Fracture Mechanics Design in Civil and Mechanical Engineering: Two High-Impact Applications

Roberto Ballarini
Thomas and Laura Hsu Professor
University of Houston

Chongqing University
December 30, 2019


Minmao Liao
A bit grouchy;
Who really did the work?

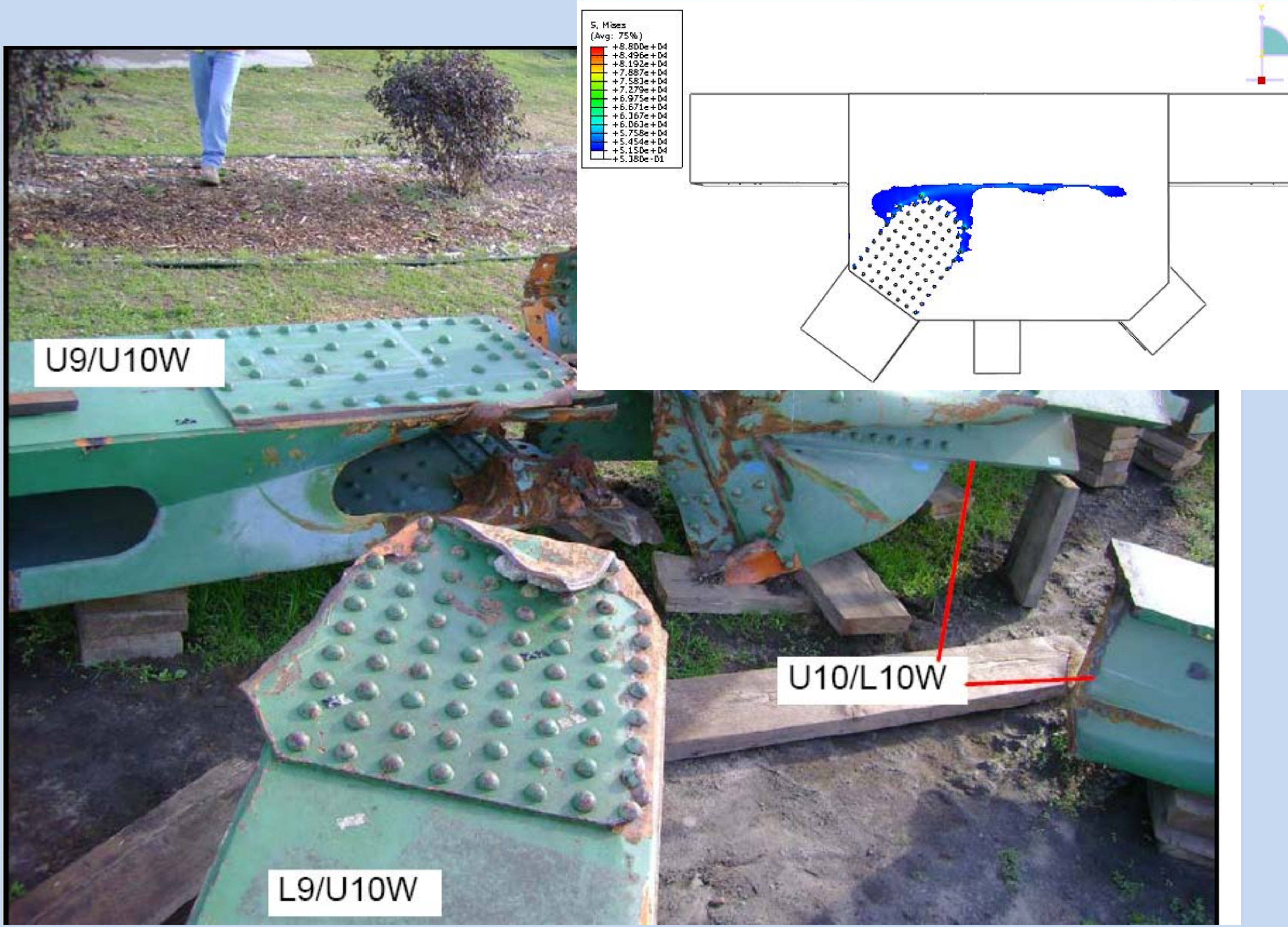
U9/U10W
U10/L10W
L9/U10W
S, Mises
(Avg: 75%)
+8.800e+04
+8.496e+04
+8.192e+04
+7.887e+04
+7.583e+04
+7.279e+04
+6.975e+04
+6.671e+04
+6.367e+04
+6.063e+04
+5.758e+04
+5.454e+04
+5.150e+04
+5.380e-01

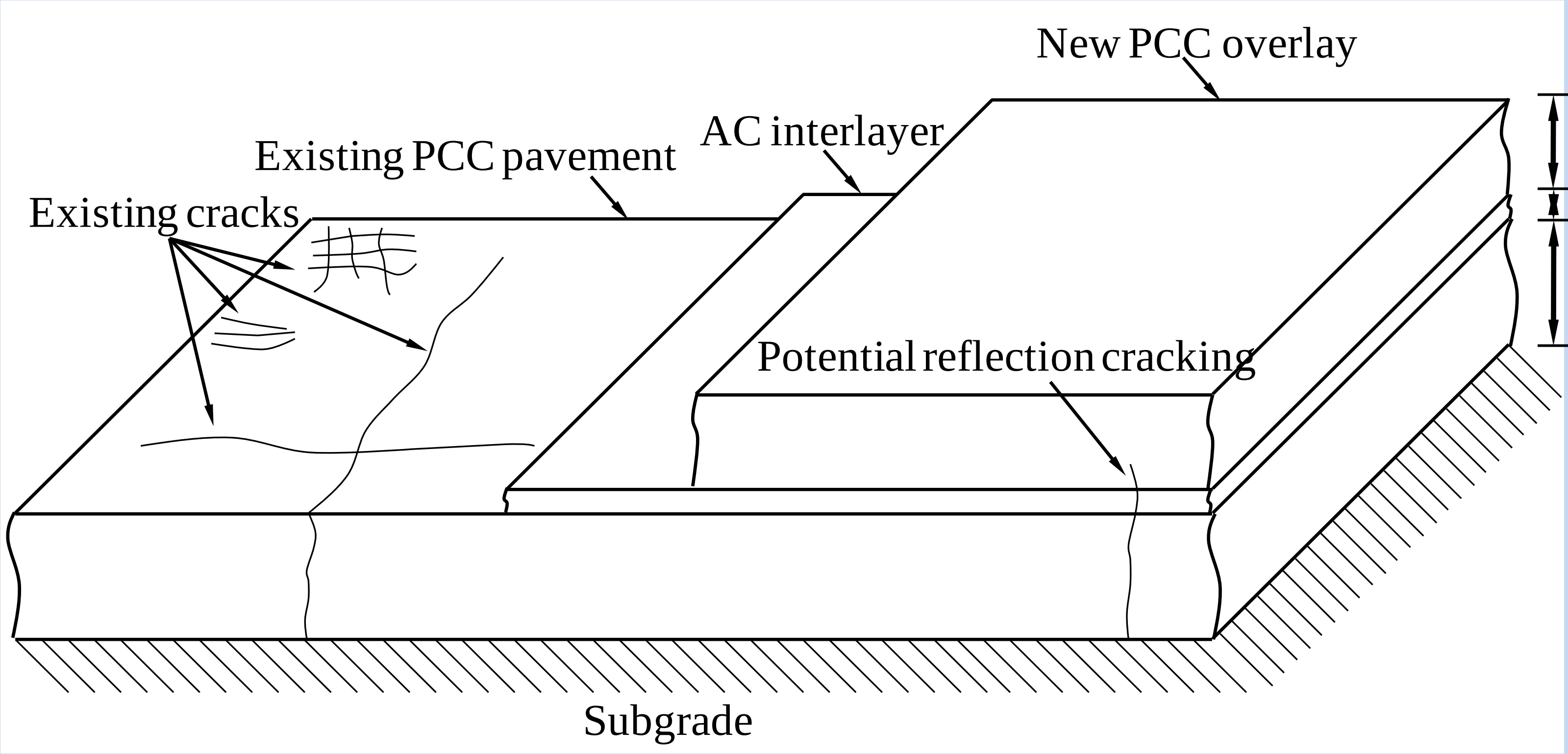

- An unbonded concrete overlay (UBCO) is a Portland cement concrete (PCC) overlay that is separated from an existing PCC pavement by an asphalt concrete (AC) interlayer.

Research methodology

- Fracture mechanics-based load-carrying capacity equivalency design paradigm

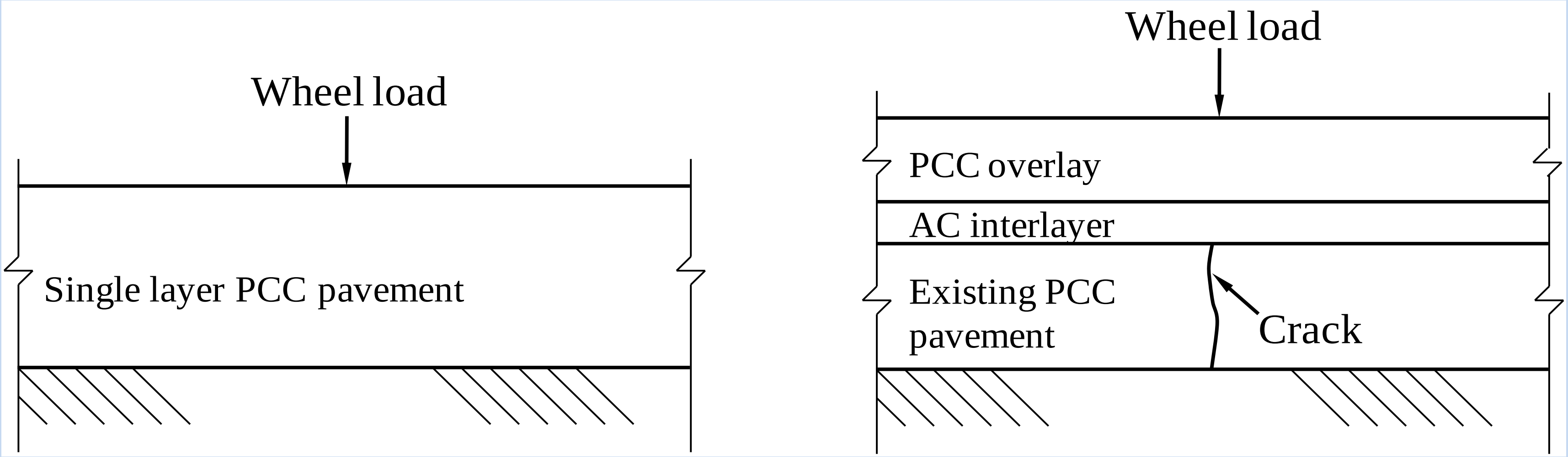

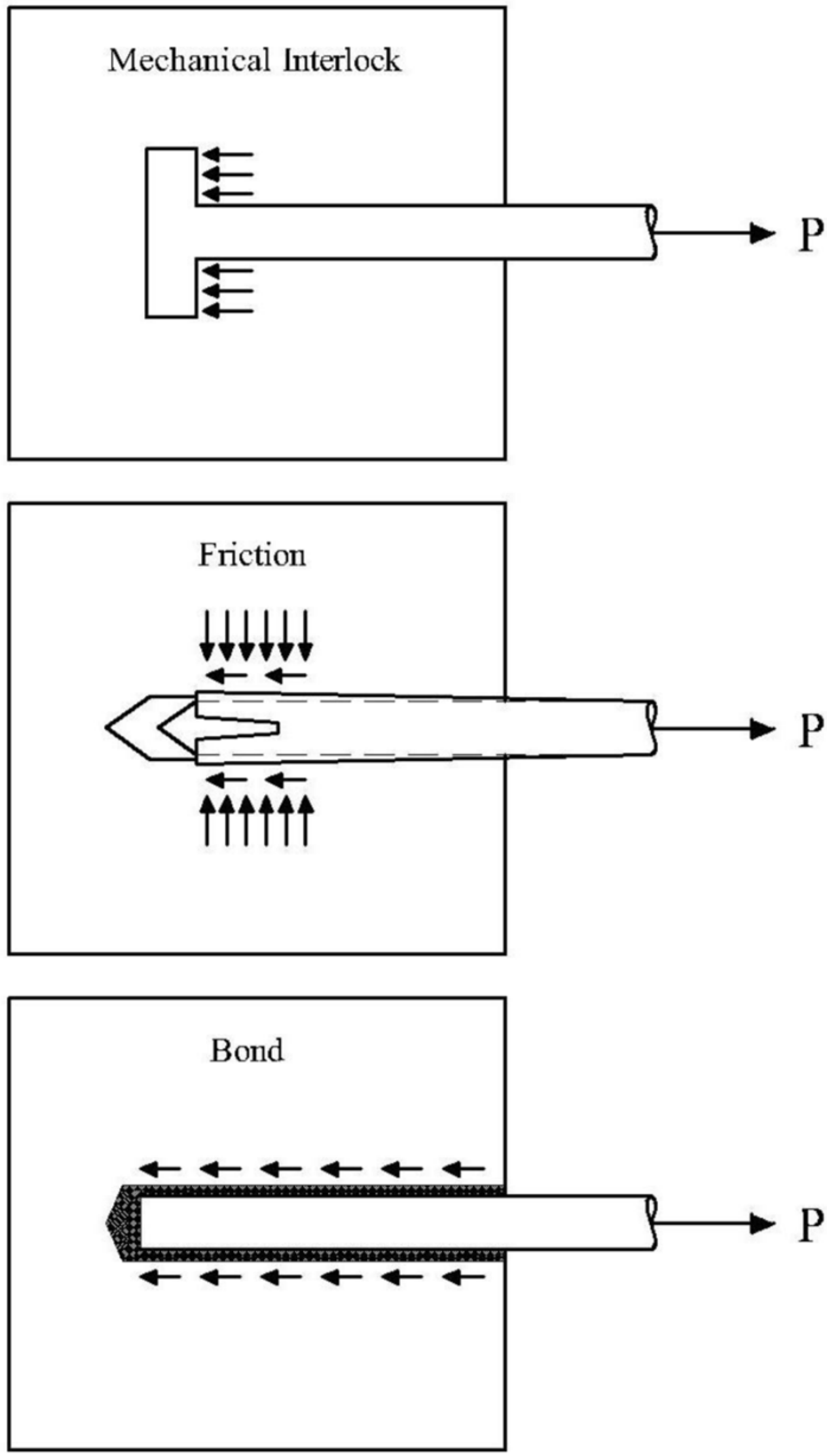
Mechanical Interlock
P
Friction
P
Bond
P

The codes up to the early 1990's

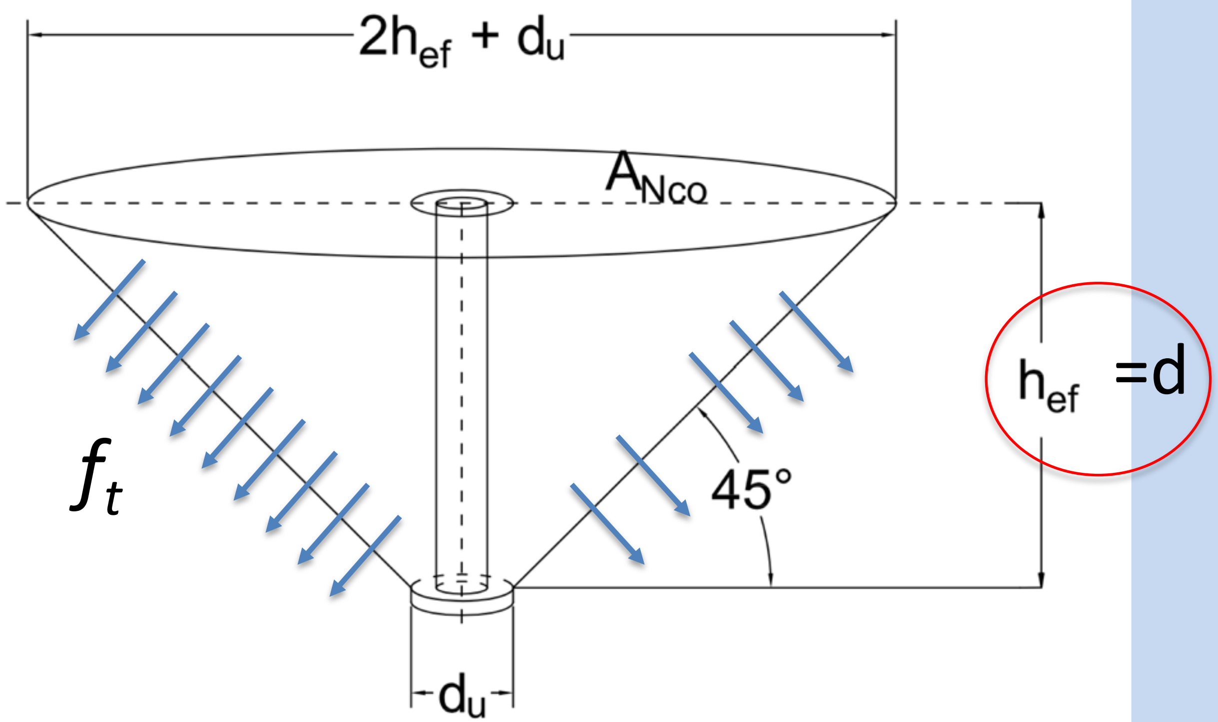

$$P_{u,ACI} = f_t \pi d^2 \left(1 + \frac{c}{d}\right) = 4\phi\sqrt{f_c'}\pi d^2 \left(1 + \frac{c}{d}\right) \approx f_t d^2$$

$\phi \; (f_t = 4\phi\sqrt{f_c'})$.

Does not agree with experimental data!
Over-predicts capacity!

Strength Theories vs. LEFM

(1) Plasticity vs. (2) Fracture Mechanics

(1)

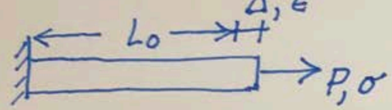

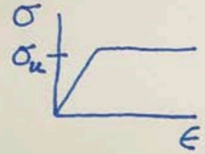

$\boxed{\sigma_{cr} \equiv \sigma_u}$

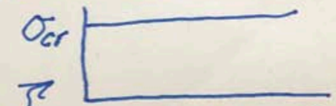

size independent "size"

(2)

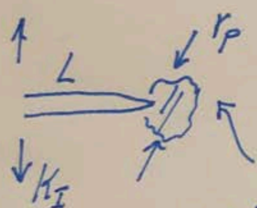

$\frac{L}{r_p} >> 1$

$\sigma_{ij} = \frac{K_I}{\sqrt{r}} f_{ij}(\theta)$

$r_p \sim \left(\frac{K_I}{\sigma_u}\right)^2$

$K_I \sim \sigma_N \sqrt{D}$

e.g. $K_I = \sigma^\infty \sqrt{\pi a}$

$\boxed{K_I \equiv K_{Ic}}$

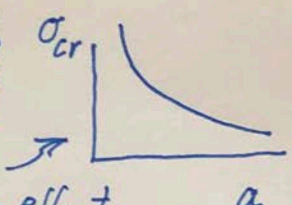

scale effect

(1) & (2)

$$\frac{\sigma_{cr}}{\sigma_u} = \begin{cases} 1, & \text{plasticity} \\ \sim \frac{1}{\sqrt{a/r_p}}, & \text{LEFM} \end{cases}$$

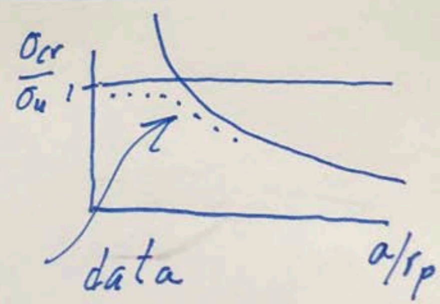

data

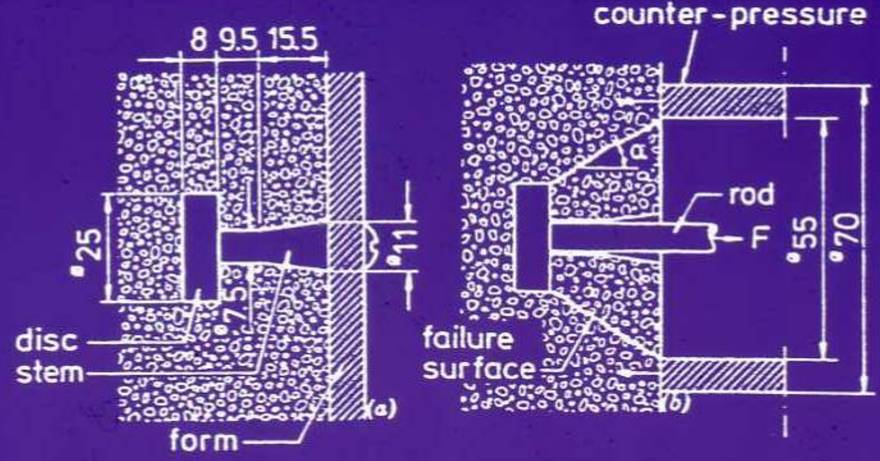

–Application and Configuration of Lok-Test (All Dimensions Are in millimeters)

FIG. 5– LOK–TEST

What material property is this test measuring?

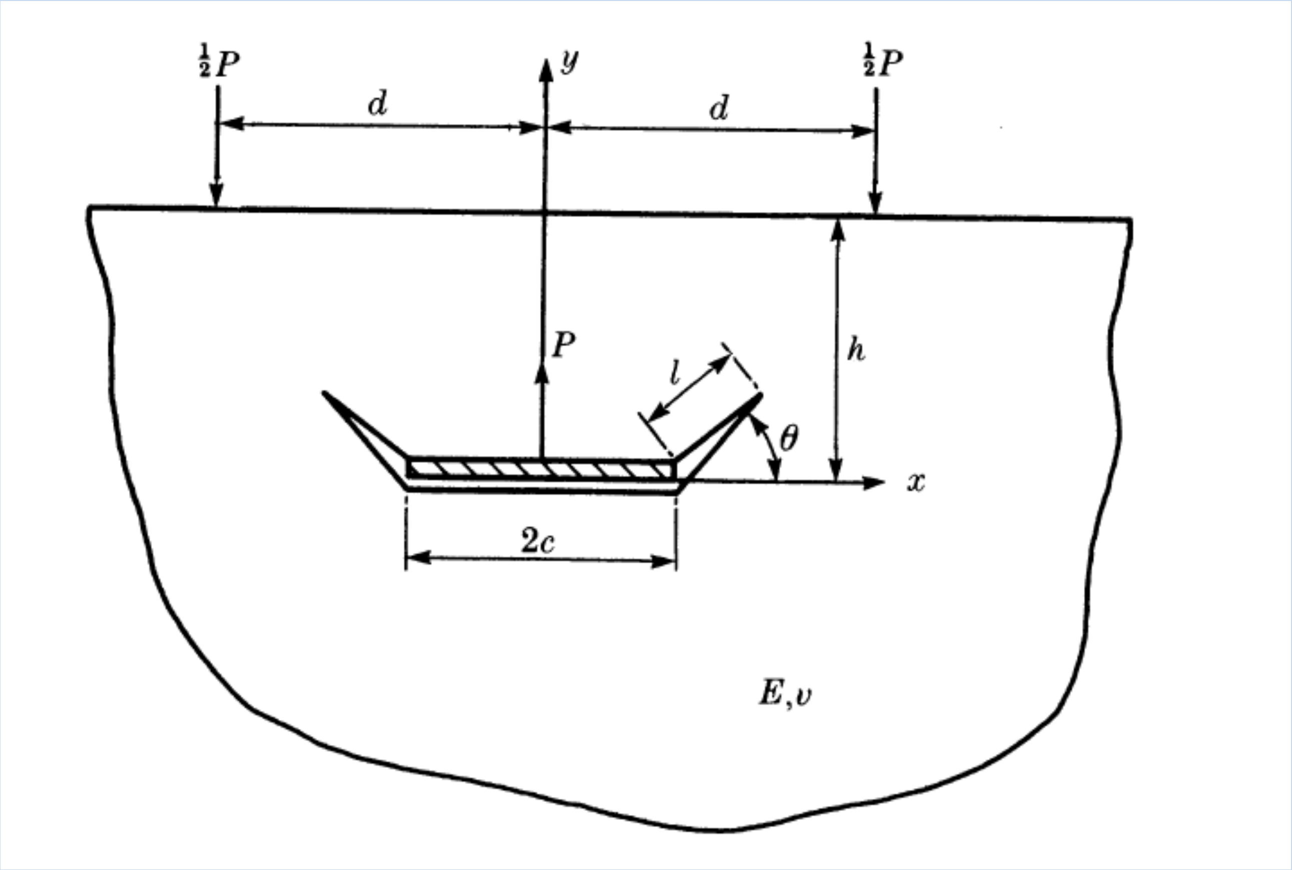

- **Failure of headed anchors reflects a progressive crack propagation process; (Ballarini *et al.*, 1985) Two-dimensional configuration**

- **Experimental and analytical investigation of LOK test and pullout problem by changing the position of the support reactions**

Stress Intensity Factors

$$\sigma_c \sim \frac{K_c}{\sqrt{a}}$$

K_I = mode I stress intensity factor

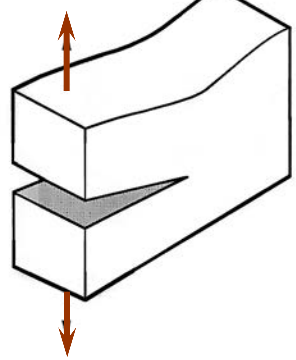

K_{II} = mode II stress intensity factor

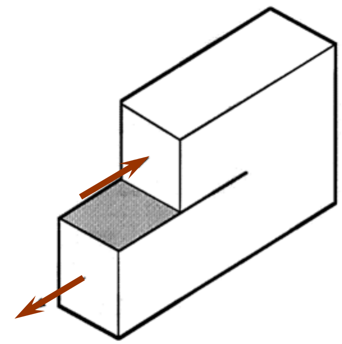

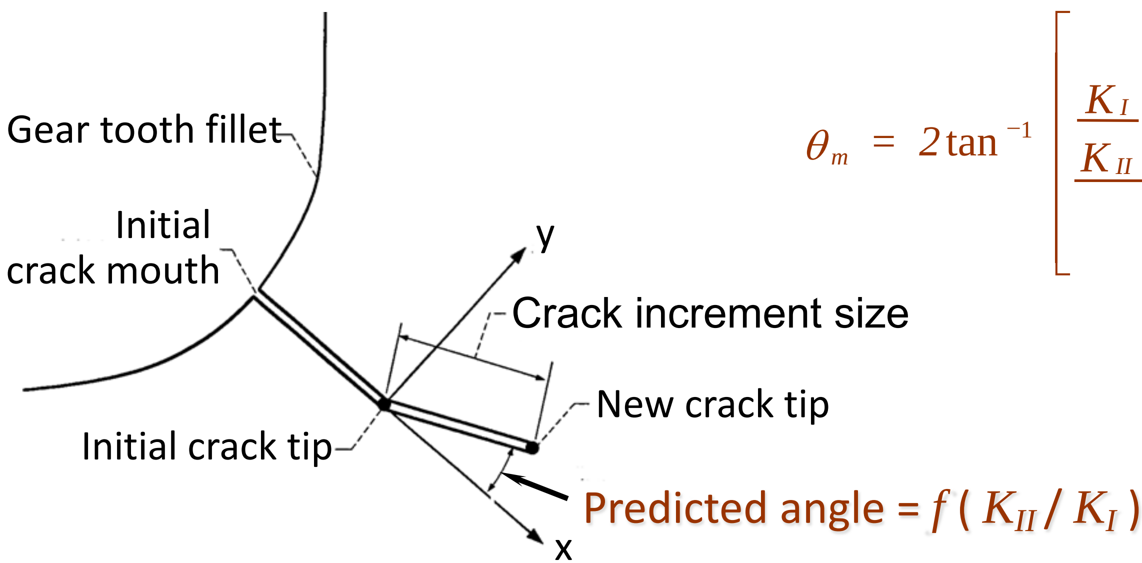

$$\theta_m = 2\tan^{-1}\left[\frac{\frac{K_I}{K_{II}} \pm \sqrt{\left(\frac{K_I}{K_{II}}\right)^2 + 8}}{4}\right]$$

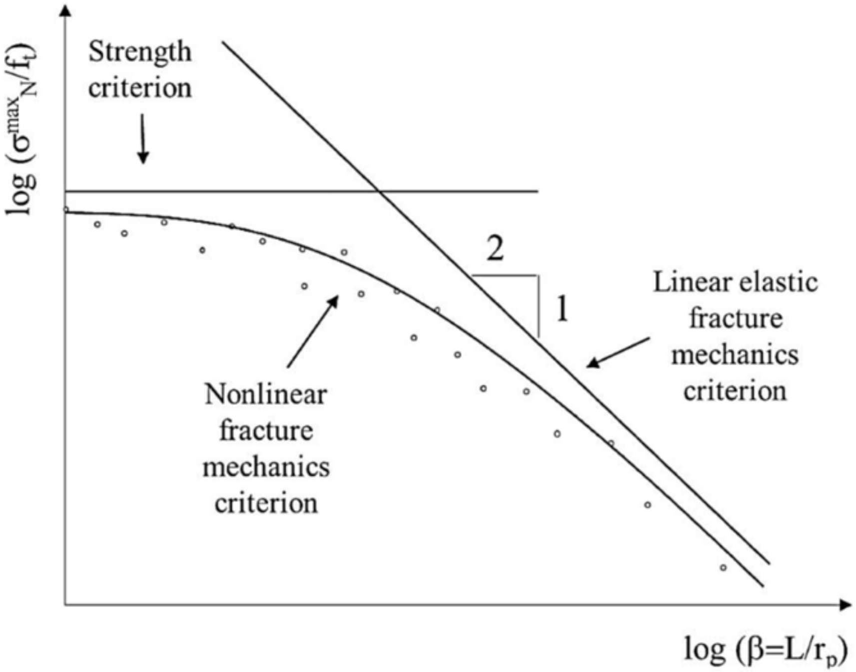

Strength criterion
$\log(\sigma^{max}_N/f_t)$
2
1
Linear elastic fracture mechanics criterion
Nonlinear fracture mechanics criterion
$\log(\beta=L/r_p)$

(a)

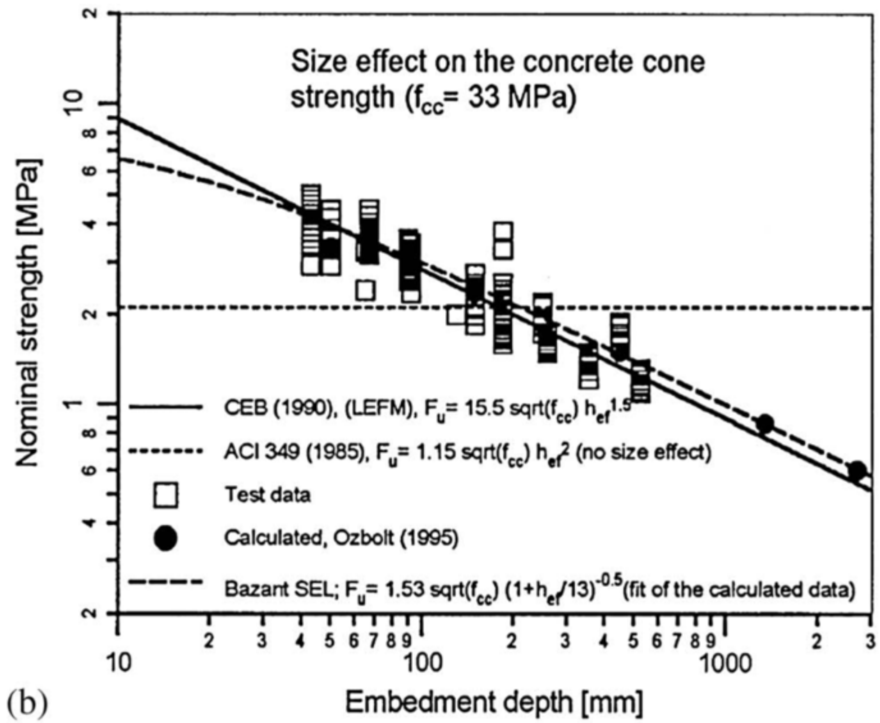

Size effect on the concrete cone strength (f_{cc}= 33 MPa)
Nominal strength [MPa]
CEB (1990), (LEFM), F_u= 15.5 sqrt(f_{cc}) $h_{ef}^{1.5}$
ACI 349 (1985), F_u= 1.15 sqrt(f_{cc}) h_{ef}^2 (no size effect)
Test data
Calculated, Ozbolt (1995)
Bazant SEL; F_u= 1.53 sqrt(f_{cc}) $(1+h_{ef}/13)^{-0.5}$(fit of the calculated data)
Embedment depth [mm]

(b)

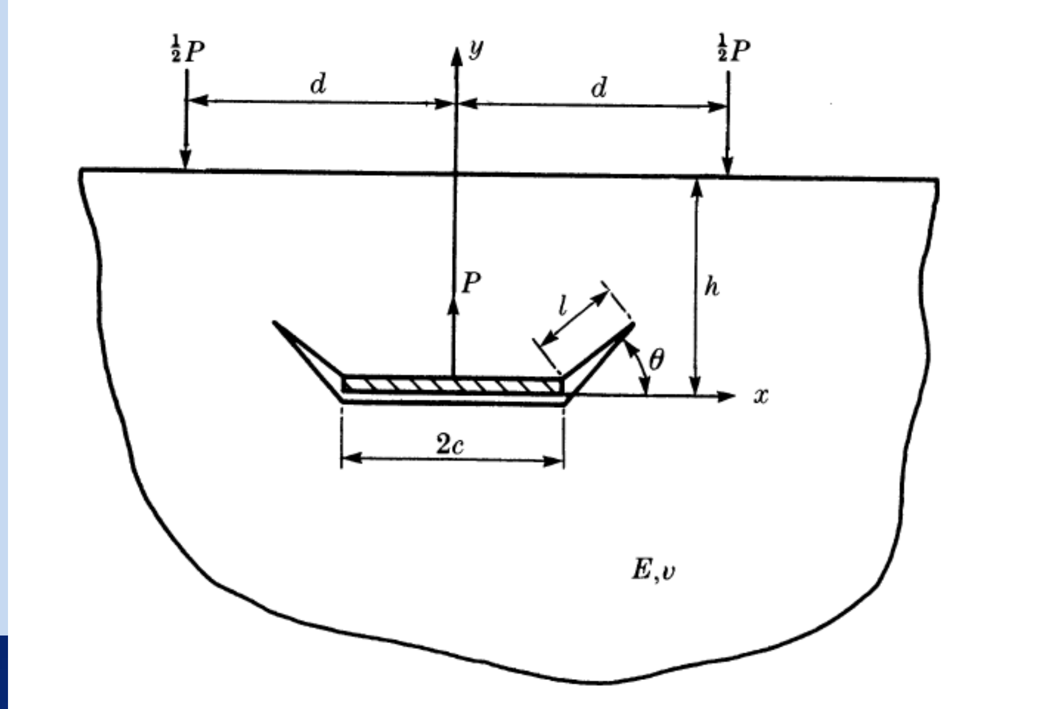

$2\mu\left(\frac{\partial u}{\partial x} + i\,\frac{\partial v}{\partial x}\right)^{+} = 0$ (bonded upper portion)

$(\sigma_{yy} - i\sigma_{xy})^{-} = 0$ (unbonded lower portion)

$\sigma_{\phi\phi} - i\sigma_{\rho\phi} = 0$ (stress free crack surface)

$$\alpha(\xi) = \frac{-1}{2\pi(\kappa+1)} \frac{\partial}{\partial \xi} (F_x + \mathrm{i} F_y),$$

$$\beta(\xi) = \frac{\mu e^{\mathrm{i}\theta}}{\pi \mathrm{i}(\kappa+1)} \frac{\partial}{\partial \xi} \{[u_r] + \mathrm{i}[v_\theta]\},$$

$$\psi(\tau) = \frac{\mu e^{\mathrm{i}\theta}}{\pi \mathrm{i}(\kappa+1)} \frac{\partial}{\partial \tau} \{[u_r] + \mathrm{i}[v_\theta]\},$$

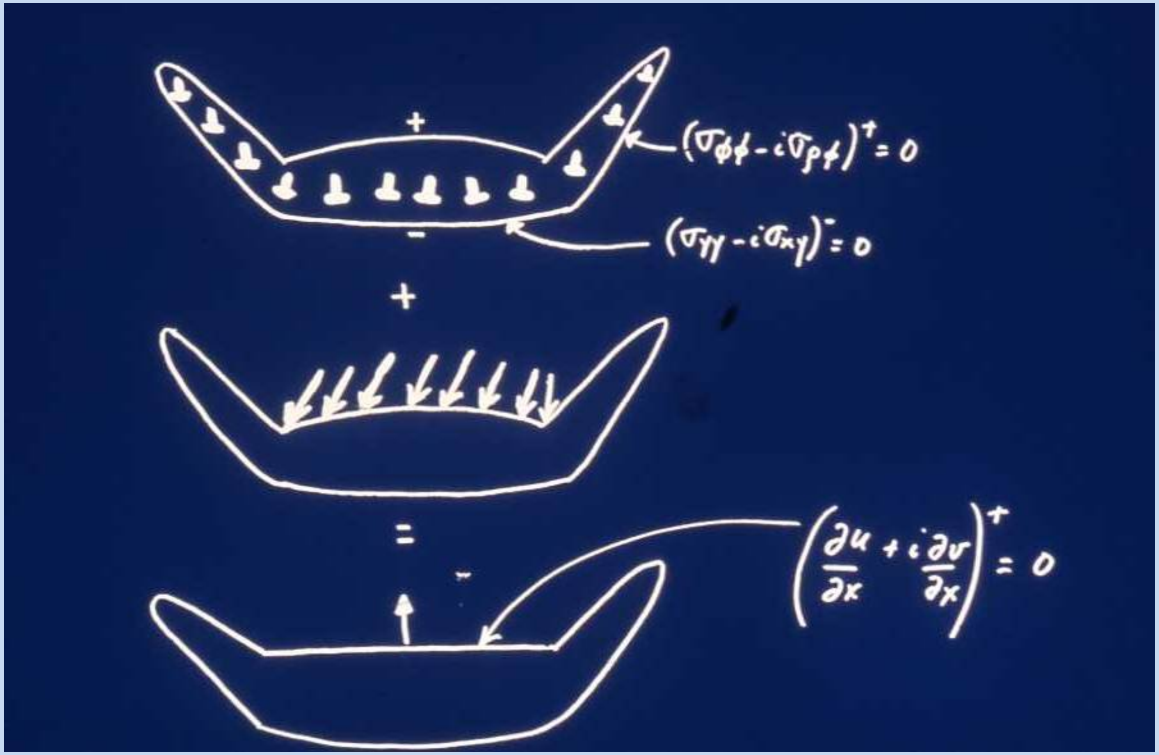
+
$(\sigma_{\phi\phi} - i\sigma_{\rho\phi})^{+} = 0$
−
$(\sigma_{yy} - i\sigma_{xy})^{-} = 0$
+
=
$\left(\frac{\partial u}{\partial x} + i\frac{\partial v}{\partial x}\right)^{+} = 0$

$$\int_0^c \alpha(\xi)\left\{\frac{\kappa-1}{\xi-x} + K_1(x,\xi) - K_2(x,-\xi)\right\} d\xi + \int_0^c \overline{\alpha(\xi)}\left\{K_2(x,\xi) - K_1(x,-\xi)\right\} d\xi$$

$$+ \pi i\,(\kappa+1)\;\alpha\,(x) + \int_0^c \beta(\rho)\left\{\frac{-2}{\rho-x} + K_3(x,\rho) - K_4(x,-\rho)\right\} d\rho$$

$$+ \int_0^c \overline{\beta(\rho)}\left\{K_4(x,\rho) - K_3(x,-\rho)\right\} d\rho$$

$$+ \int_0^\ell \psi(\tau)\,K_9(x,\tau)\,d\tau + \int_0^\ell \overline{\psi(\tau)}\,K_{10}\,(x,\tau)\,d\tau + f_1(x) = 0 \qquad -c \le x \le c$$

$$\int_0^c \left[\alpha(\xi) - \overline{\alpha(\xi)}\right] d\xi = \frac{P}{2\pi i(\kappa+1)}$$

$$\int_0^c \left[\beta(\xi) - \overline{\beta(\xi)}\right] d\xi + \int_0^\ell \left[\psi(\tau) - \overline{\psi(\tau)}\right] d\tau = 0$$

All physical quantities can be obtained after solving numerically the equations (3.4)–(3.8). In particular, the stress intensity factor, defined by

$$K_{\mathrm{I}}-\mathrm{i}K_{\mathrm{II}} = \lim_{\tau\to l^{+}} \sqrt{[2\pi(\tau-l)]}\,(\sigma_{\phi\phi}-\mathrm{i}\sigma_{\phi\phi}) \tag{3.10}$$

can be directly related to the dislocation density $\psi(\tau)$ by taking the asymptotic form of (3.6). In terms of dimensionless quantities arising from the numerical scheme, the result is

$$(K_{\mathrm{I}}-\mathrm{i}K_{\mathrm{II}})\,(c^{\frac{1}{2}}/P) = 2^{\frac{1}{2}}\pi^{\frac{3}{2}}\mathrm{e}^{-\mathrm{i}\theta}\sqrt{(l/c)}\,\overset{*}{\psi}(1), \tag{3.11}$$

where

$$\psi(\tau) = \frac{\overset{*}{\psi}(s)}{(1-s^{2})^{\frac{1}{2}}}\frac{P}{c}; \quad s = \frac{2\tau}{l}-1. \tag{3.12}$$

FIG. 13— MINIMUM PRINCIPAL STRESSES

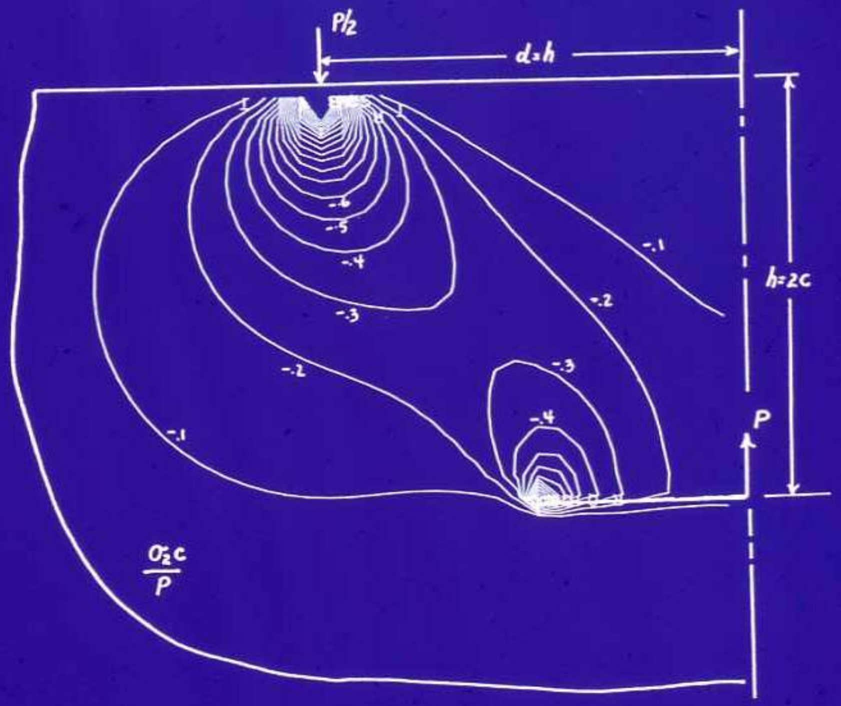

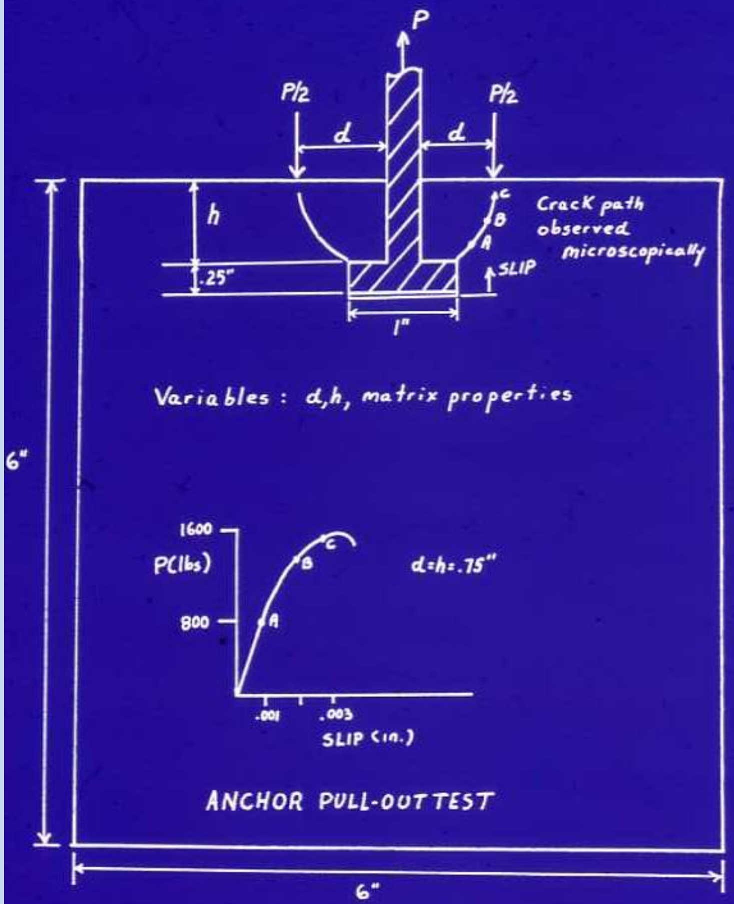

FIG. 6— CONFIGURATION OF 2–D

PULL–OUT TEST

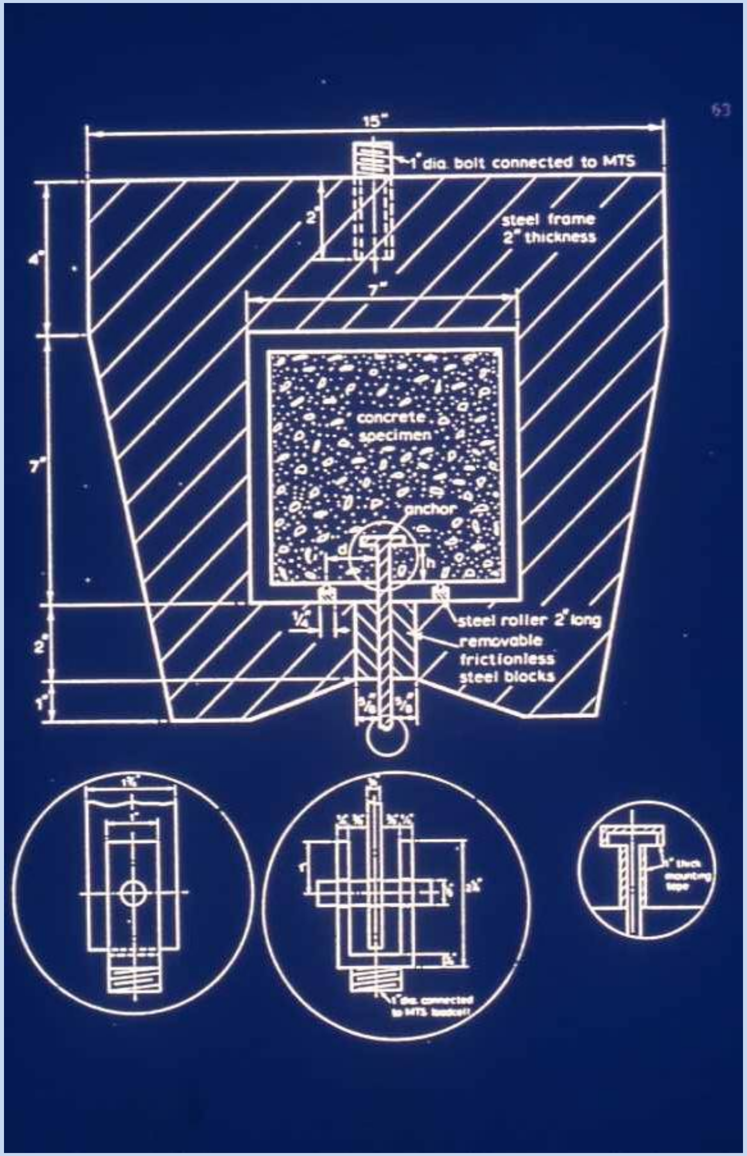

15"
1" dia. bolt connected to MTS
steel frame
2" thickness
2"
4"
7"
concrete
specimen
anchor
d
h
7"
1/4"
steel roller 2" long
removable
frictionless
steel blocks
2"
1"
5/8"
5/8"

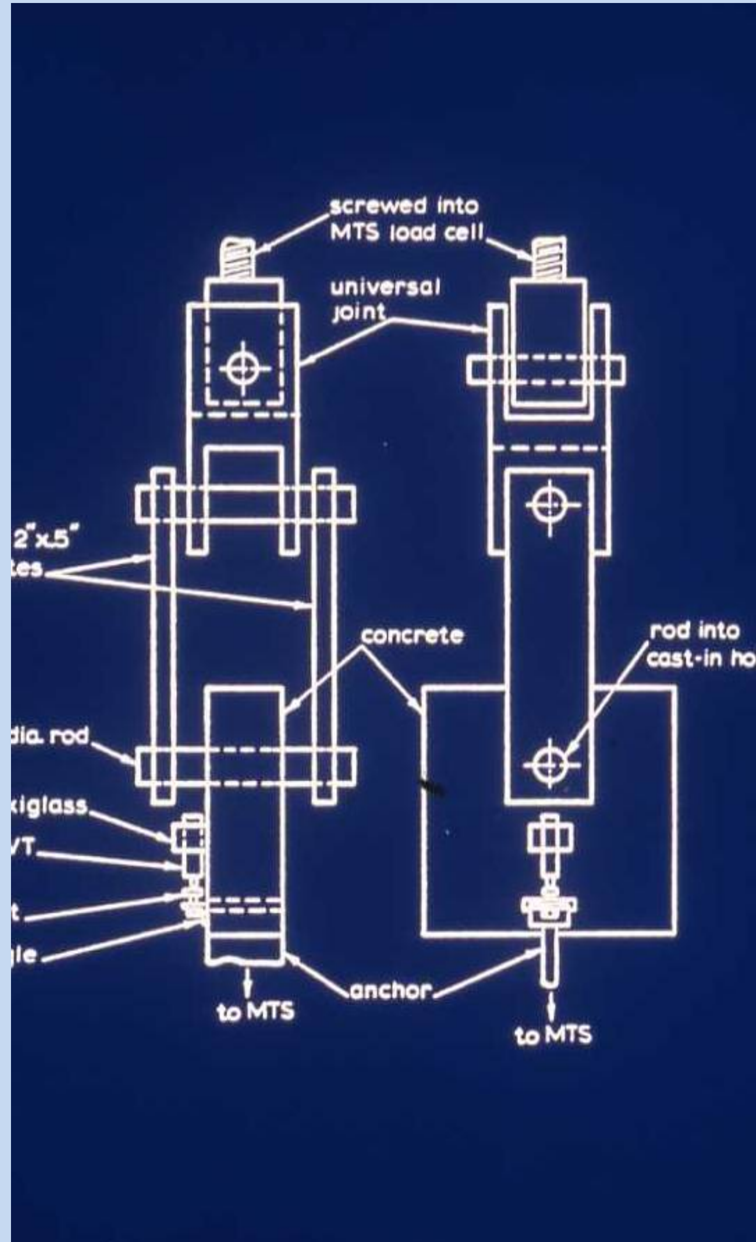

screwed into
MTS load cell
universal
joint
2"x.5"
tes
concrete
rod into
cast-in hole
dia. rod
xiglass
VT
t
le
to MTS
anchor
to MTS

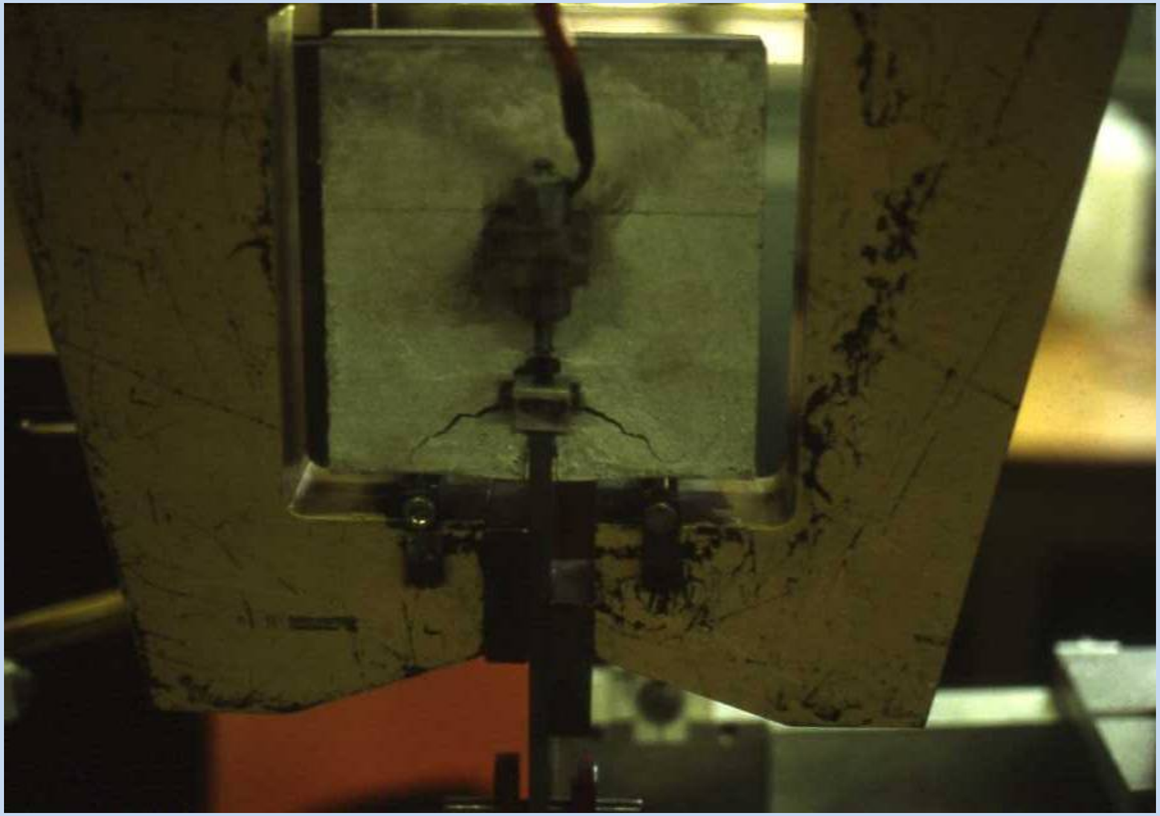

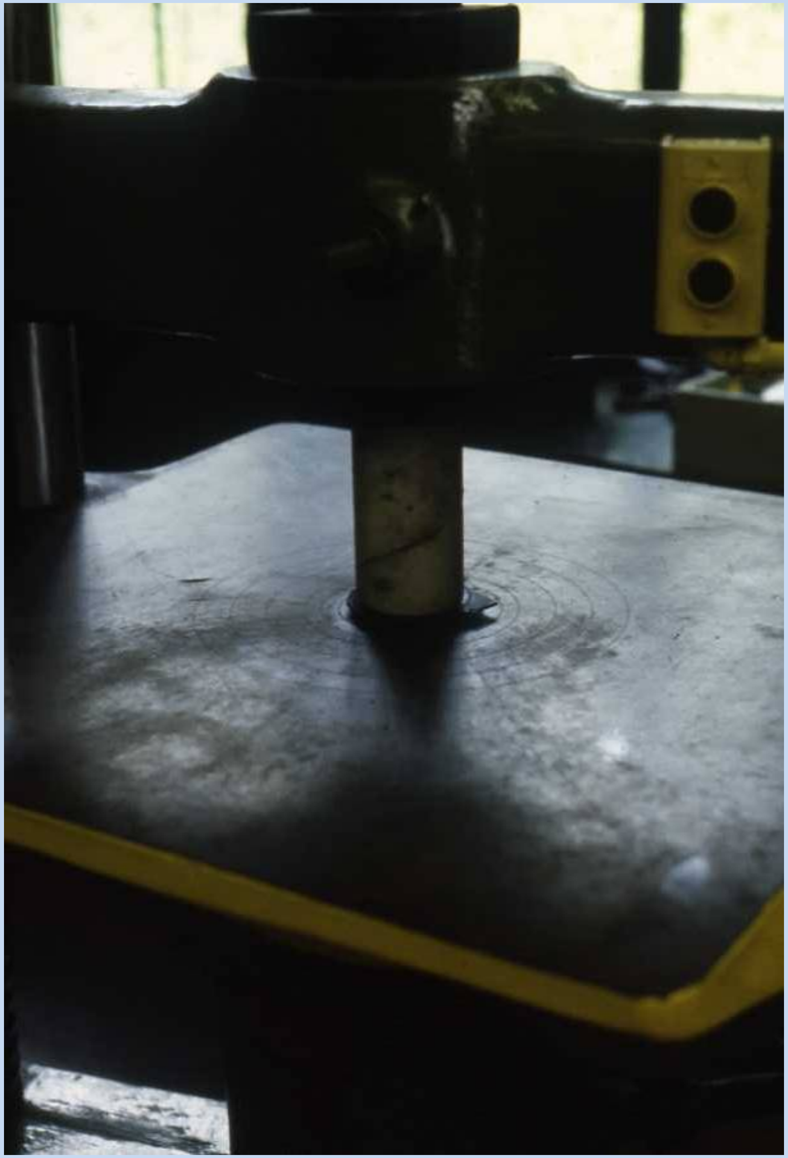

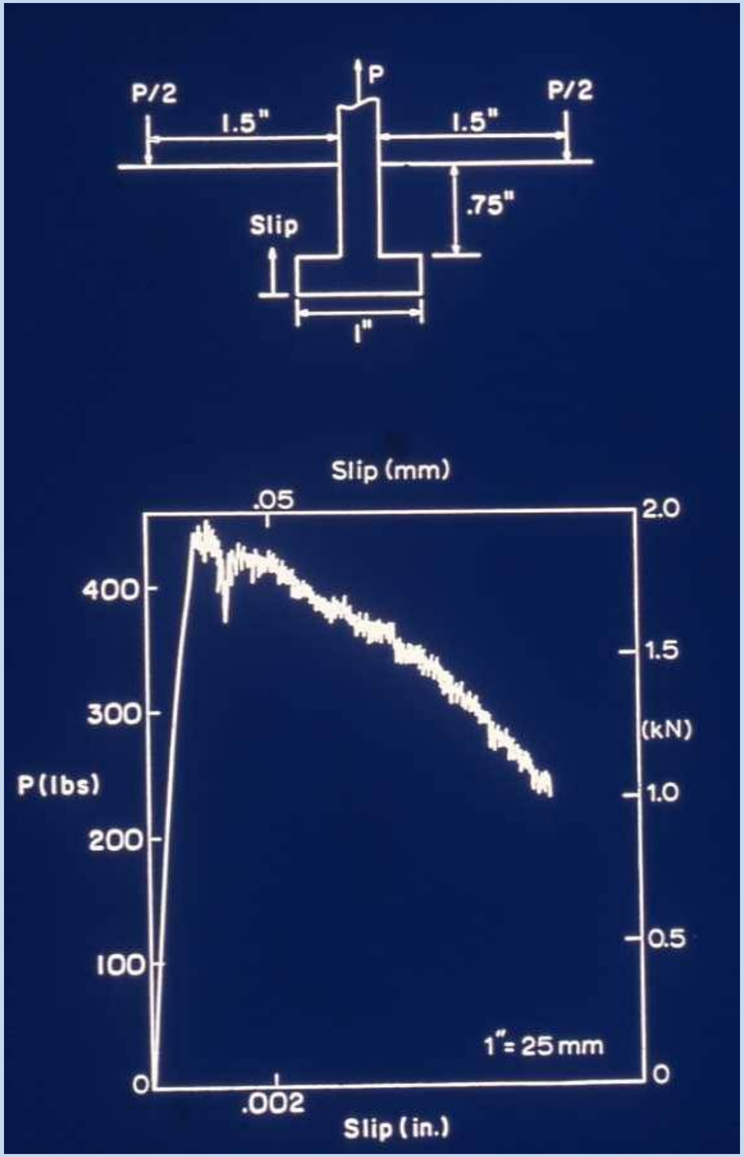

P
P/2
1.5"
1.5"
P/2
.75"
Slip
1"
Slip (mm)
.05
2.0
400
1.5
300
(kN)
P (lbs)
1.0
200
0.5
100
1" = 25 mm
0
0
.002
Slip (in.)

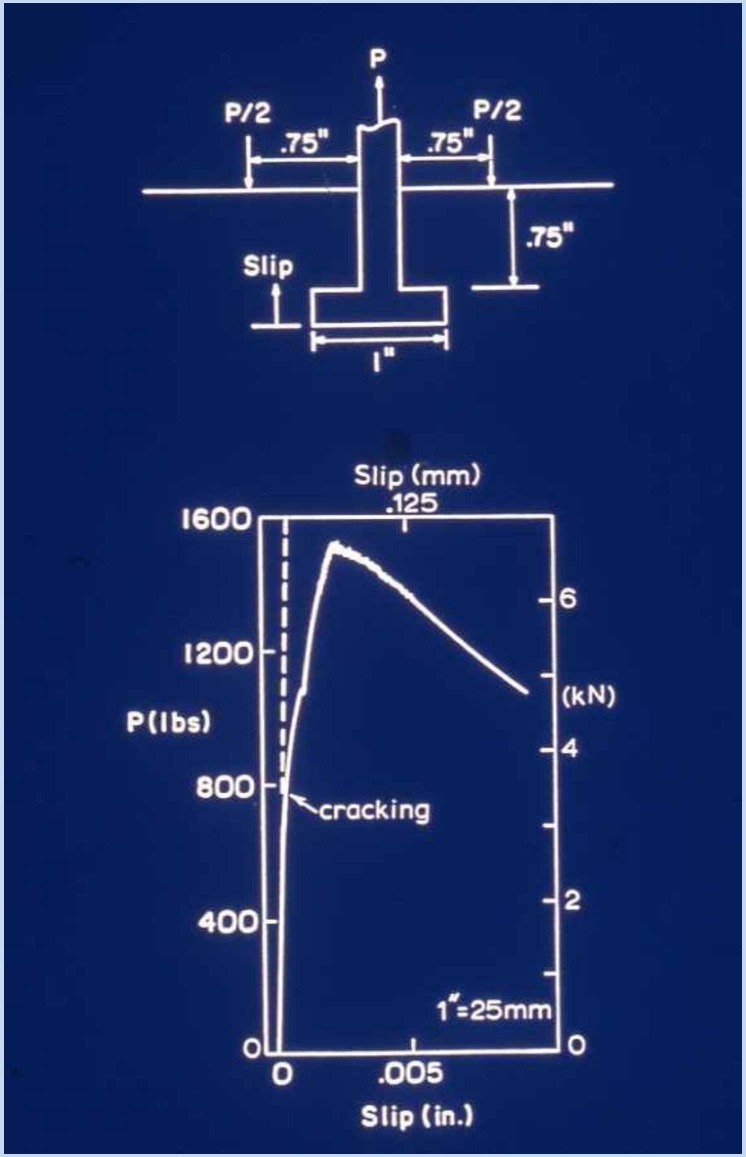

P
P/2
.75"
.75"
P/2
.75"
Slip
1"
Slip (mm)
.125
1600
6
1200
(kN)
P (lbs)
4
800
cracking
2
400
1"=25mm
0
0
0
.005
Slip (in.)

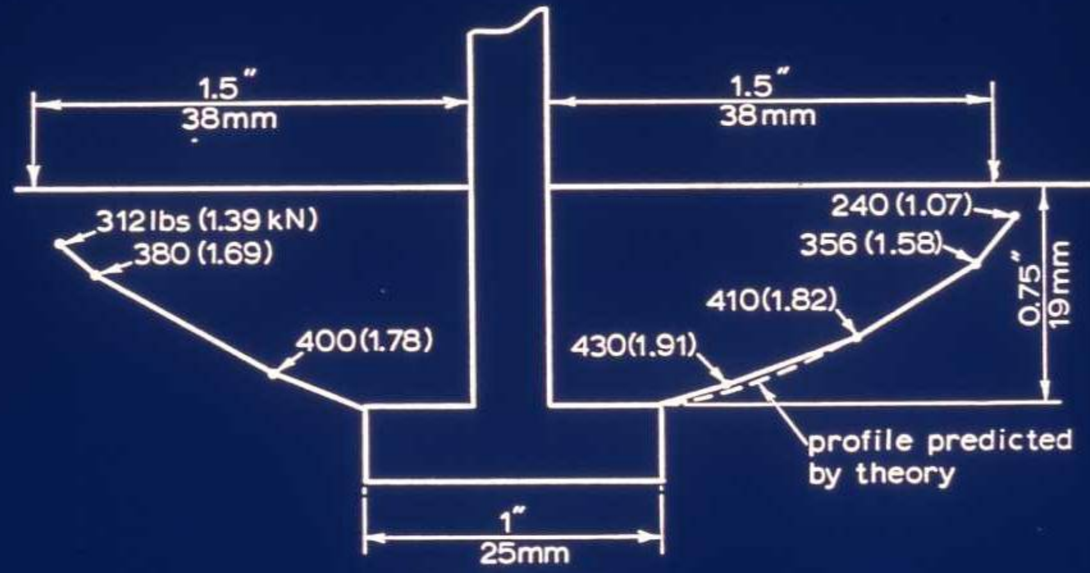

Specimen 4A

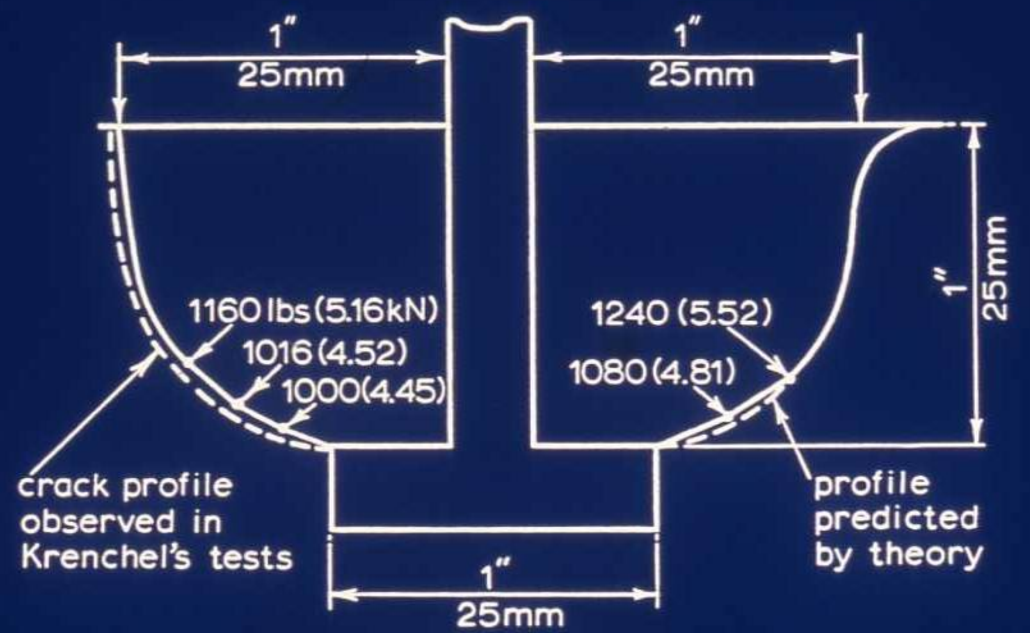

Specimen 7A

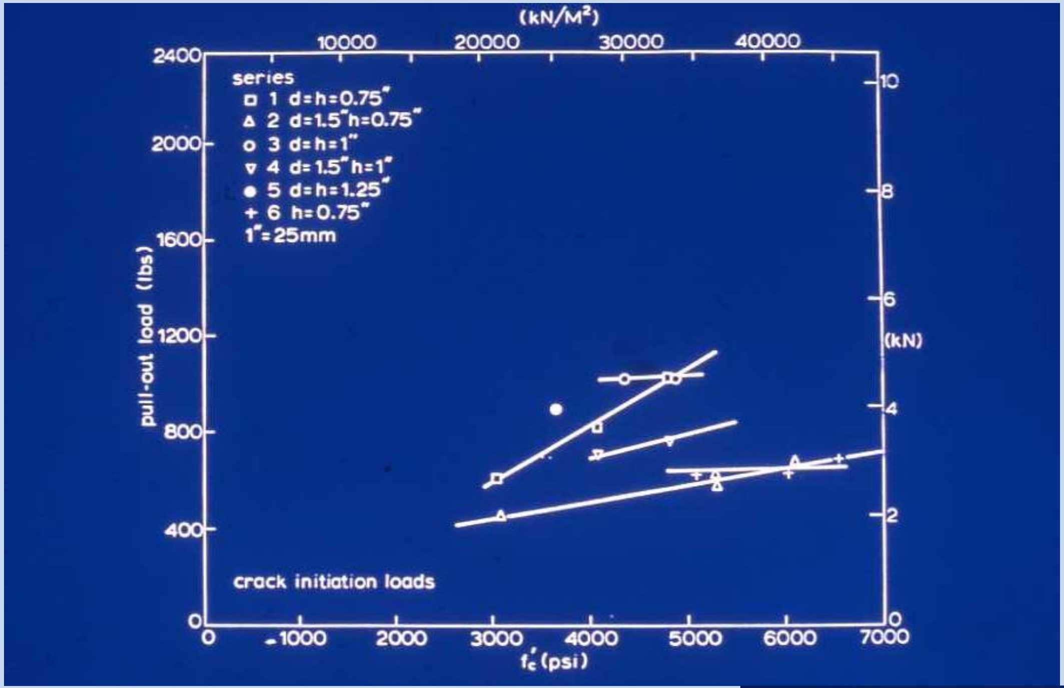
(kN/M²)
10000 20000 30000 40000
2400 2000 1600 1200 800 400 0
pull-out load (lbs)
series
1 d=h=0.75"
2 d=1.5" h=0.75"
3 d=h=1"
4 d=1.5" h=1"
5 d=h=1.25"
6 h=0.75"
1"=25mm
10 8 6 4 2 0
(kN)
crack initiation loads
0 1000 2000 3000 4000 5000 6000 7000
f'c (psi)

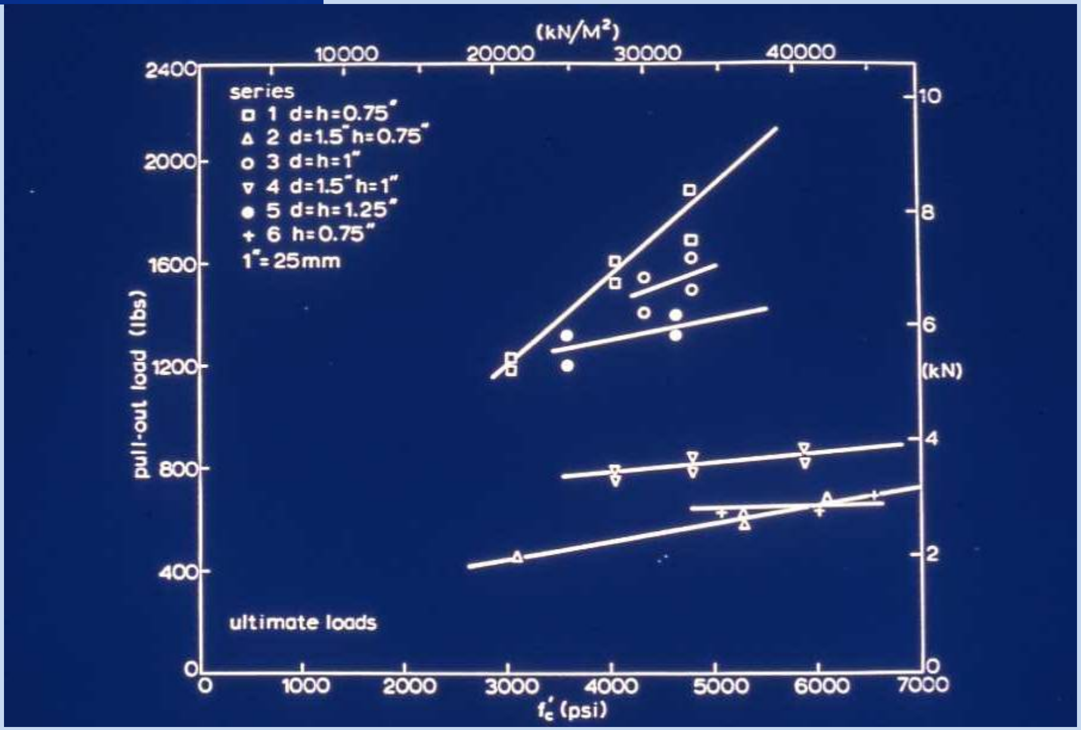
(kN/M²)
10000 20000 30000 40000
2400 2000 1600 1200 800 400 0
pull-out load (lbs)
series
1 d=h=0.75"
2 d=1.5" h=0.75"
3 d=h=1"
4 d=1.5" h=1"
5 d=h=1.25"
6 h=0.75"
1"=25mm
10 8 6 4 2 0
(kN)
ultimate loads
0 1000 2000 3000 4000 5000 6000 7000
f'c (psi)

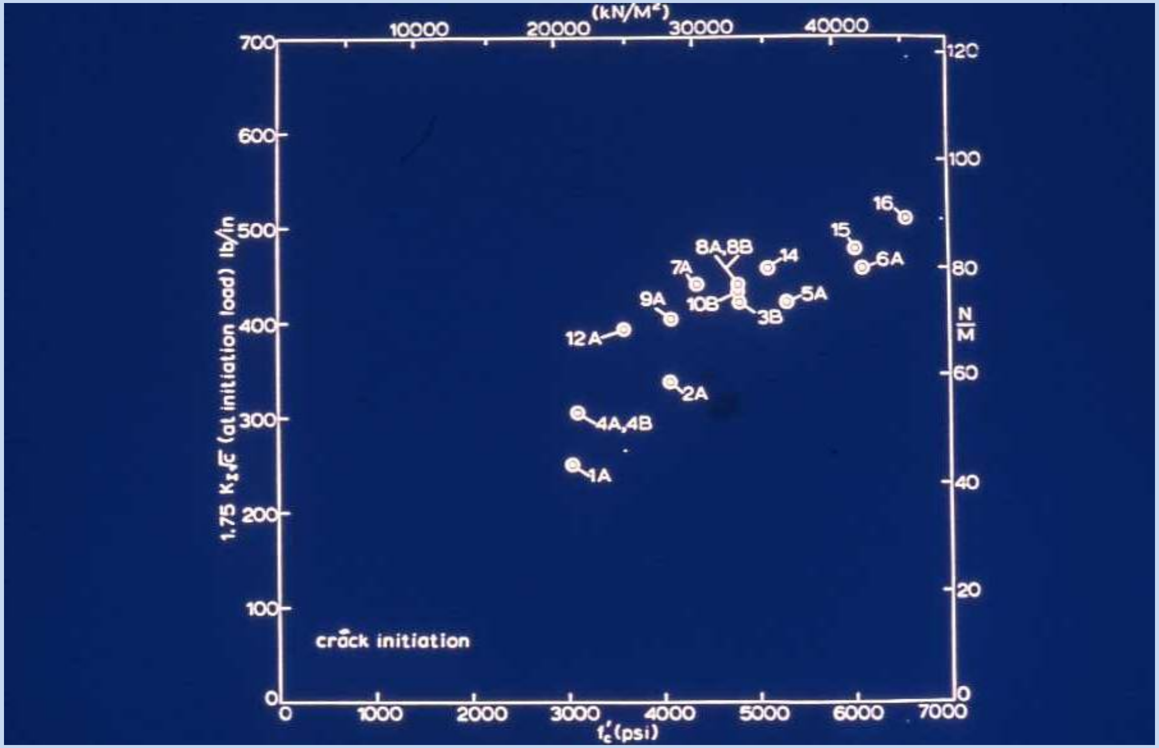

(kN/M²)
10000
20000
30000
40000
700
600
500
400
300
200
100
0
120
100
80
60
40
20
0
N/M
1.75 K_I√E (at initiation load) lb/in
16
15
6A
8A,8B
14
7A
9A
10B
3B
5A
12A
2A
4A,4B
1A
crack initiation
0
1000
2000
3000
4000
5000
6000
7000
f'c (psi)

The new code formulas are based on LEFM

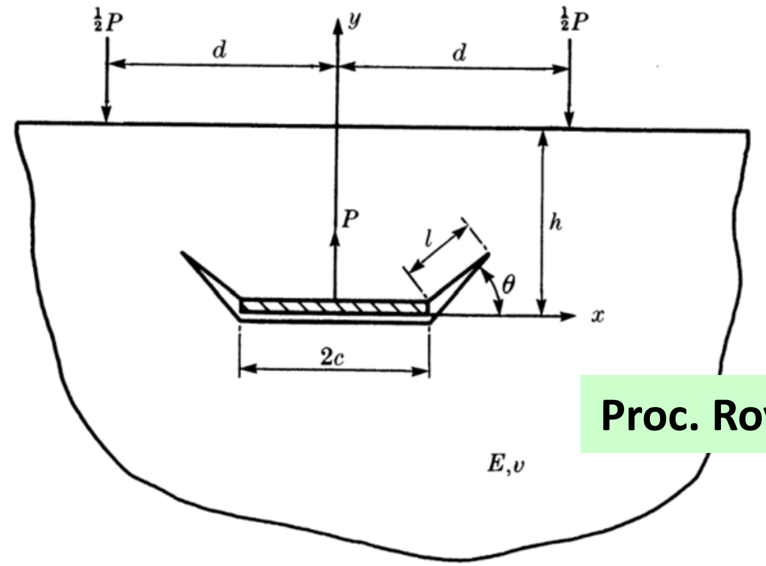

Proc. Royal Society of London, 1986

$$P_{LEFM} \approx K_c d^{3/2} \approx k_c \sqrt{f_c'}\, d^{3/2}$$

Ballarini *et al.* 1986,1987; Elfgren 1998; Elfgren and Ohlsoon 1992; Eligehausen and Sawade 1989; Eligehausen and Balogh 1995; Eligehausen *et al*. 2006; Fuchs *et al*. 1995; Karihaloo 1996; Krenchel and Shah 1985; Ozbolt et al. 1992,1999; Vogel and Ballarini 1999; Piccinin *et al*. 2010,2012

The pullout test is basically a fracture toughness test; it obeys The strongest size effect (-1/2)

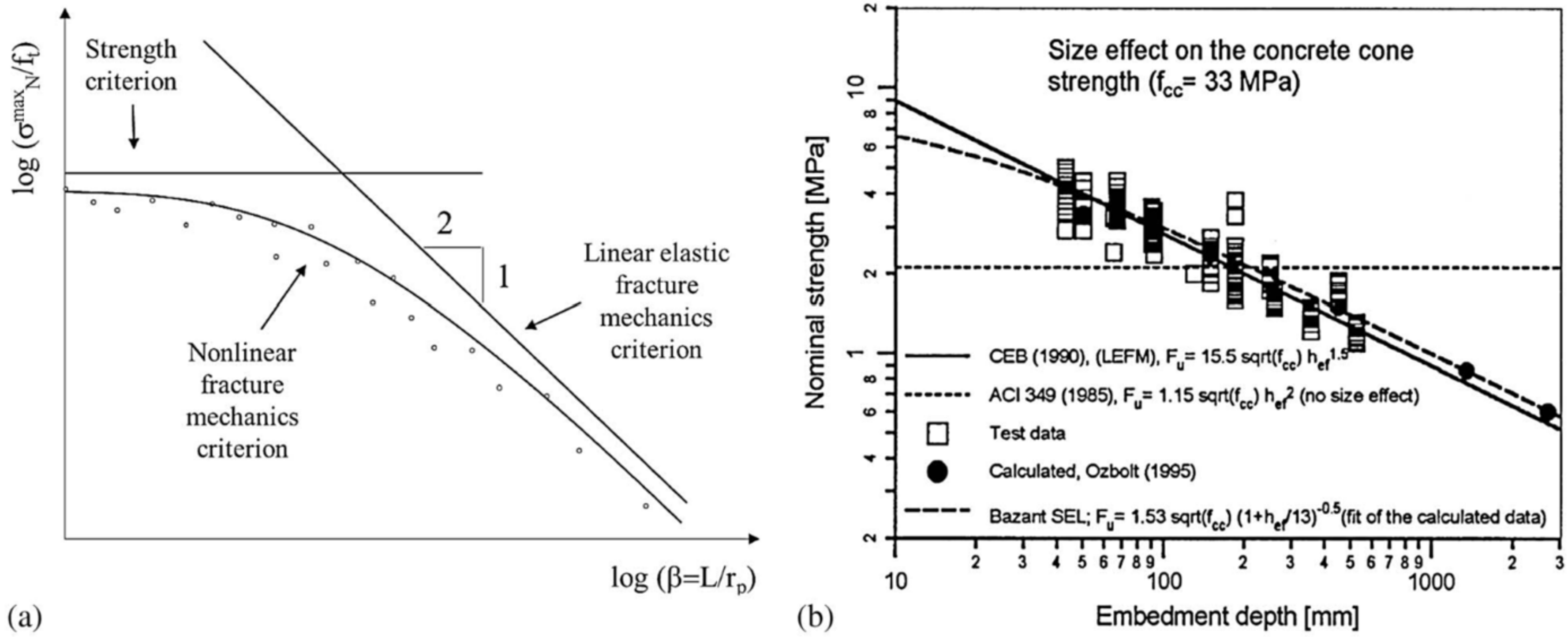


Roberto Piccinin
Now at Hilti, Liechtenstein

Very shallow embedments and with prestress

Experiments

Crack Profiles: *d/c=2*

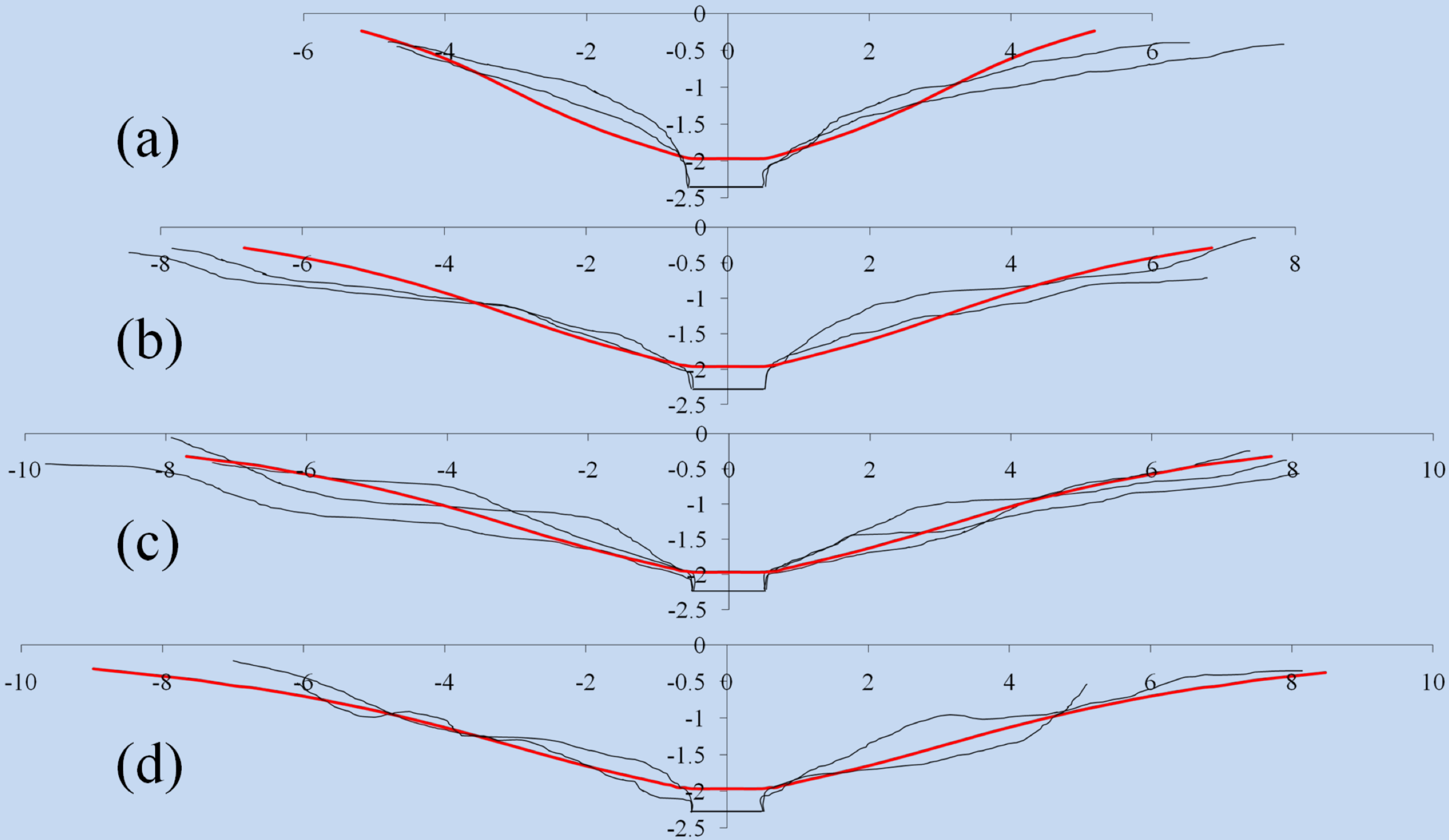

- **Crack profiles obtained from visual inspection;**
- **LEFM captures inclination and shape;**

Group anchors and anchors near free edges

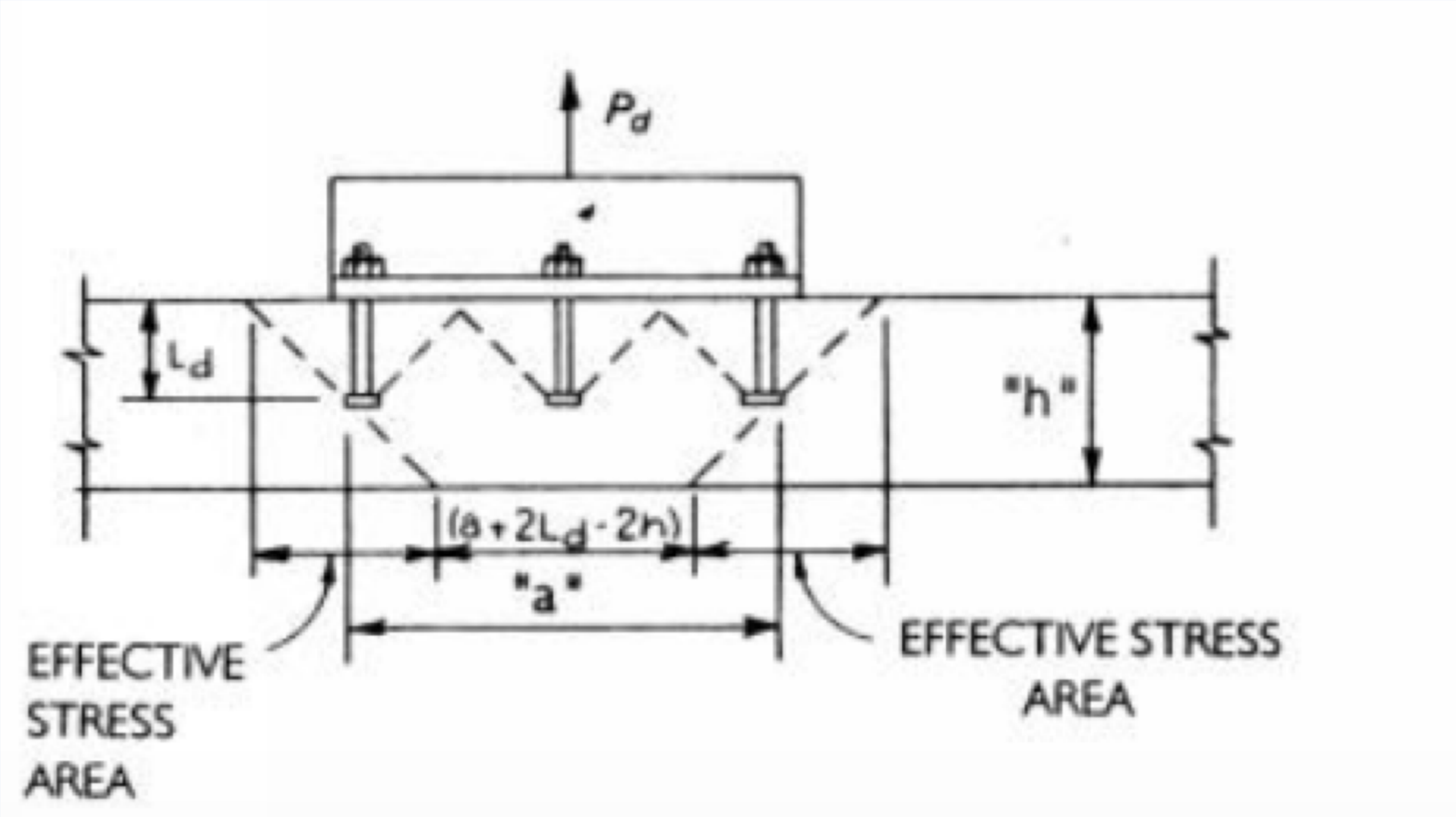

The codes still maintain some of the old approach: for a group, multiply the LEFM formula by:

$$\frac{A_{Nc}}{A_{Nco}}$$

The ratio of the projected areas of the break out cone associated with a group of *N* anchors and an isolated anchor, respectively does not correctly reflect the edge effects. It is overly conservative.

The Commentary then continues with modifications to the design formulas that reduce the conservatism in the design, with certain restrictions.

Toy problem showing this is incorrect

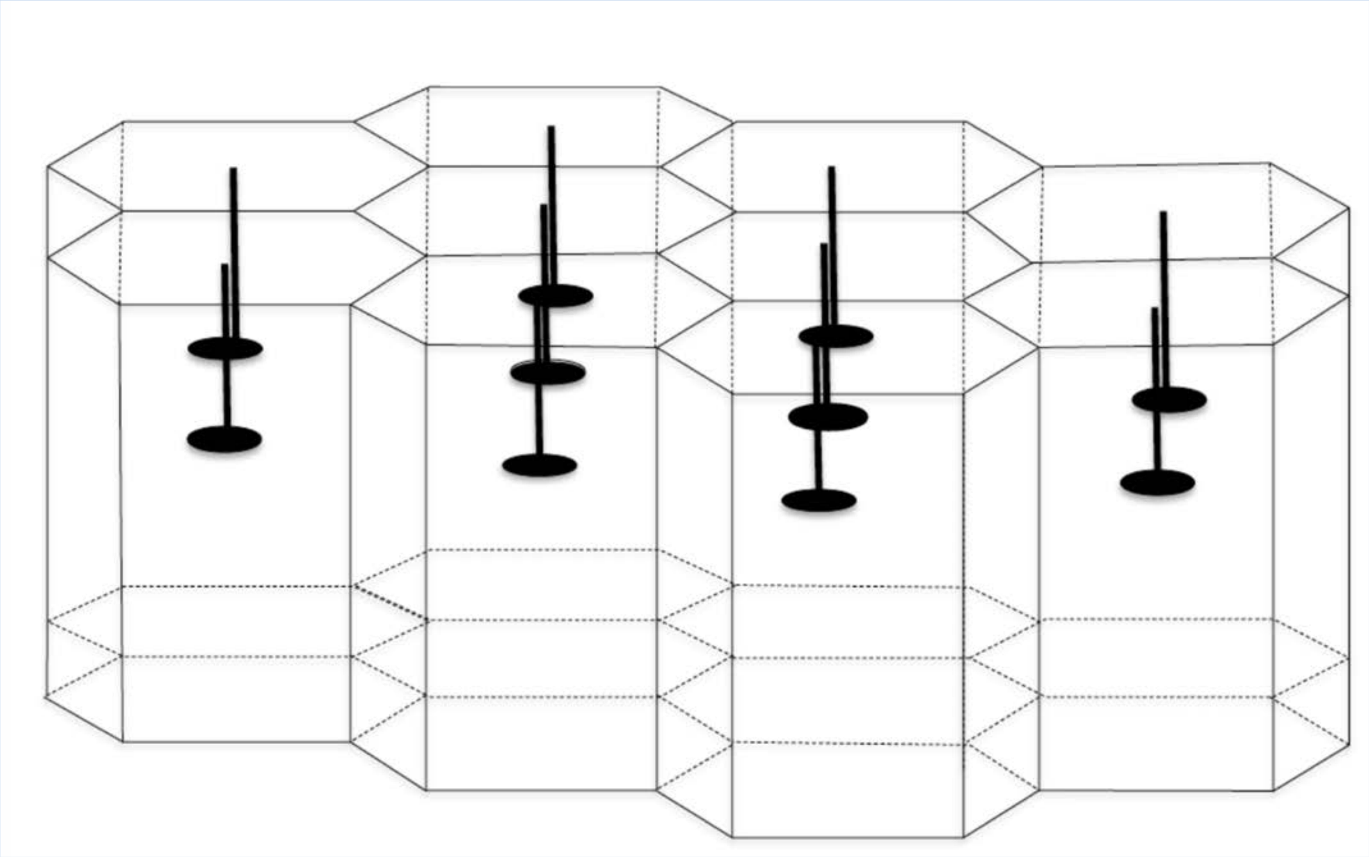

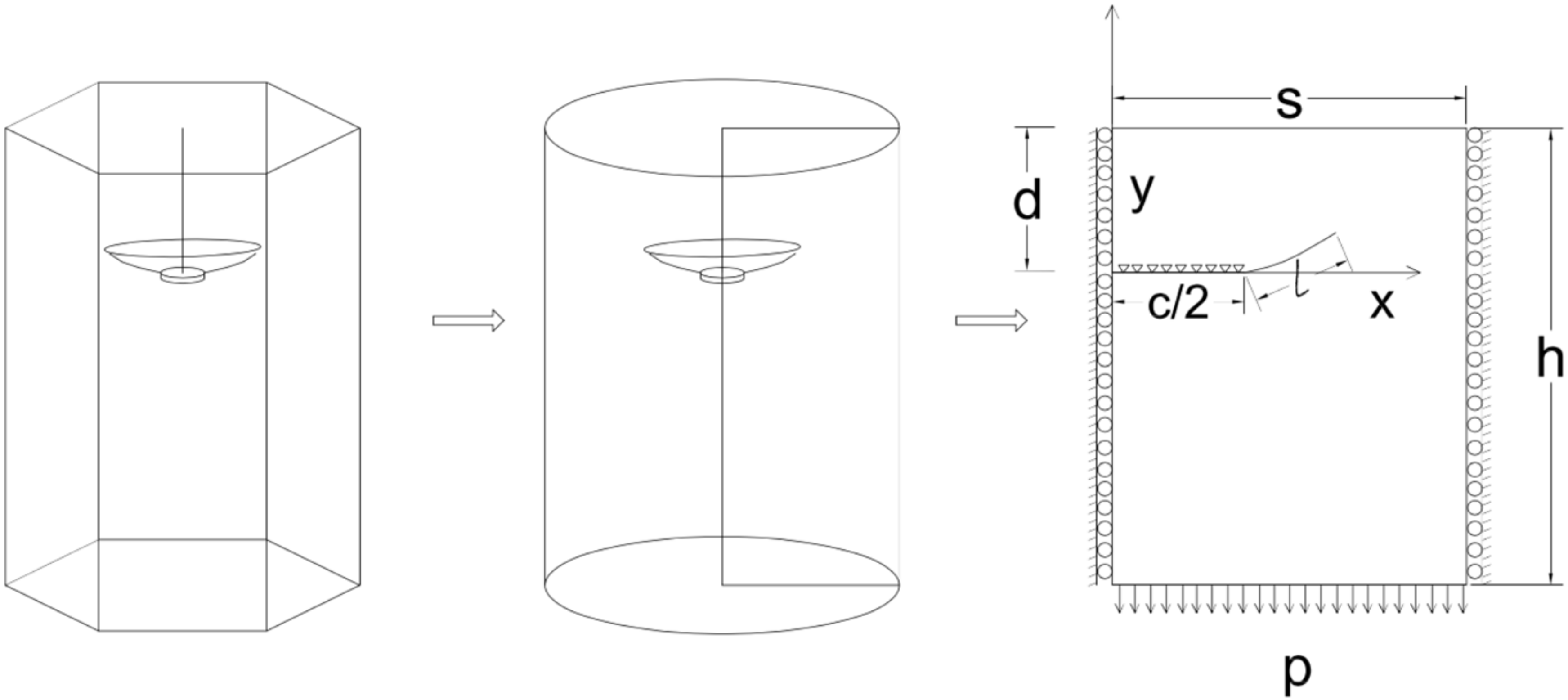

s
d
y
c/2
l
x
h
p

$$K_{Ic} = P_c d^{-3/2} f\left(\frac{l}{c}, \frac{d}{c}, \frac{s}{d}, \upsilon\right)$$

$$\frac{P_c}{K_{Ic} d^{3/2}} \equiv g = \min\left[1/f\right]$$

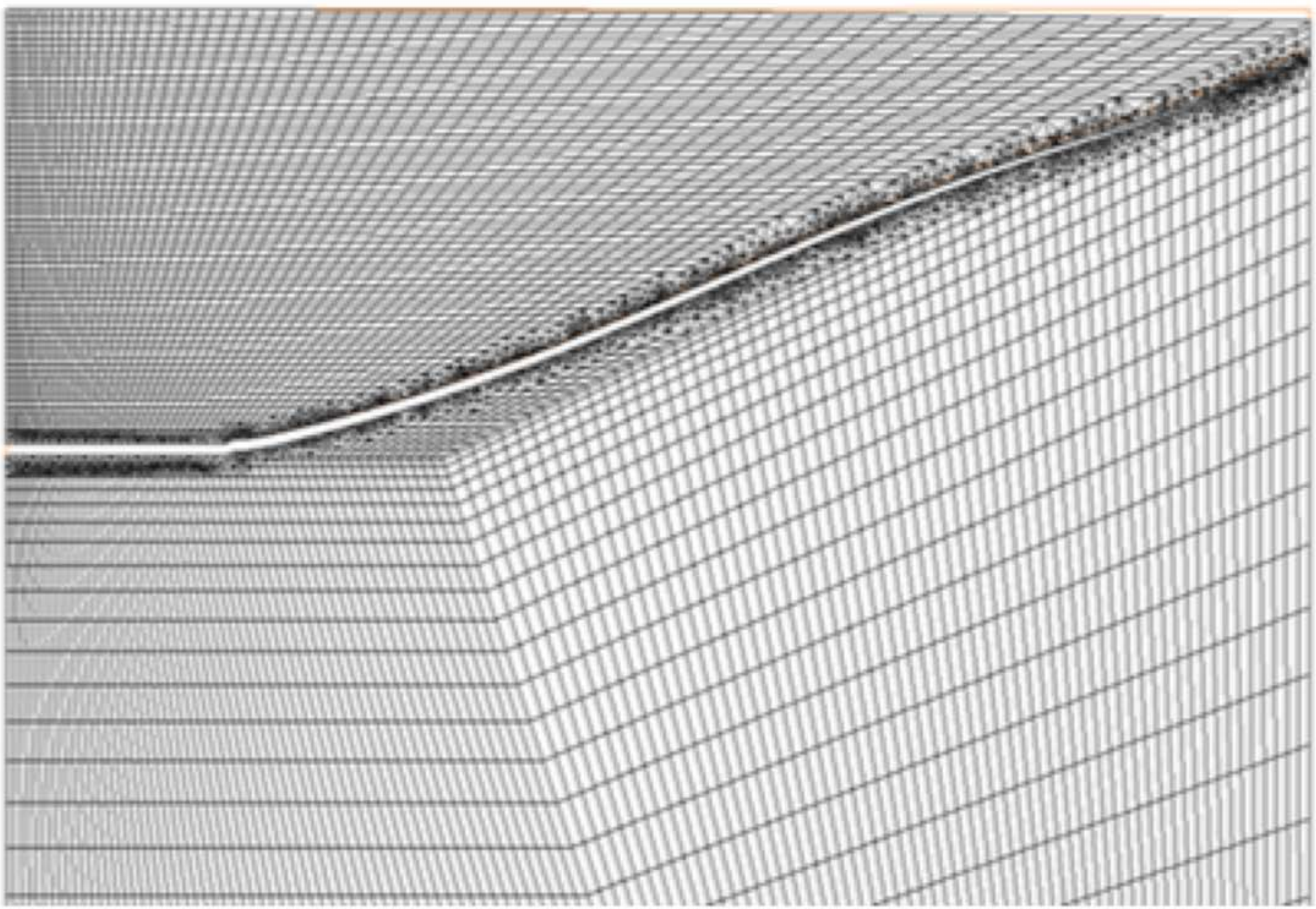

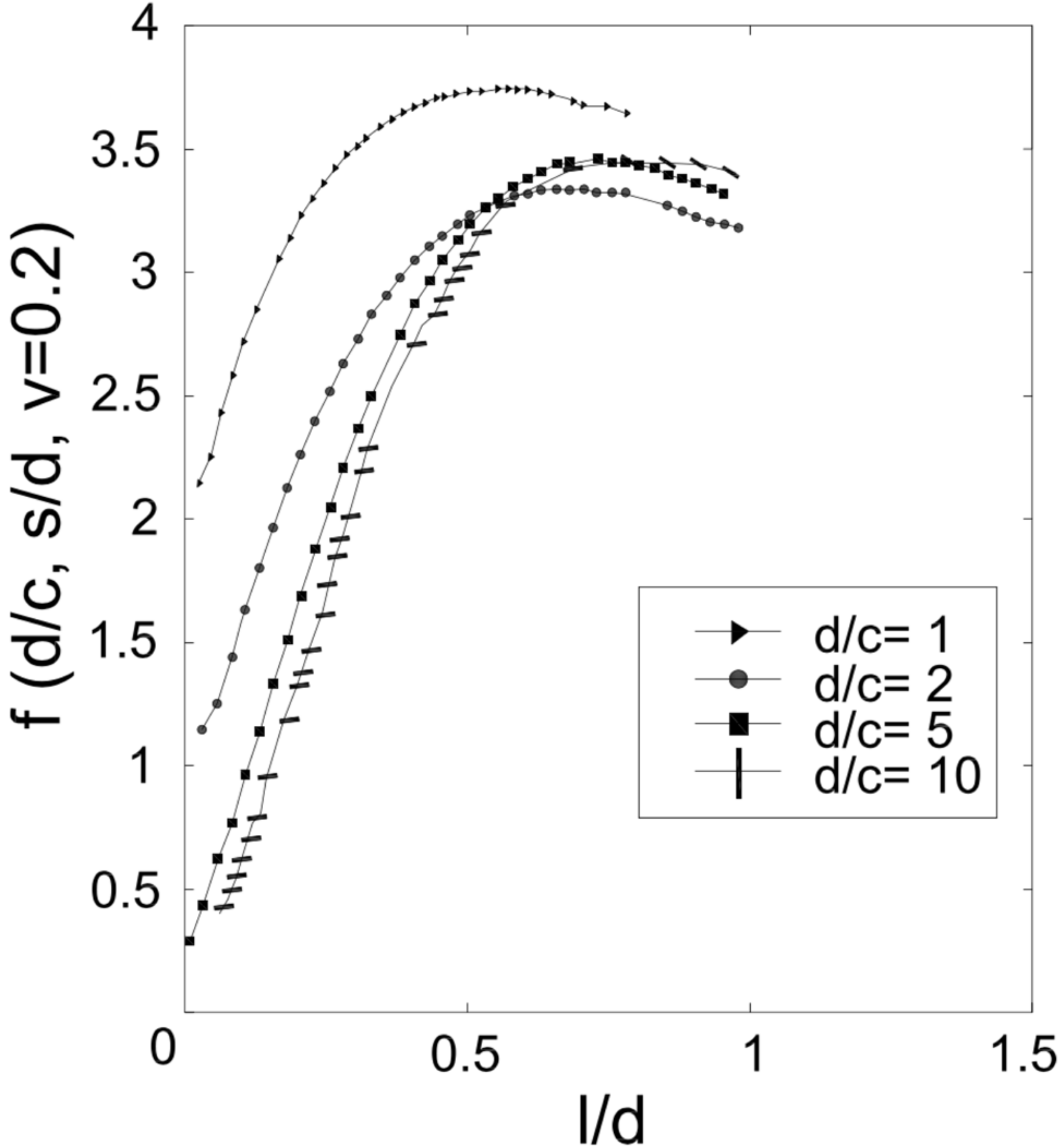

f (d/c, s/d, v=0.2)
l/d
d/c= 1
d/c= 2
d/c= 5
d/c= 10
0
0.5
1
1.5
2
2.5
3
3.5
4

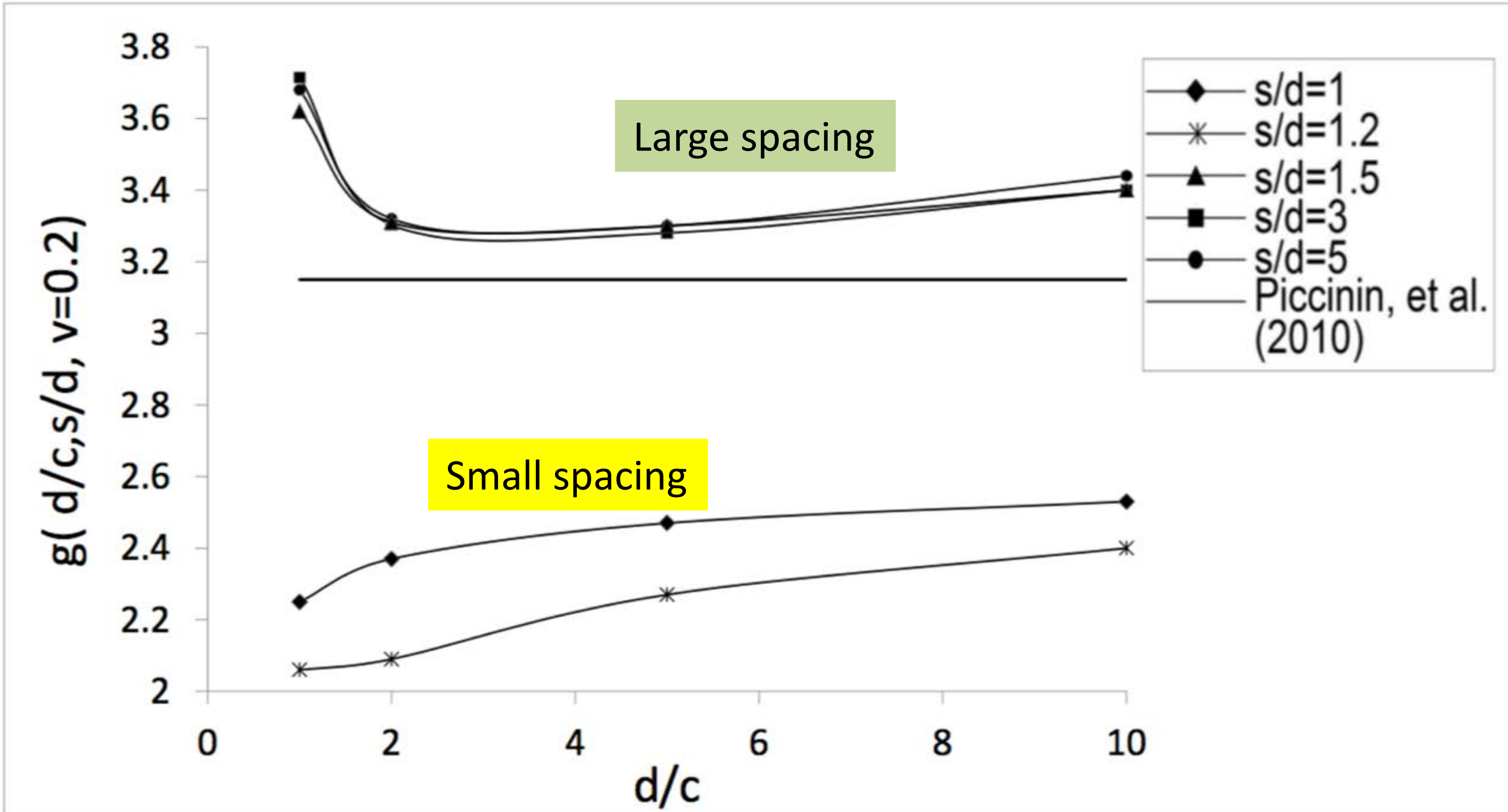

Large spacing
Small spacing
g(d/c,s/d, v=0.2)
d/c
3.8
3.6
3.4
3.2
3
2.8
2.6
2.4
2.2
2
0
2
4
6
8
10
s/d=1
s/d=1.2
s/d=1.5
s/d=3
s/d=5
Piccinin, et al. (2010)

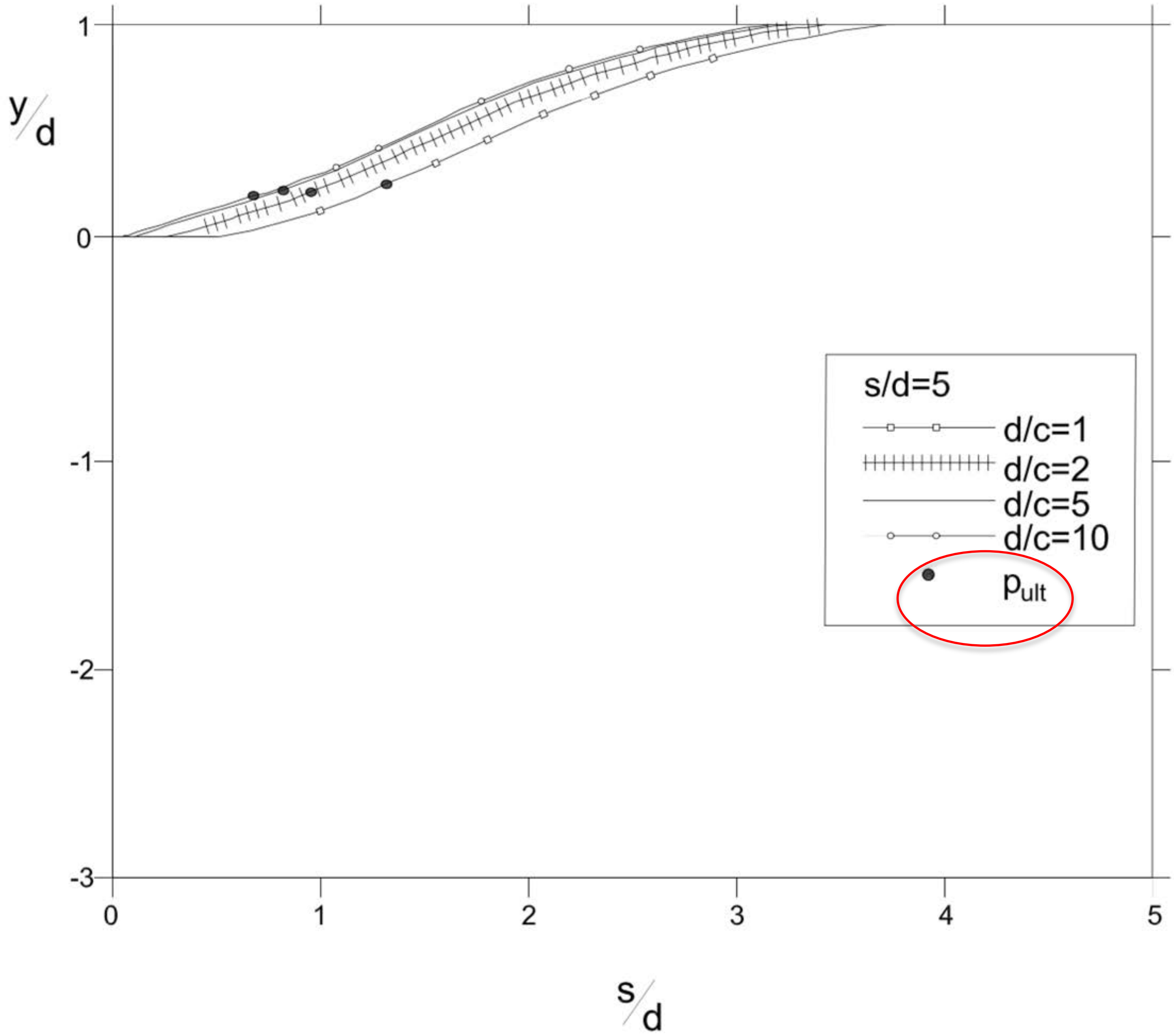

y/d
1
0
-1
-2
-3
0
1
2
3
4
5
s/d
s/d=5
d/c=1
d/c=2
d/c=5
d/c=10
p_ult

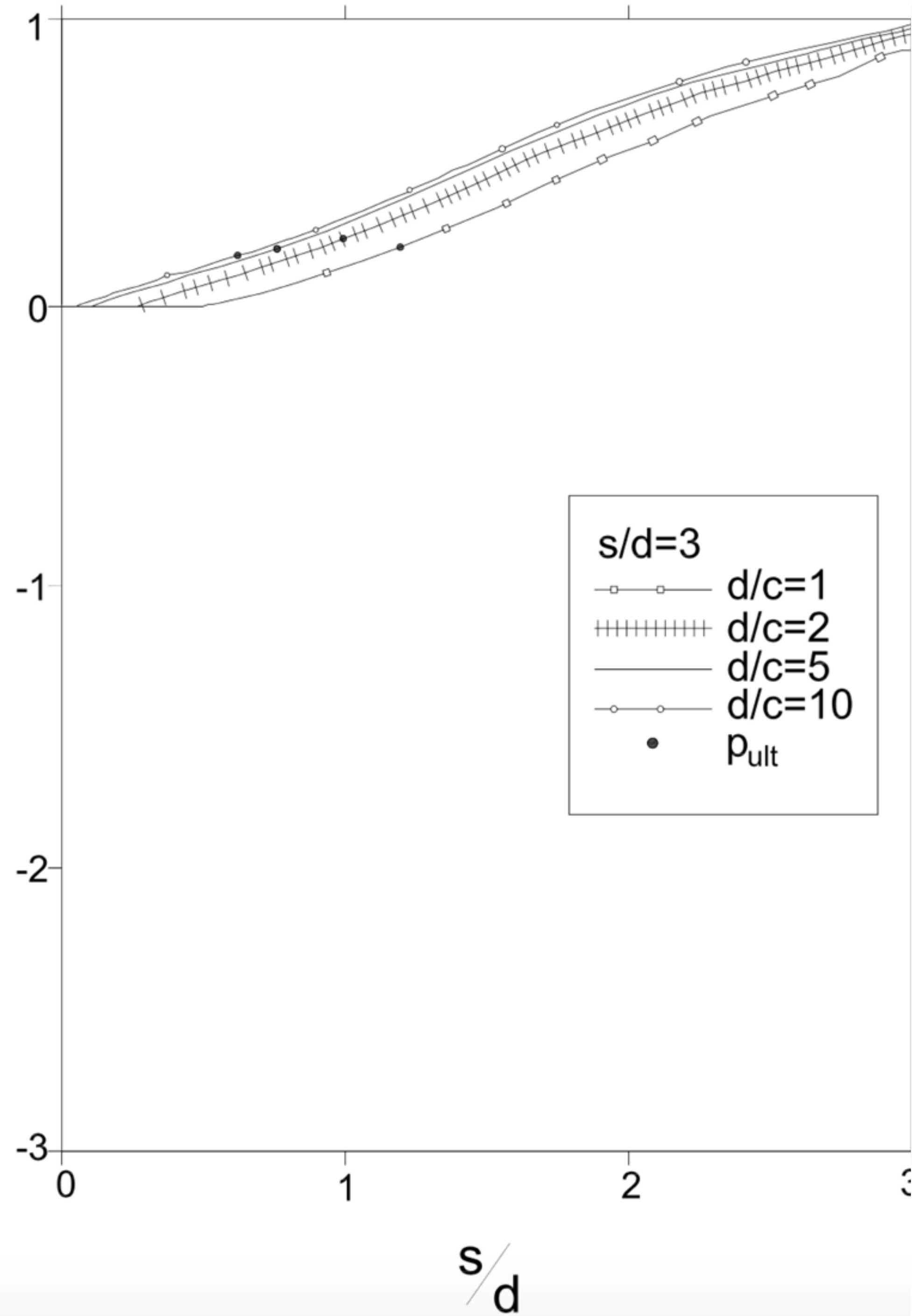

s/d=3
d/c=1
d/c=2
d/c=5
d/c=10
p_{ult}
s/d
1
0
-1
-2
-3
0
1
2

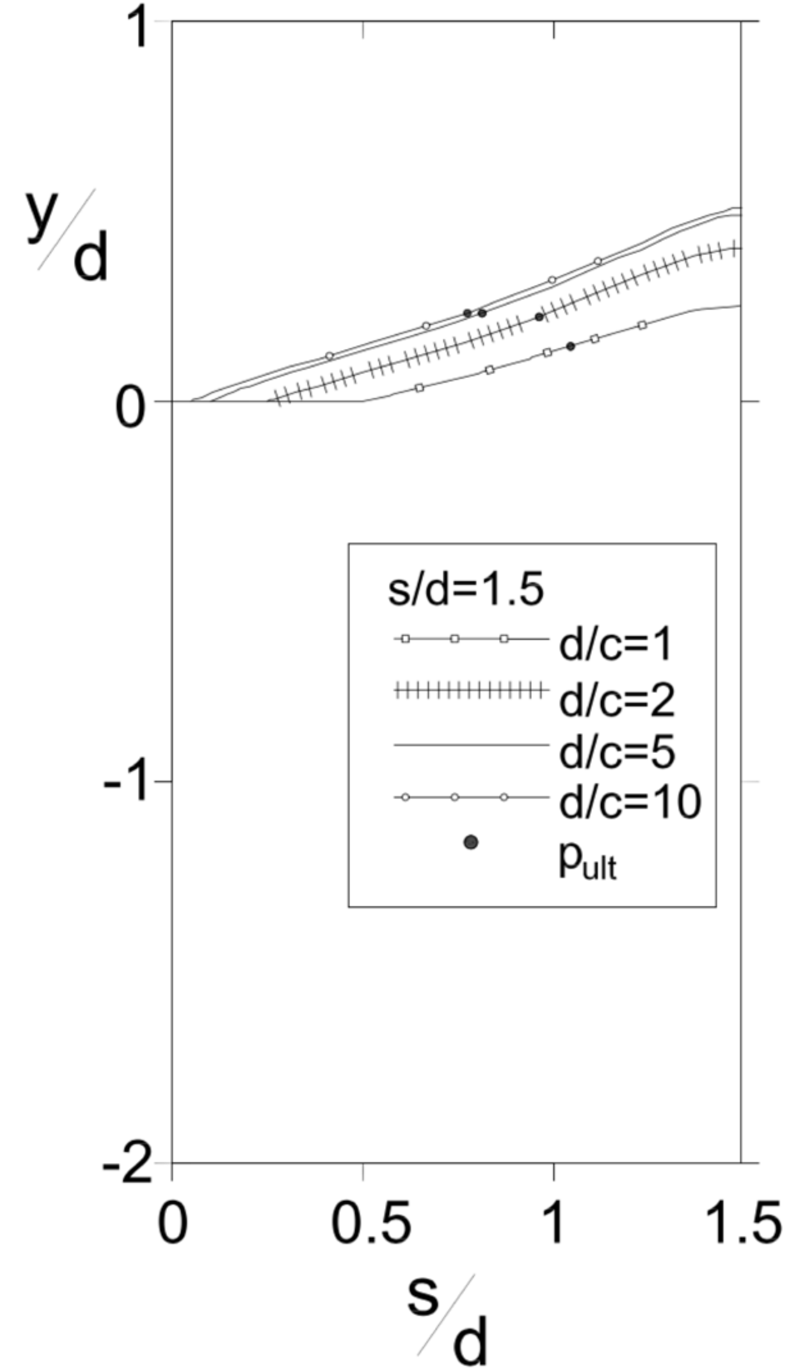

y/d
s/d=1.5
d/c=1
d/c=2
d/c=5
d/c=10
p_{ult}
s/d
1
0
-1
-2
0
0.5
1
1.5

$$A_{Nc} = \left[\left(\sqrt{N} - 1\right)s + 3h_{ef}\right]^2$$

$$\frac{P_{ult,N}}{NP_{ult,o}} = \frac{\left[\left(\sqrt{N} - 1\right)\frac{s}{3h_{ef}} + 1\right]^2}{N}$$

setting $N = \infty$

$$\frac{P_{ult,N=\infty}}{NP_{ult,o}} = \left(\frac{s}{3d}\right)^2$$

s/d=5,3,1.5,1.2,1.0 the capacity ratios are 1.0, 1.0, 0.25, 0.16 and 0.11, respectively (for $s/d=5$ and s/d=1 the Code considers the anchors as non-interacting). The 75-90% range of the reduction prescribed by the Code is significantly larger than the ~20-30% reduction predicted by the simulations.

Suggestion

With the advent of powerful and sophisticated computational approaches to fracture simulation, derive capacity formulas through simulation.

Background

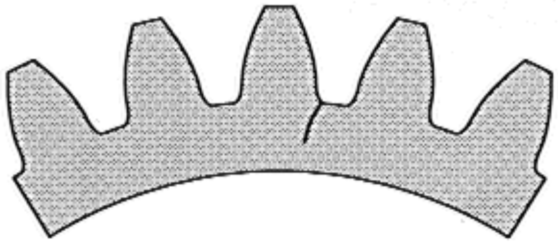

Thin rim -
catastrophic rim fracture

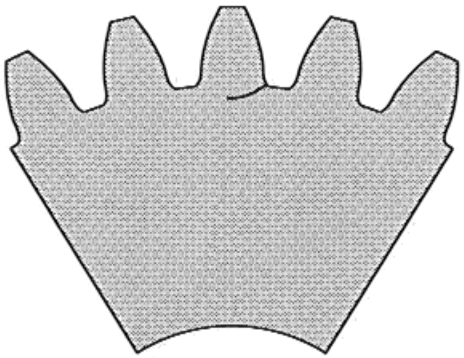

Thick rim -
"benign" tooth fracture

- Thin-rim gears desired for reduced weight.
- Stress fields and failure characteristics significantly different for thin-rim gears compared to conventional gears.
- Catastrophic failures have occurred in thin-rim gears.
- Safety and reliability can not be sacrificed.

Definition of Backup Ratio (m_B)

$$m_B = \frac{b}{h}$$

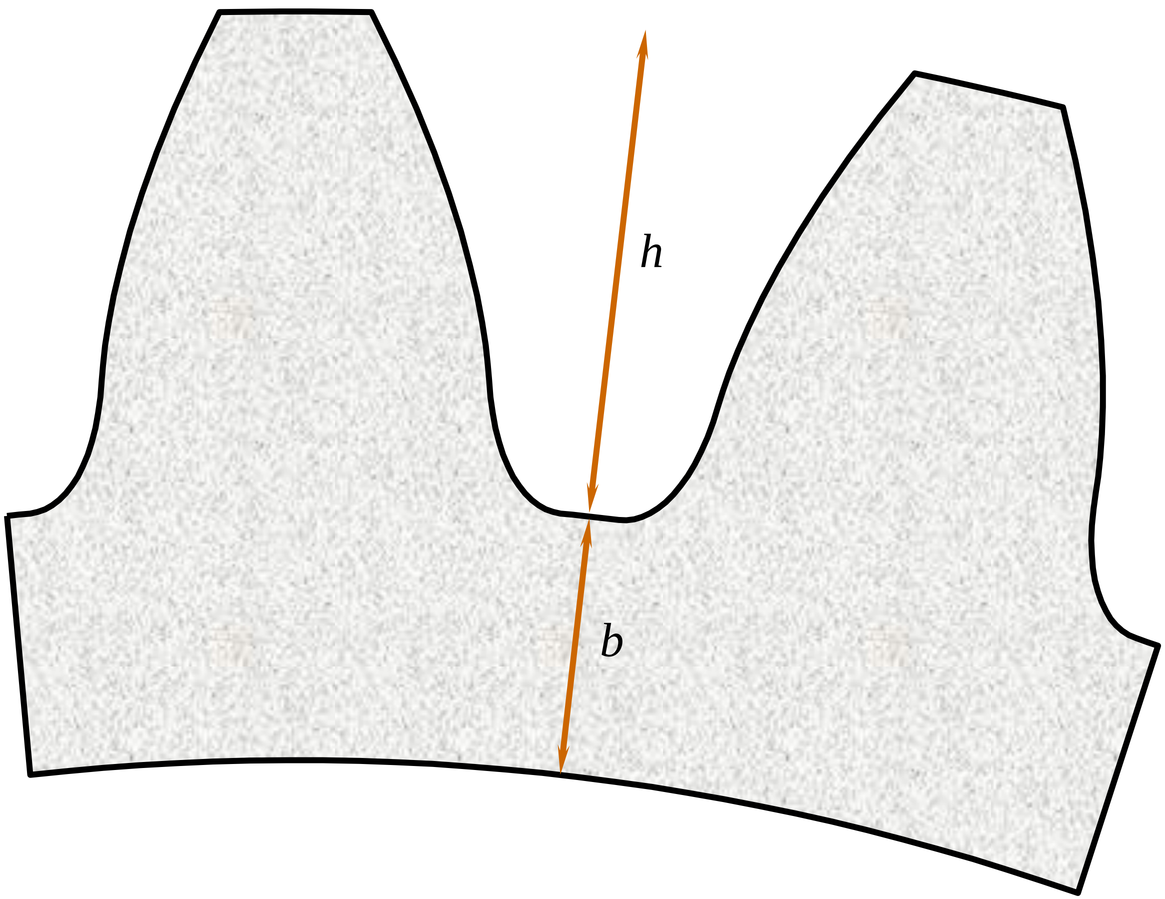

Bending stress index

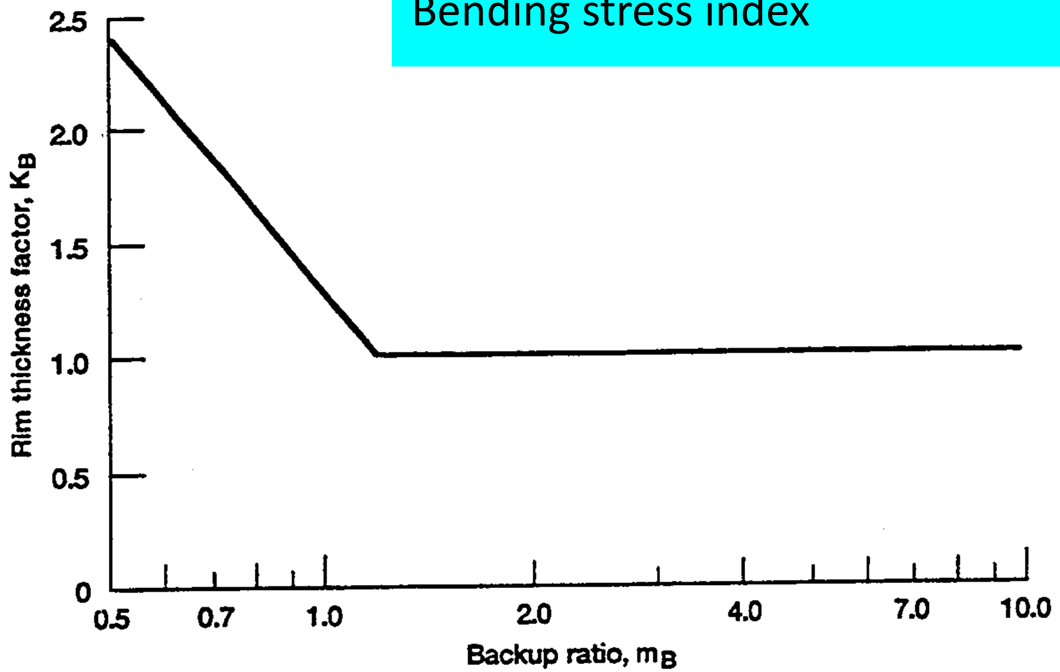

Figure 1.2.1.—Gear tooth bending stress index rim thickness correction factor (AGMA, 1990).

Objectives

Develop design guidelines to prevent rim fracture failure modes in gear tooth bending fatigue.

Crack Modeling Using Finite Element Method

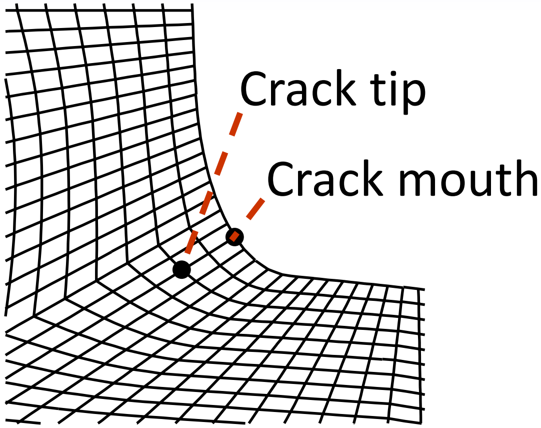

User-defined initial crack

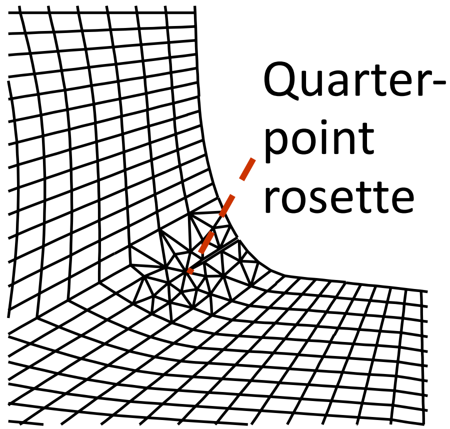

Final mesh of initial crack

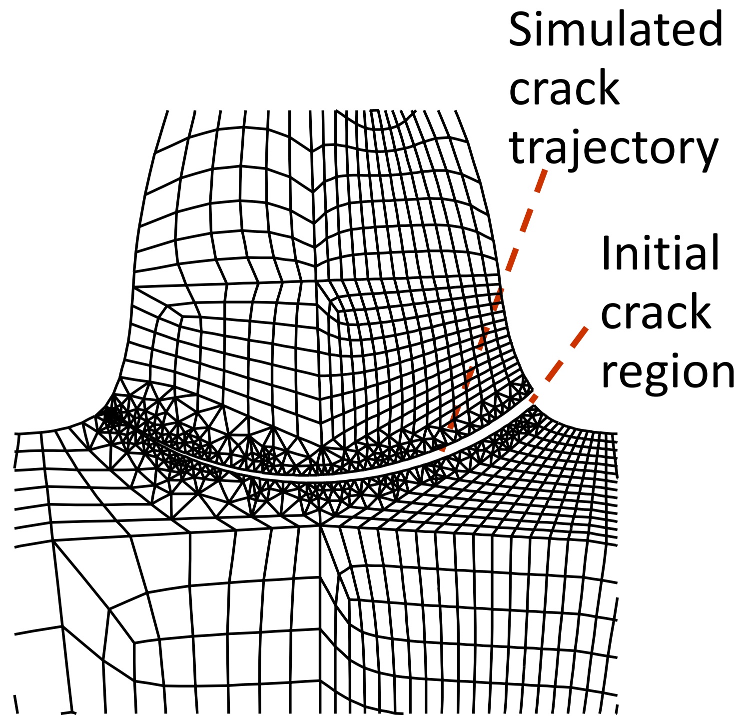

Predicted crack path

Crack Propagation Angle and Growth Rate

$$\theta_m = 2\tan^{-1}\left[\frac{\frac{K_I}{K_{II}} \pm \sqrt{\left(\frac{K_I}{K_{II}}\right)^2 + 8}}{4}\right]$$

3 Paris equation, $n = 2.264$, $C = 1.149\times10^{-15}$ in./cyc/(psi$\sqrt{\text{in.}}$)^n (Au and Ke, 1981)
4 Paris equation, $n = 2.954$, $C = 6.027\times10^{-19}$ in./cyc/(psi$\sqrt{\text{in.}}$)^n (Au and Ke, 1981)
5 Paris equation, $n = 2.555$, $C = 2.721\times10^{-17}$ in./cyc/(psi$\sqrt{\text{in.}}$)^n (Au and Ke, 1981)
6 Paris equation, $n = 2.420$, $C = 1.084\times10^{-16}$ in./cyc/(psi$\sqrt{\text{in.}}$)^n (Au and Ke, 1981)
10 Collipriest equation, $n = 1.63$, $C = 8.36\times10^{-9}$ in./cyc/(ksi$\sqrt{\text{in.}}$)^n, $\Delta K_{th} = 3.5$ ksi$\sqrt{\text{in.}}$, $K_{IC} = 200$ ksi$\sqrt{\text{in.}}$, $R = 0$ (Forman and Hu, 1984)

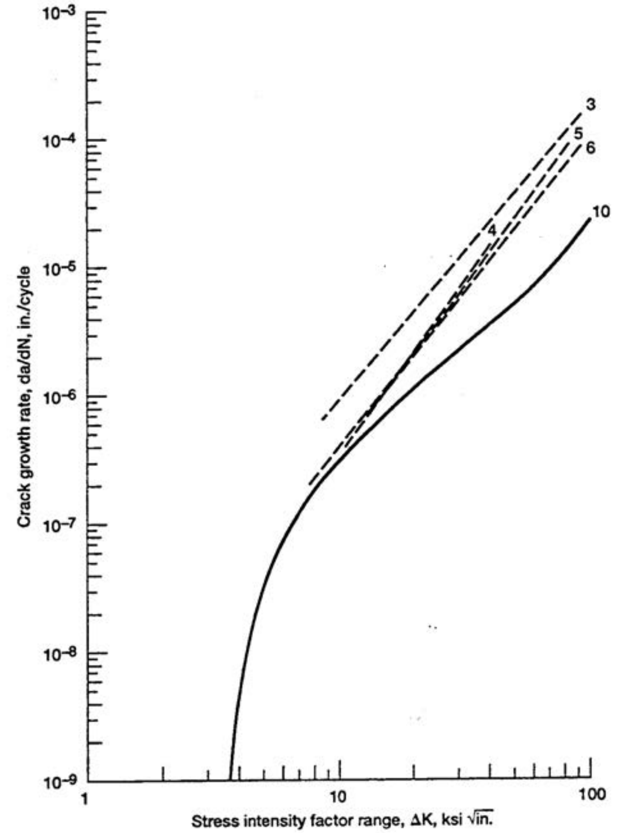

Figure 3.7.3.—Comparison of fatigue crack growth rates using Paris equation and Collipriest equation for AISI 9310 steel.

Analysis Procedure

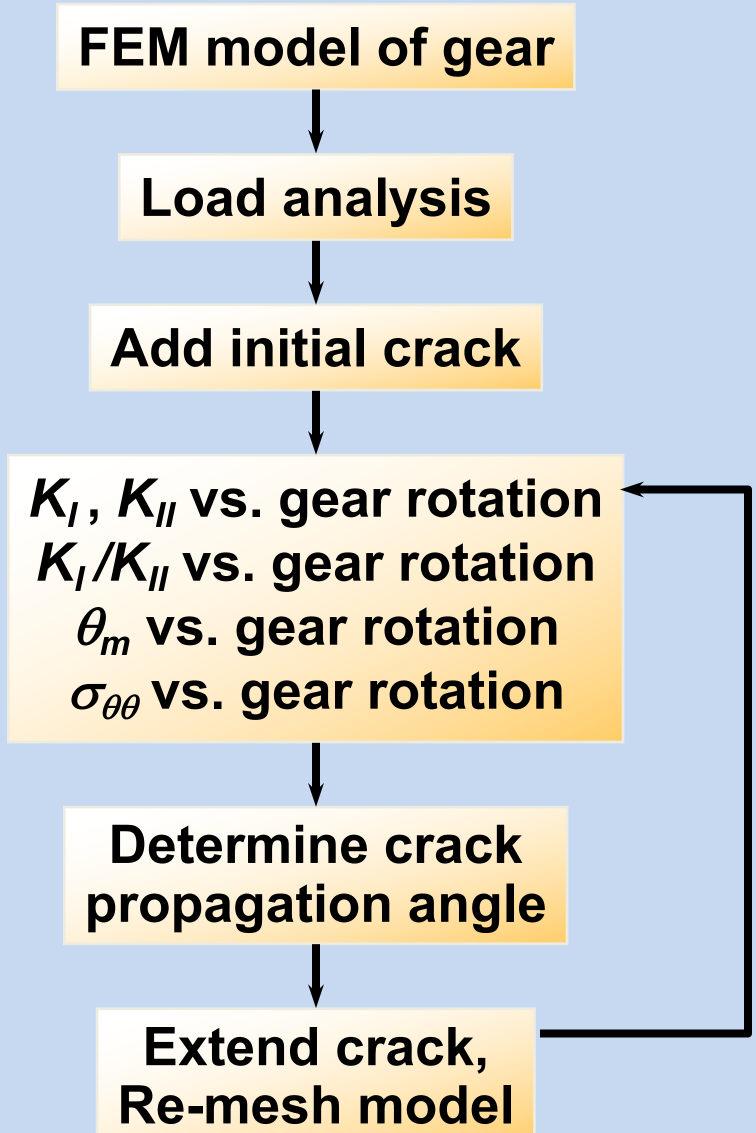

Typical Finite Element Gear Model

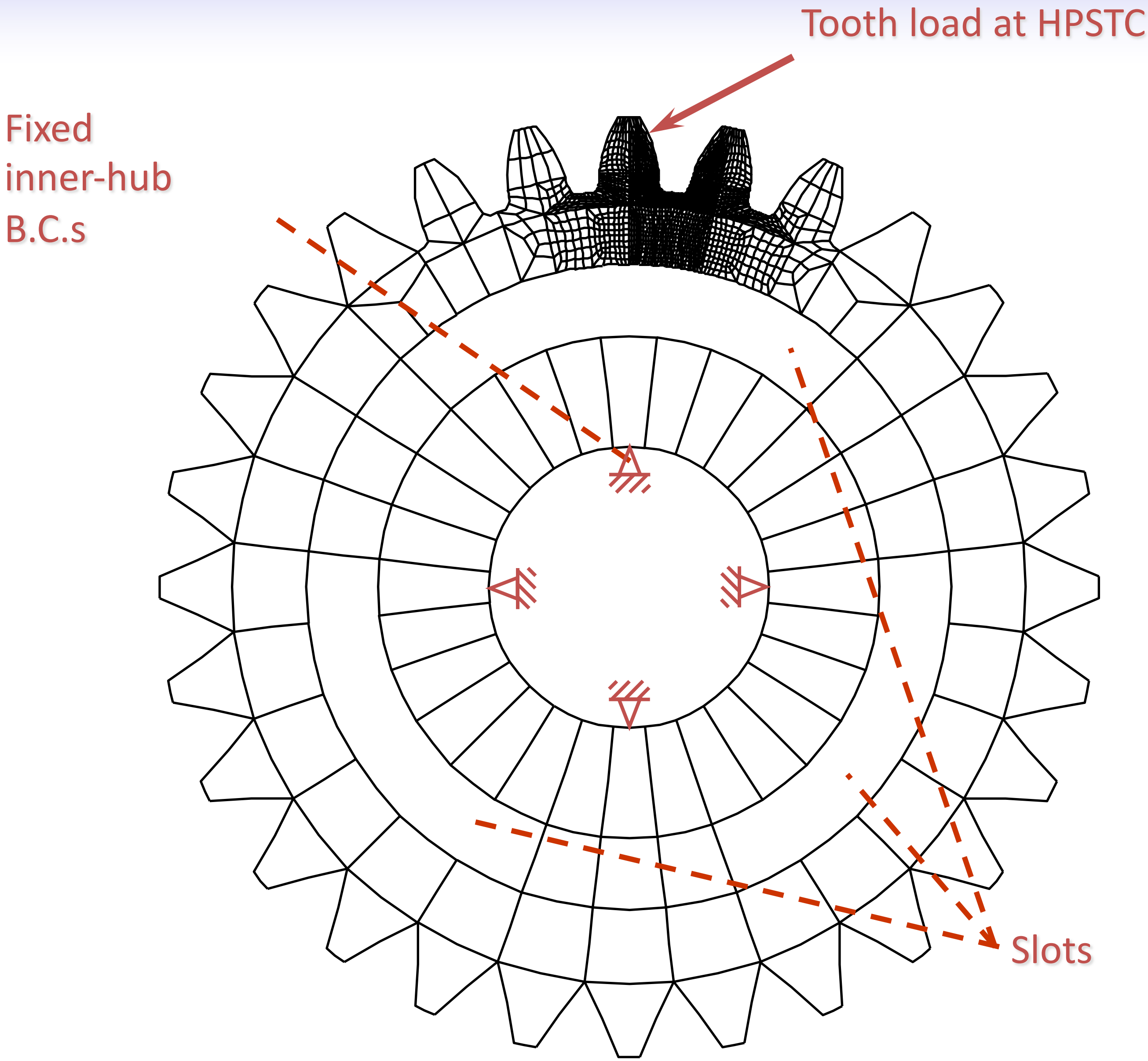

Load Case Locations for FEM

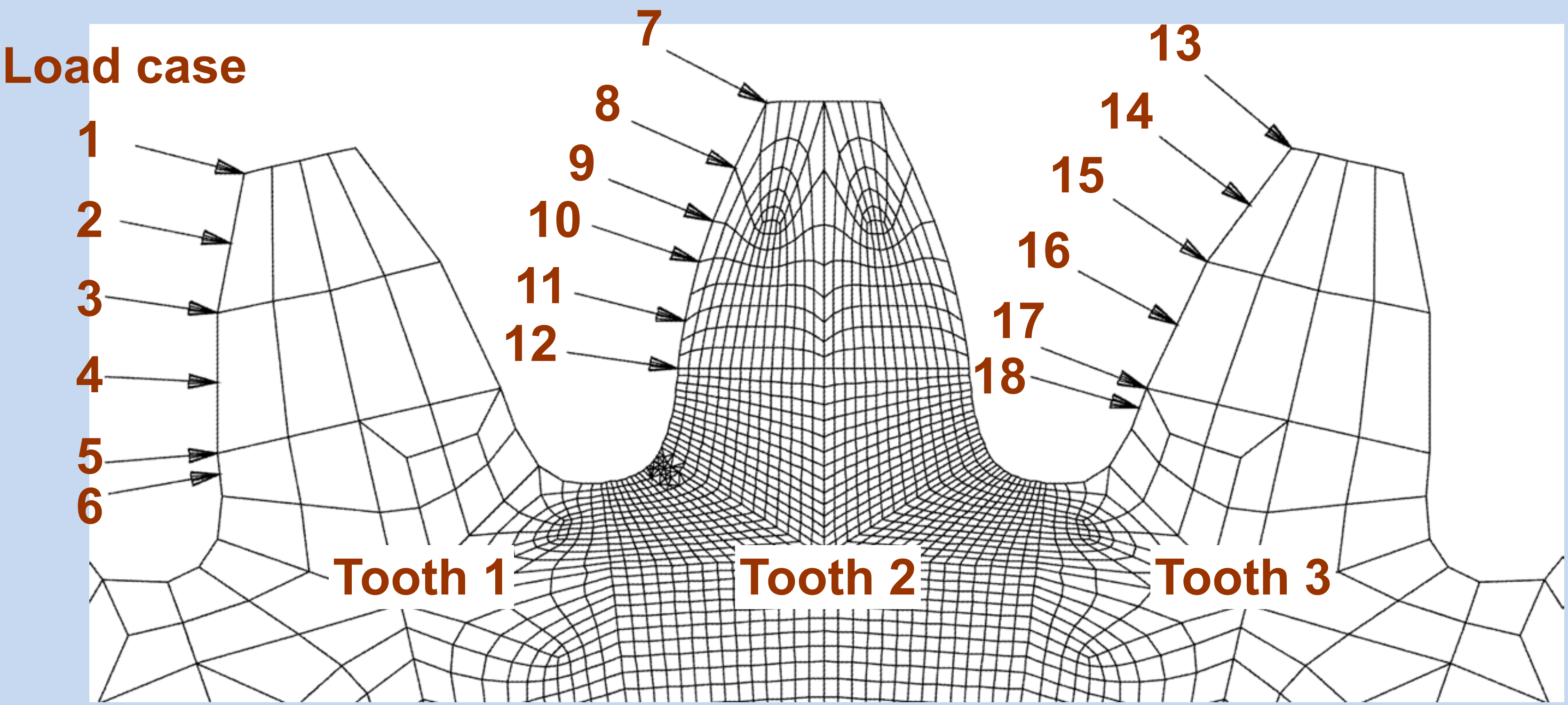

0.26-mm crack size, 68 N-m driver gear torque.

Test Gears

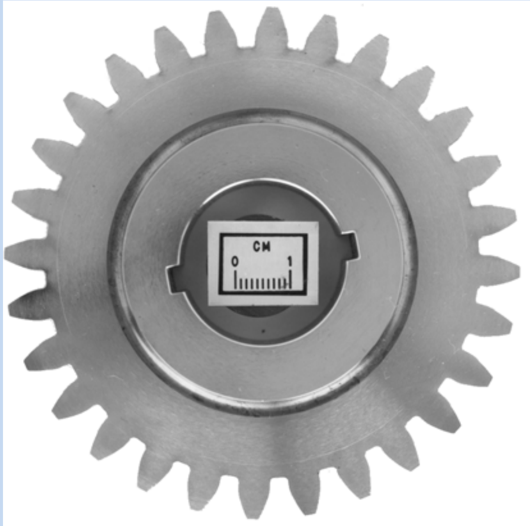

Backup ratio = 3.3

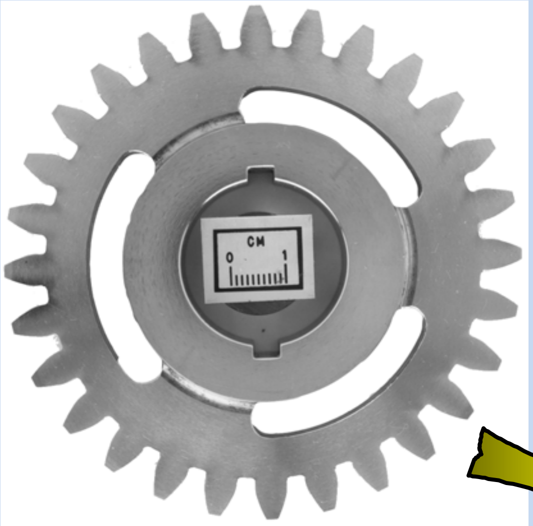

Backup ratio = 1.0

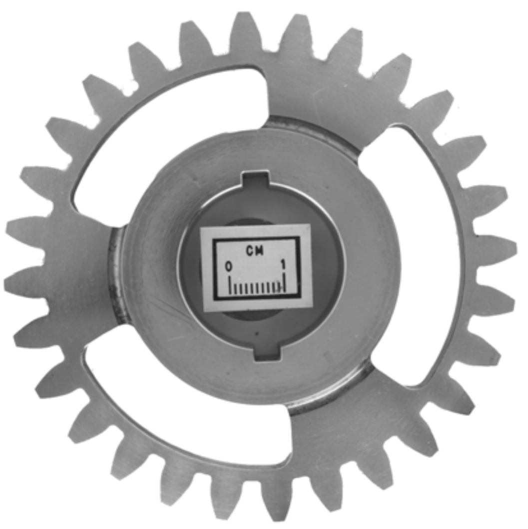

Backup ratio = 0.3

Notch inserted in tooth fillet

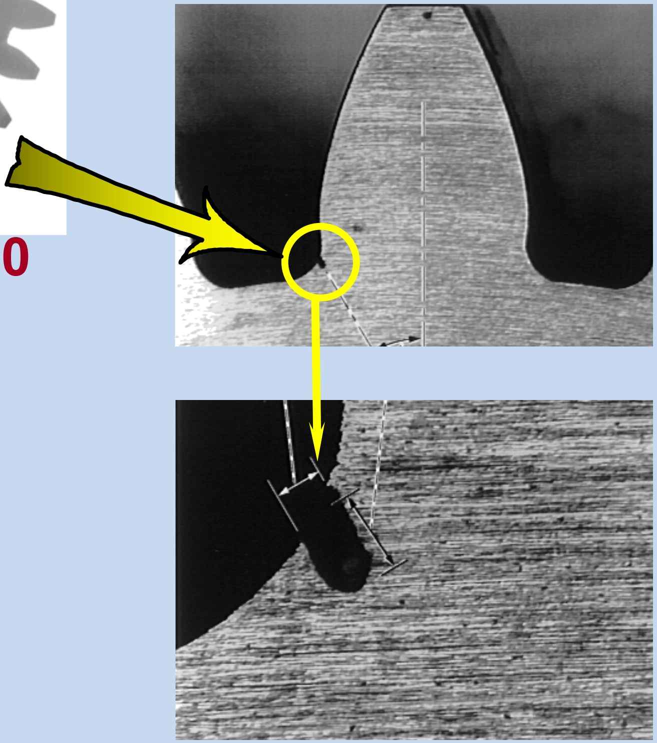

Definition of Backup Ratio (m_B)

$$m_B = \frac{b}{h}$$

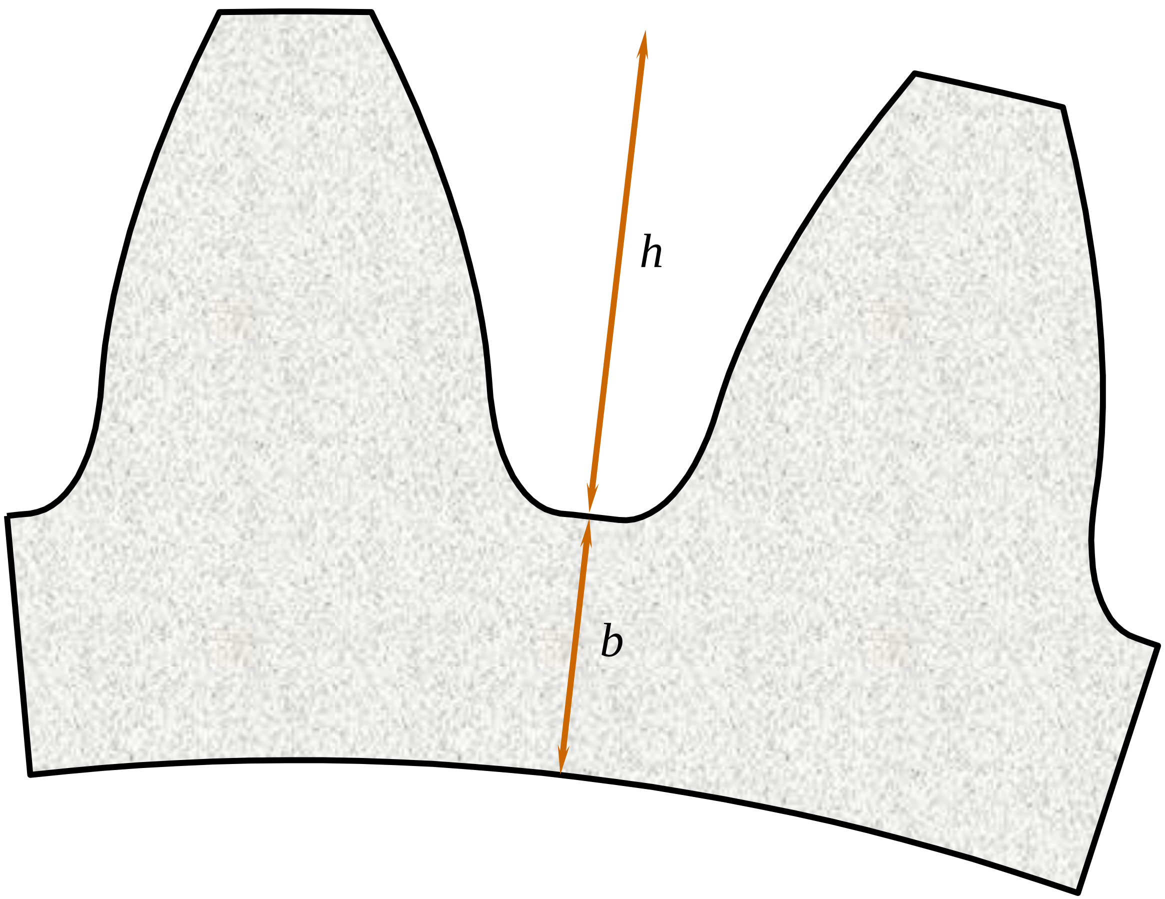

Definition of Initial Crack Location (θ_0)

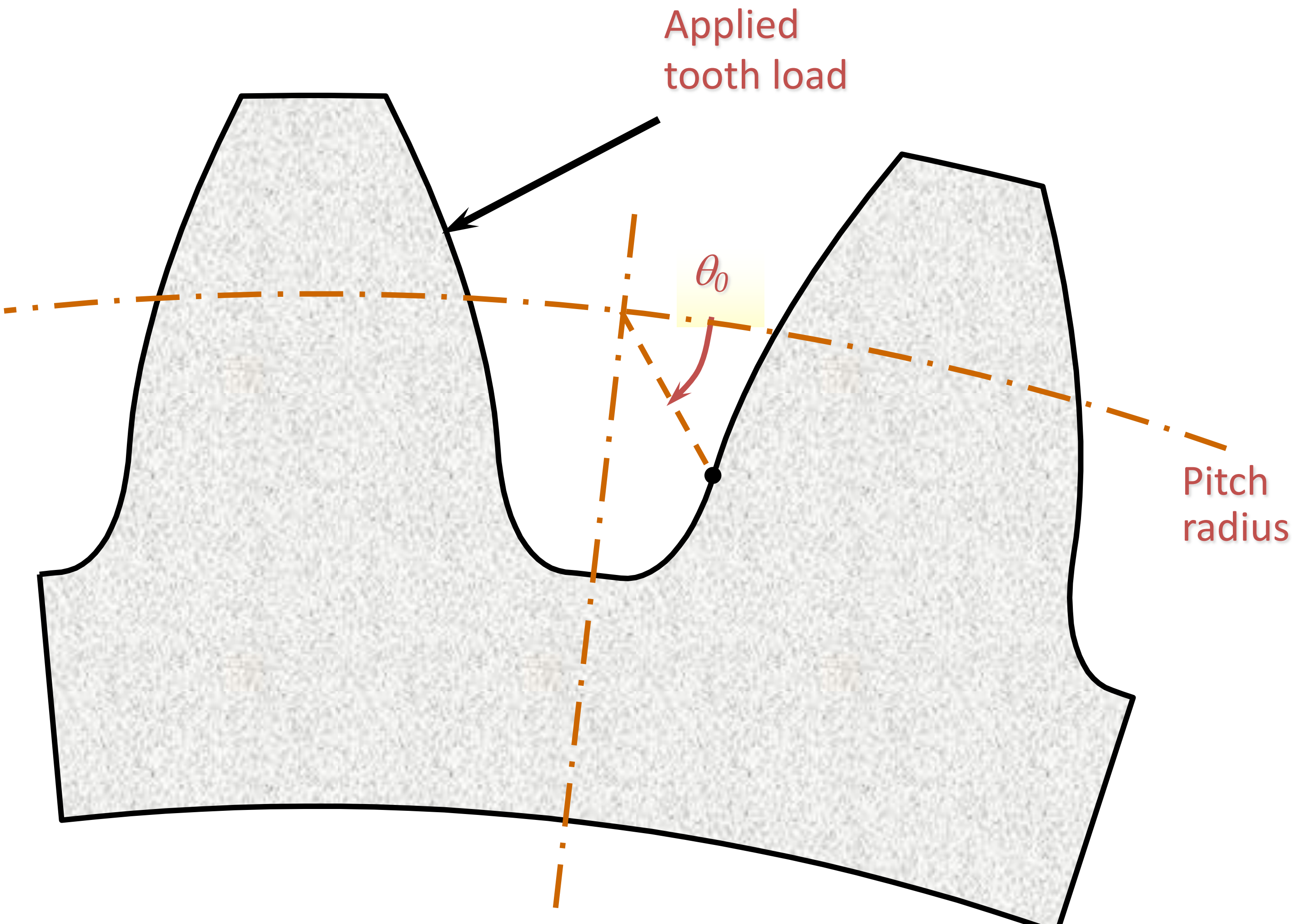

Effect of Initial Crack Location on Crack Path

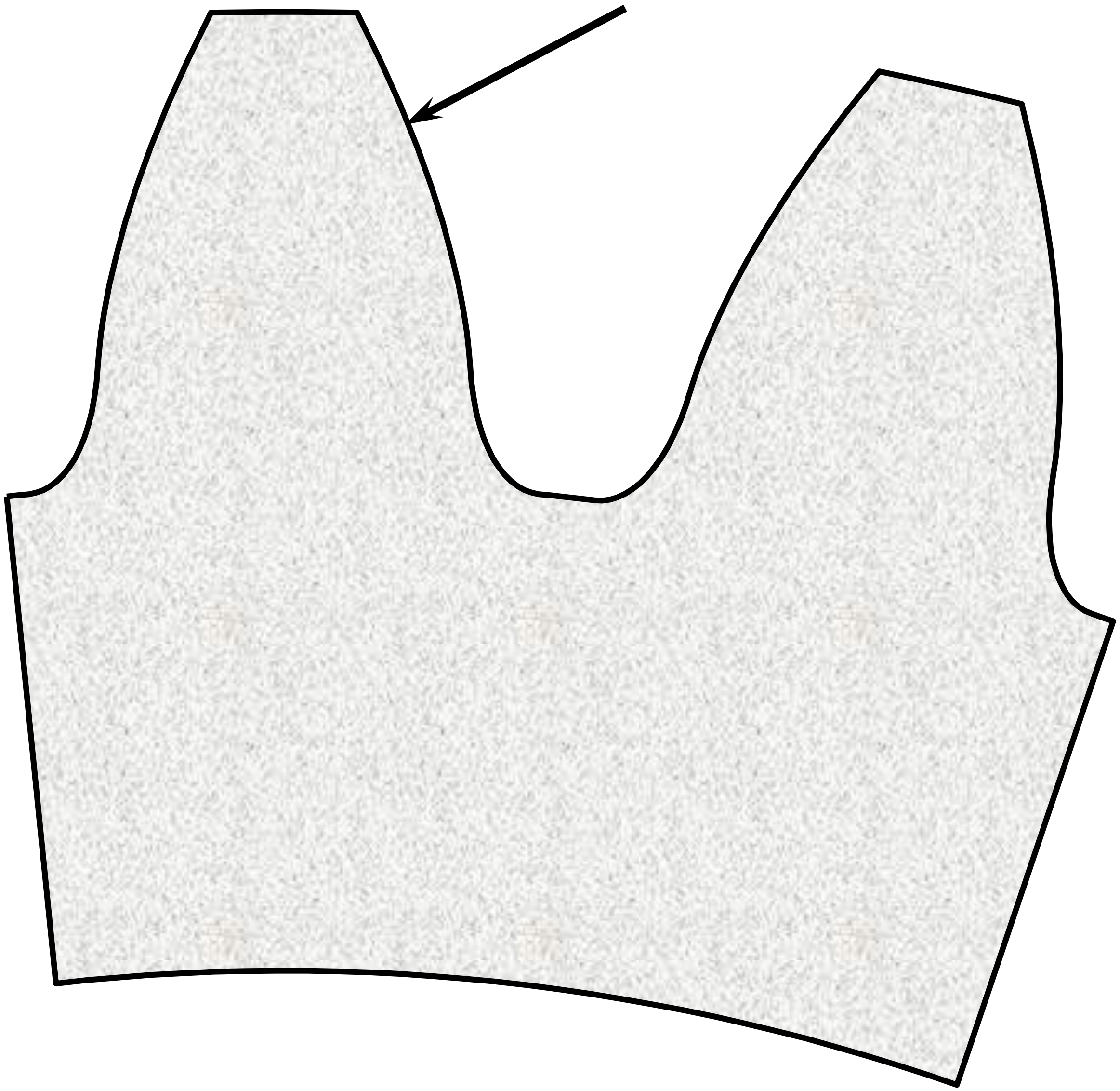

Gear Parameters:

- 28 teeth
- 8 pitch
- 1.75" pitch rad
- 20° press angle
- m_B = 1.0

Effect of Initial Crack Location on Crack Path

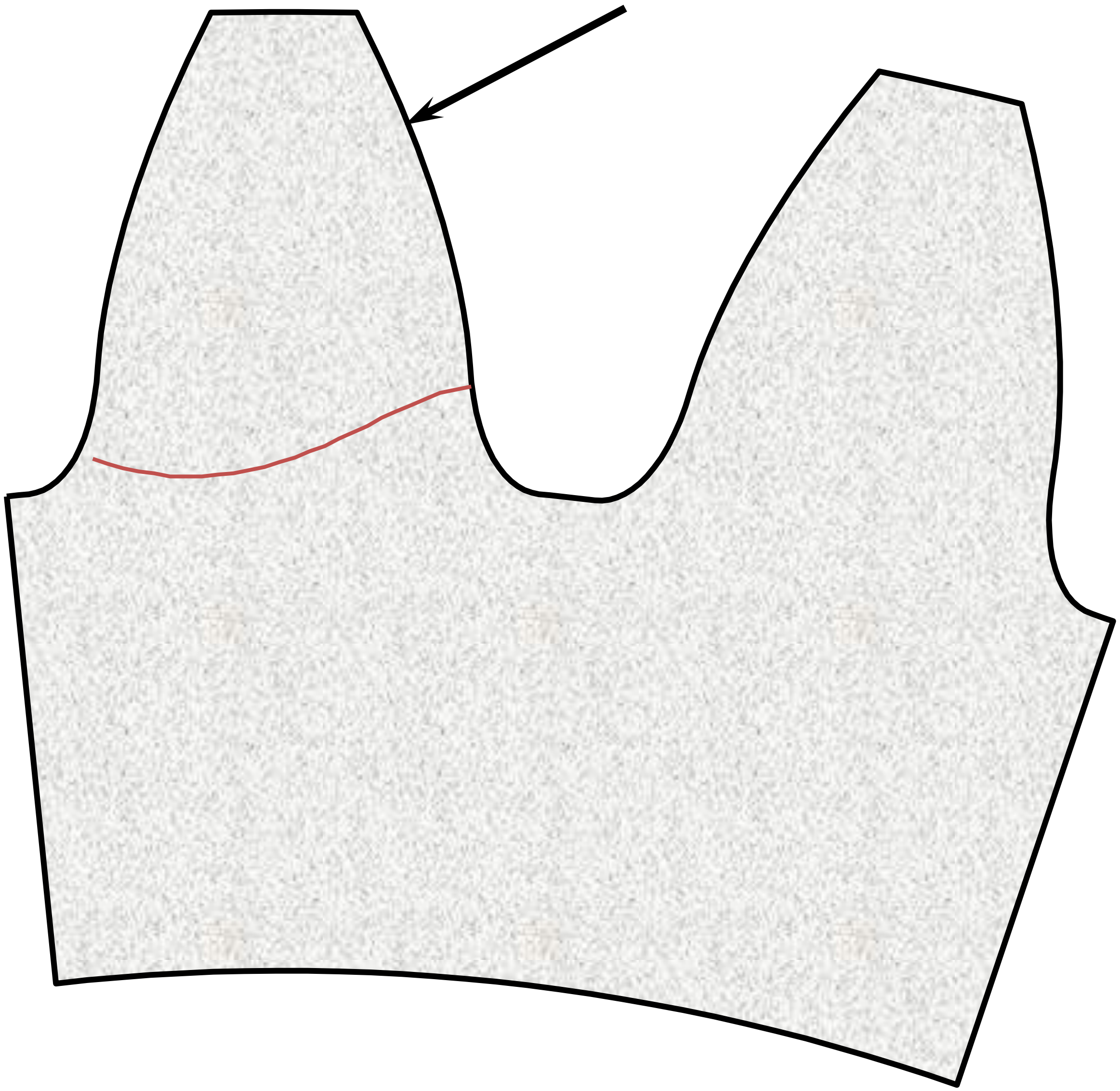

Initial crack location:
$\theta_0 = 120^\circ$

Failure mode:
Tooth fracture

Effect of Initial Crack Location on Crack Path

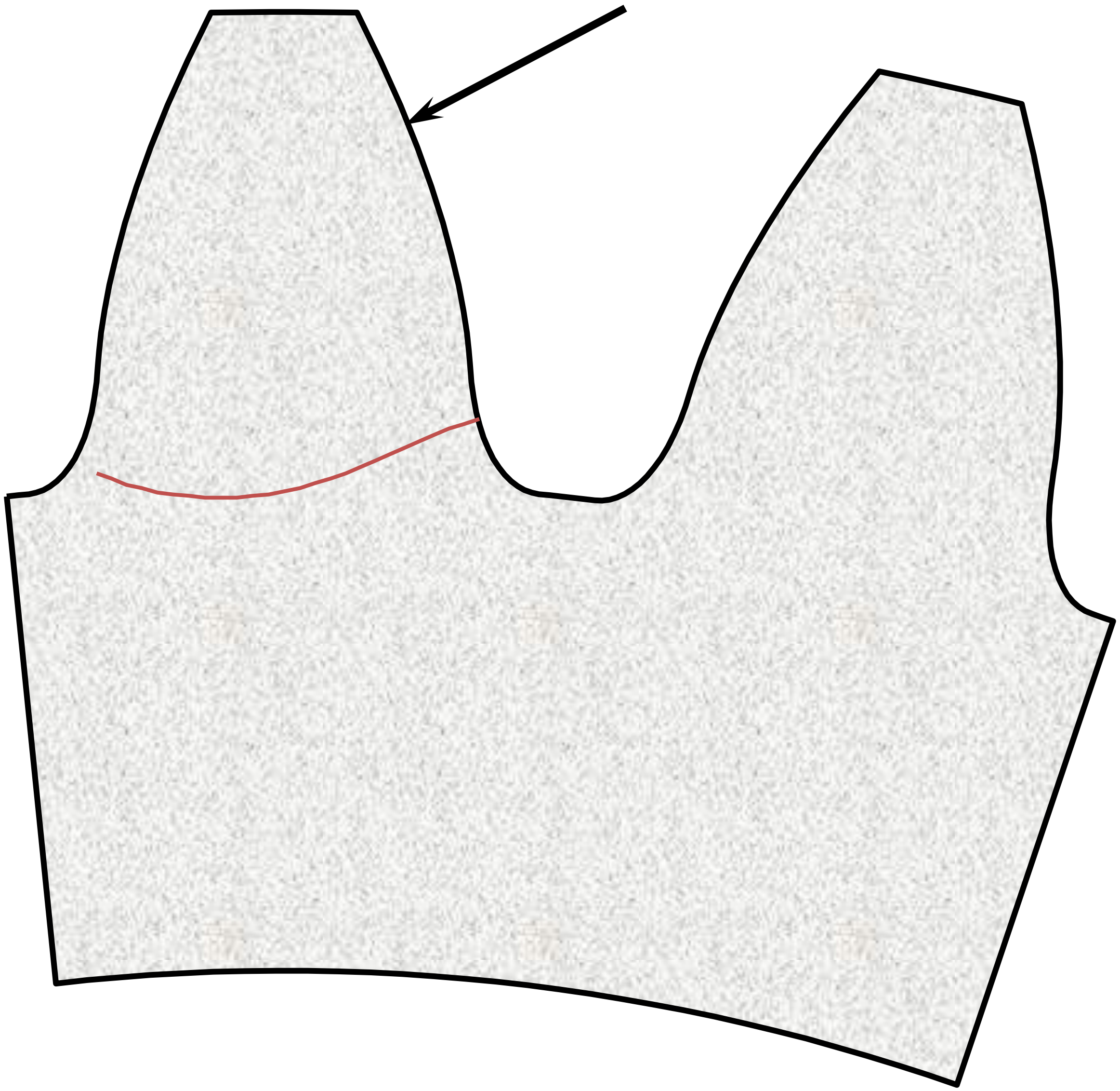

Initial crack location:
θ_0 = 114°

Failure mode:
Tooth fracture

Effect of Initial Crack Location on Crack Path

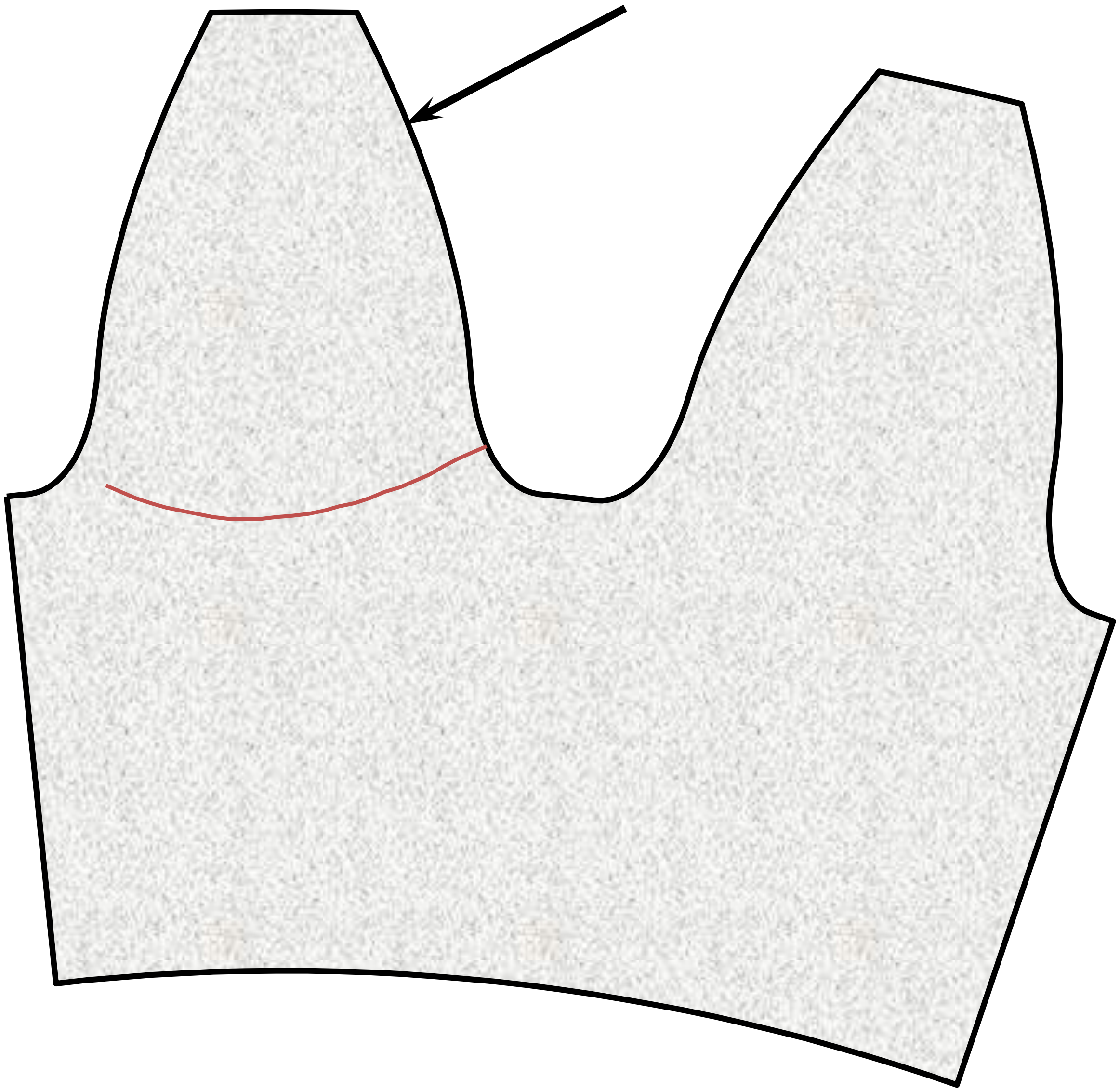

Initial crack location:
$\theta_0 = 109^\circ$

Failure mode:
Tooth fracture

Effect of Initial Crack Location on Crack Path

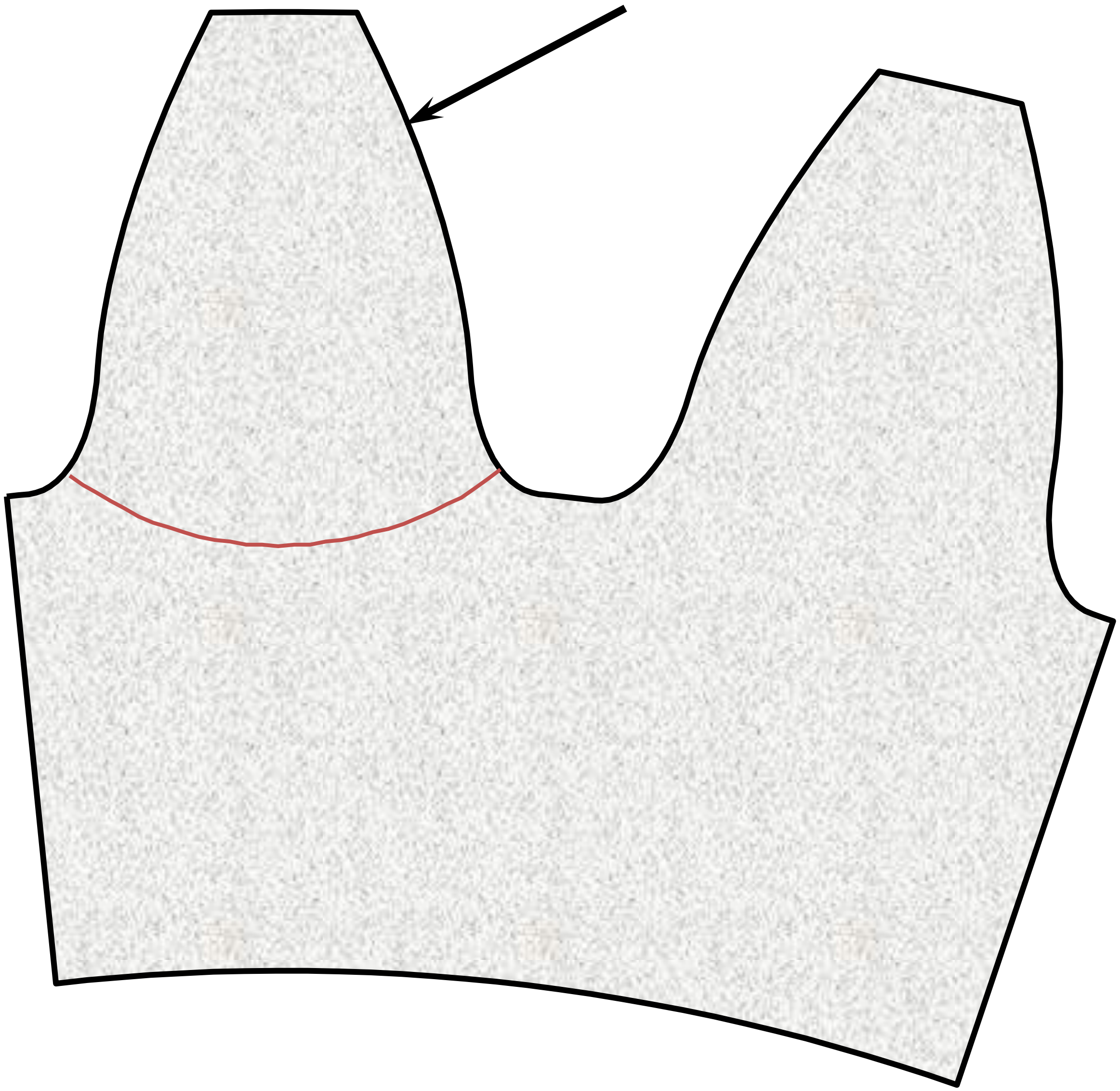

Initial crack location:
θ_0 = 104˚
(max tensile)

Failure mode:
Tooth fracture

Effect of Initial Crack Location on Crack Path

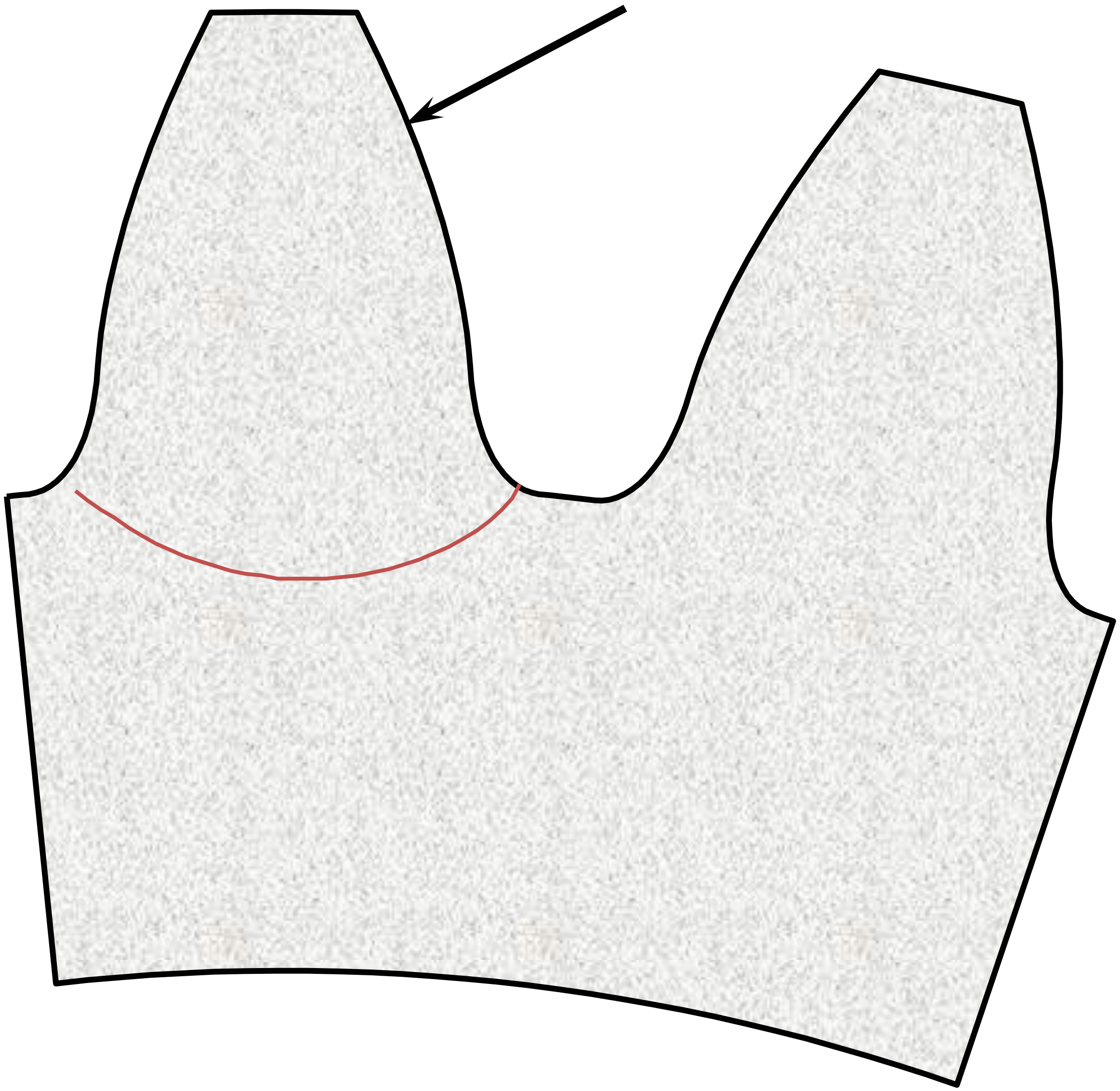

Initial crack location:
θ_0 = 99°

Failure mode:
Tooth fracture

Effect of Initial Crack Location on Crack Path

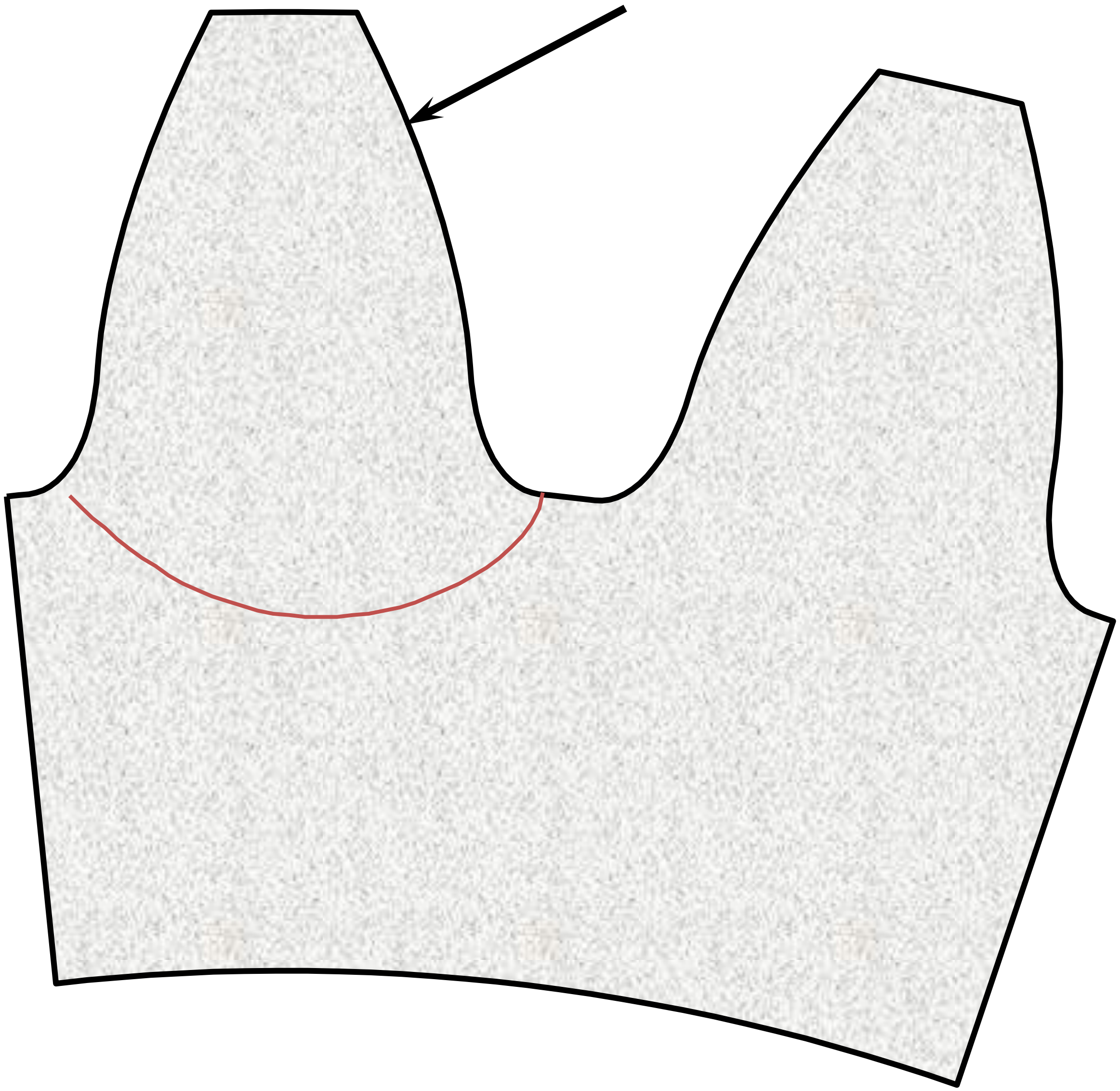

Initial crack location:
θ_0 = 94°

Failure mode:
Tooth fracture

Effect of Initial Crack Location on Crack Path

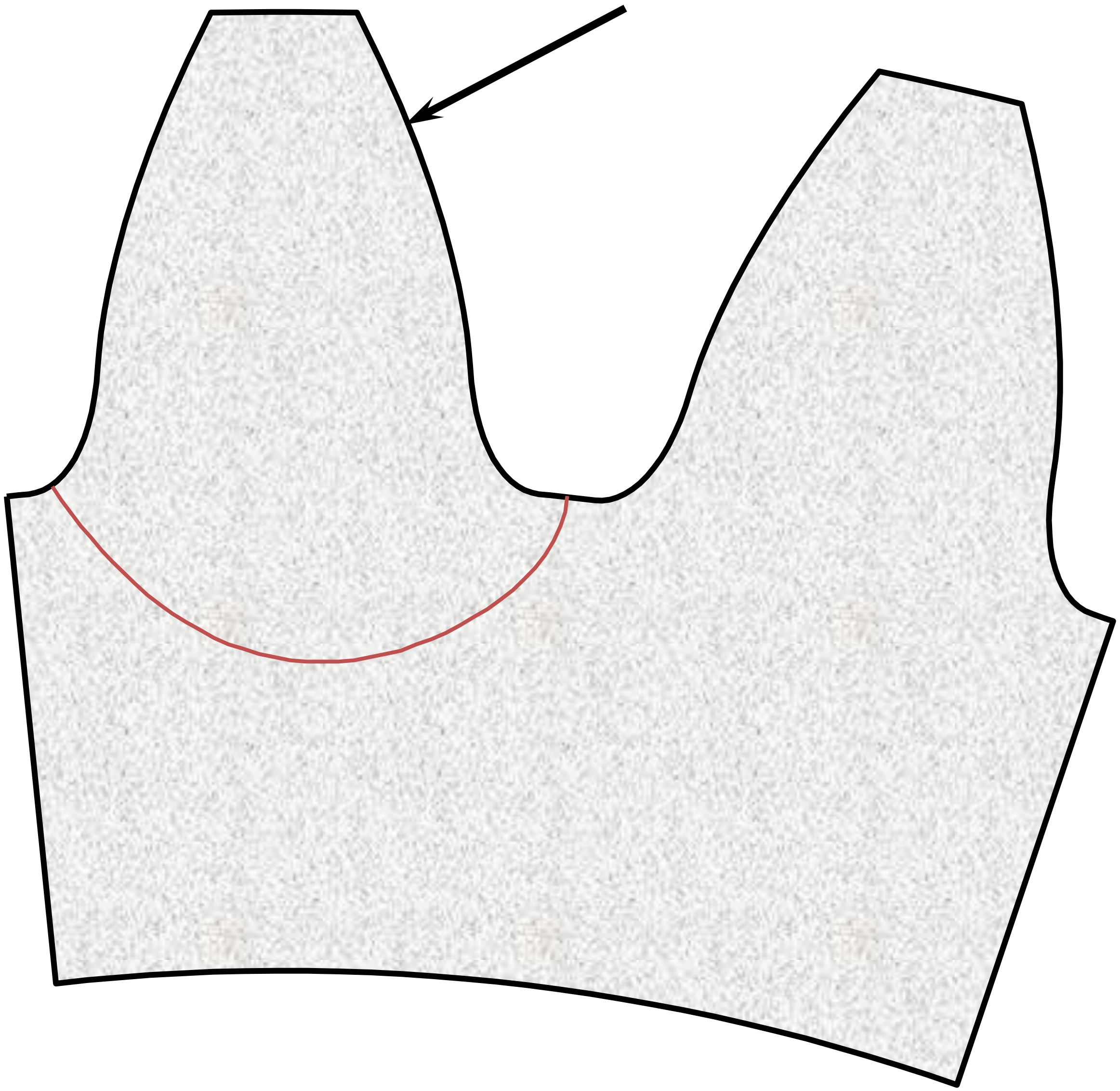

Initial crack location:
θ_0 = 88°
(root centerline)

Failure mode:
Tooth fracture

Effect of Initial Crack Location on Crack Path

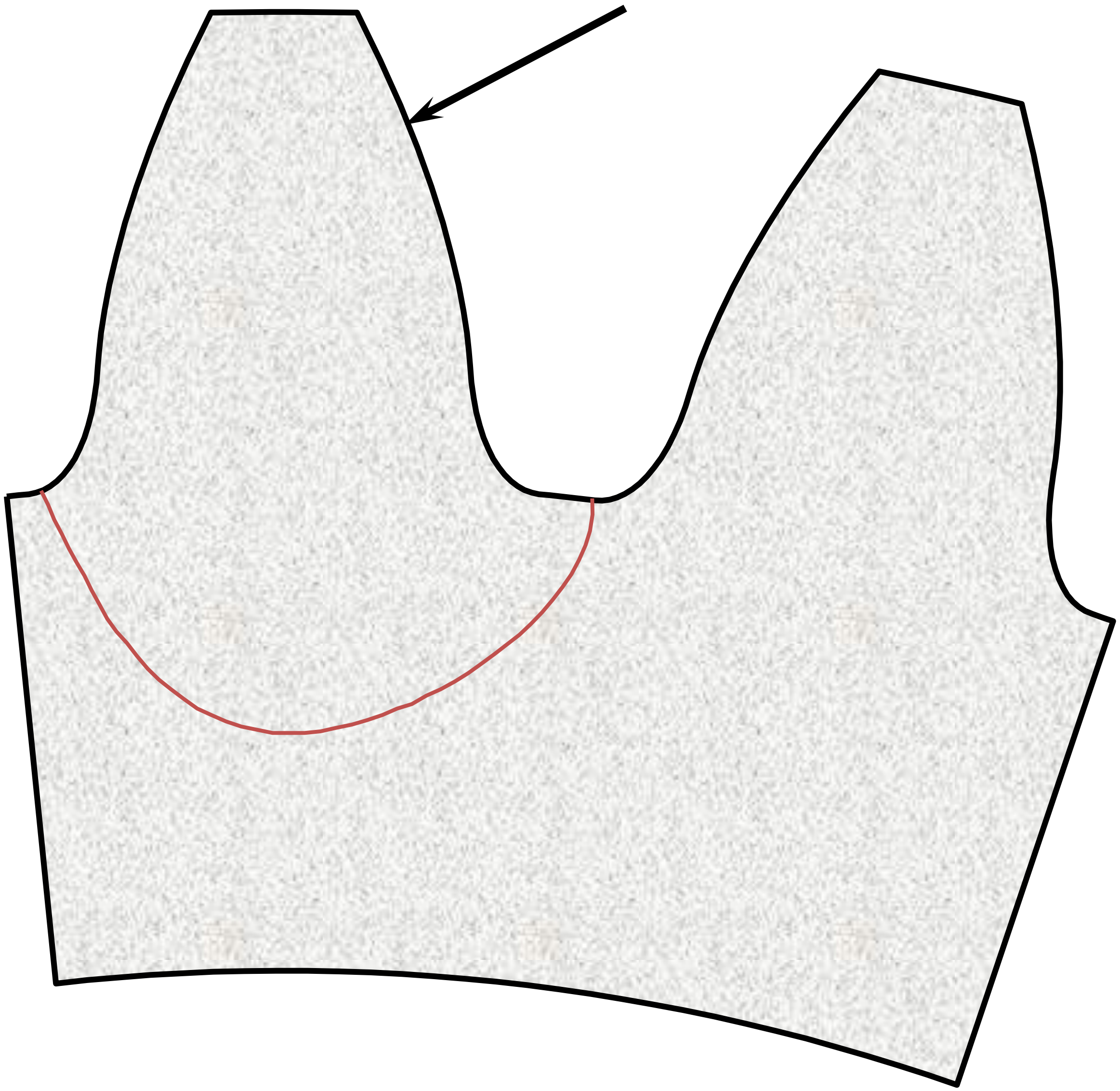

Initial crack location:
$\theta_0 = 83°$

Failure mode:
Tooth fracture

Effect of Initial Crack Location on Crack Path

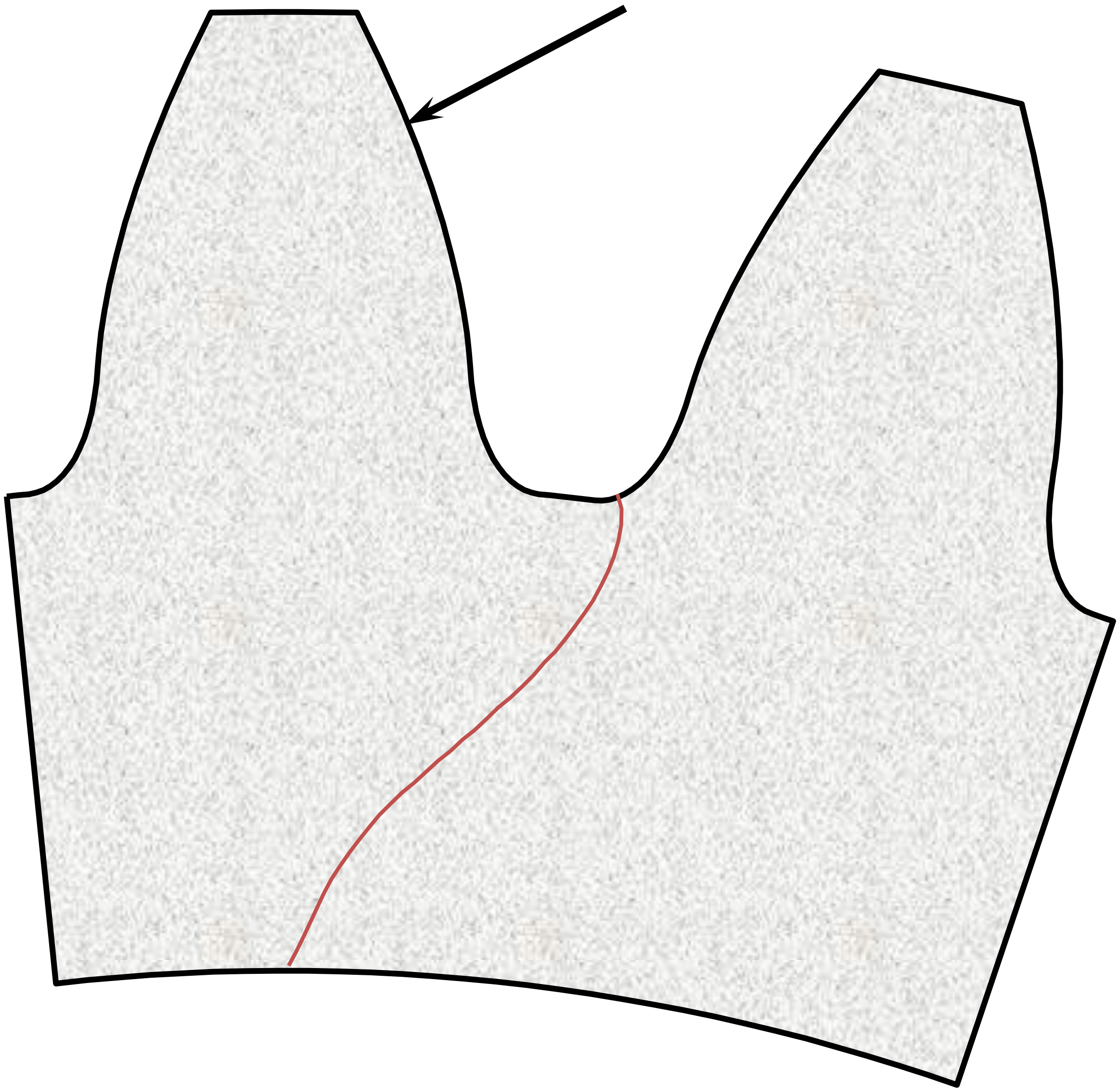

Initial crack location:
θ_0 = 78°

Failure mode:
Rim fracture

Effect of Initial Crack Location on Crack Path

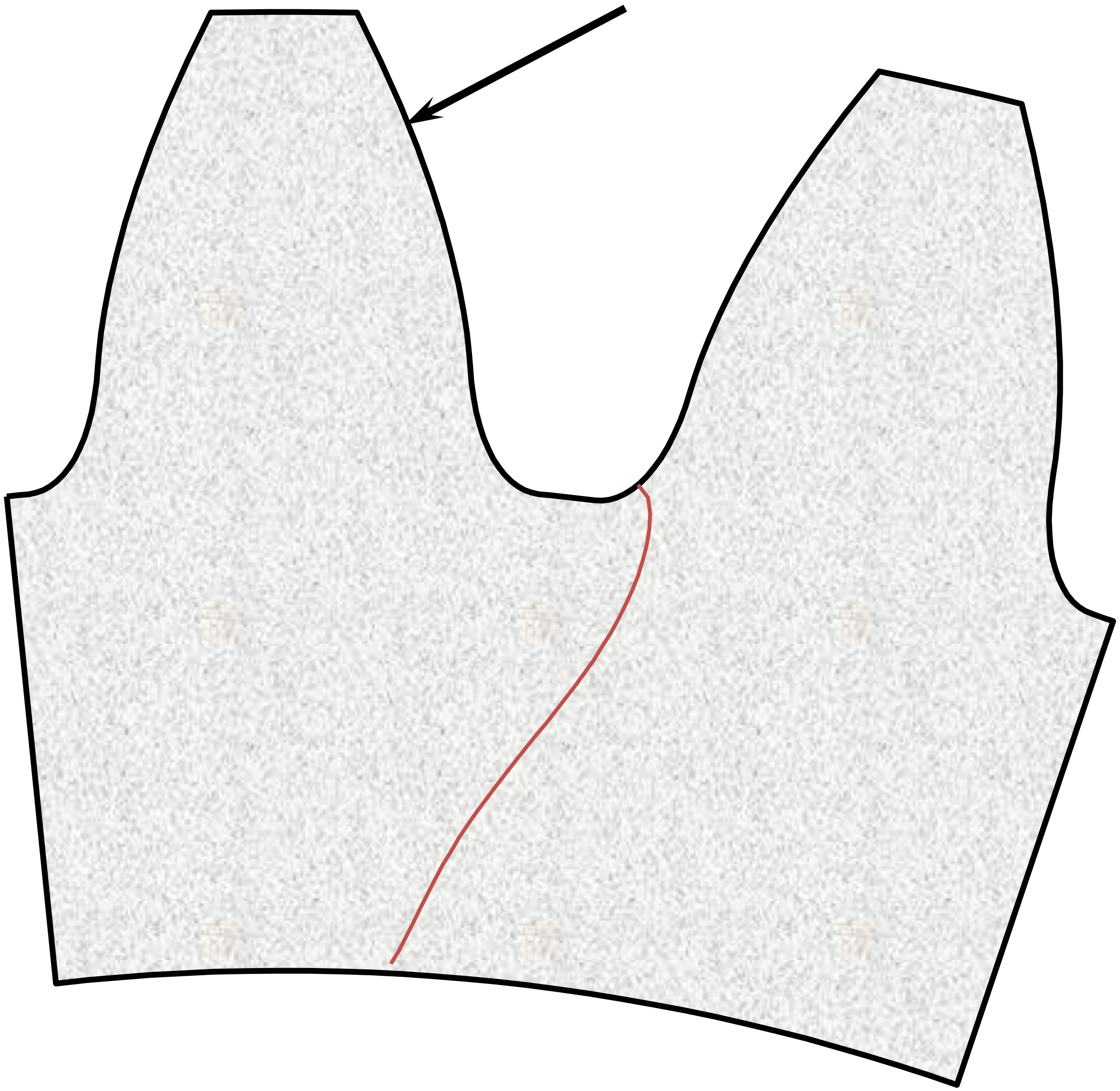

Initial crack location:
$\theta_0 = 73^\circ$

Failure mode:
Rim fracture

Effect of Initial Crack Location on Crack Path

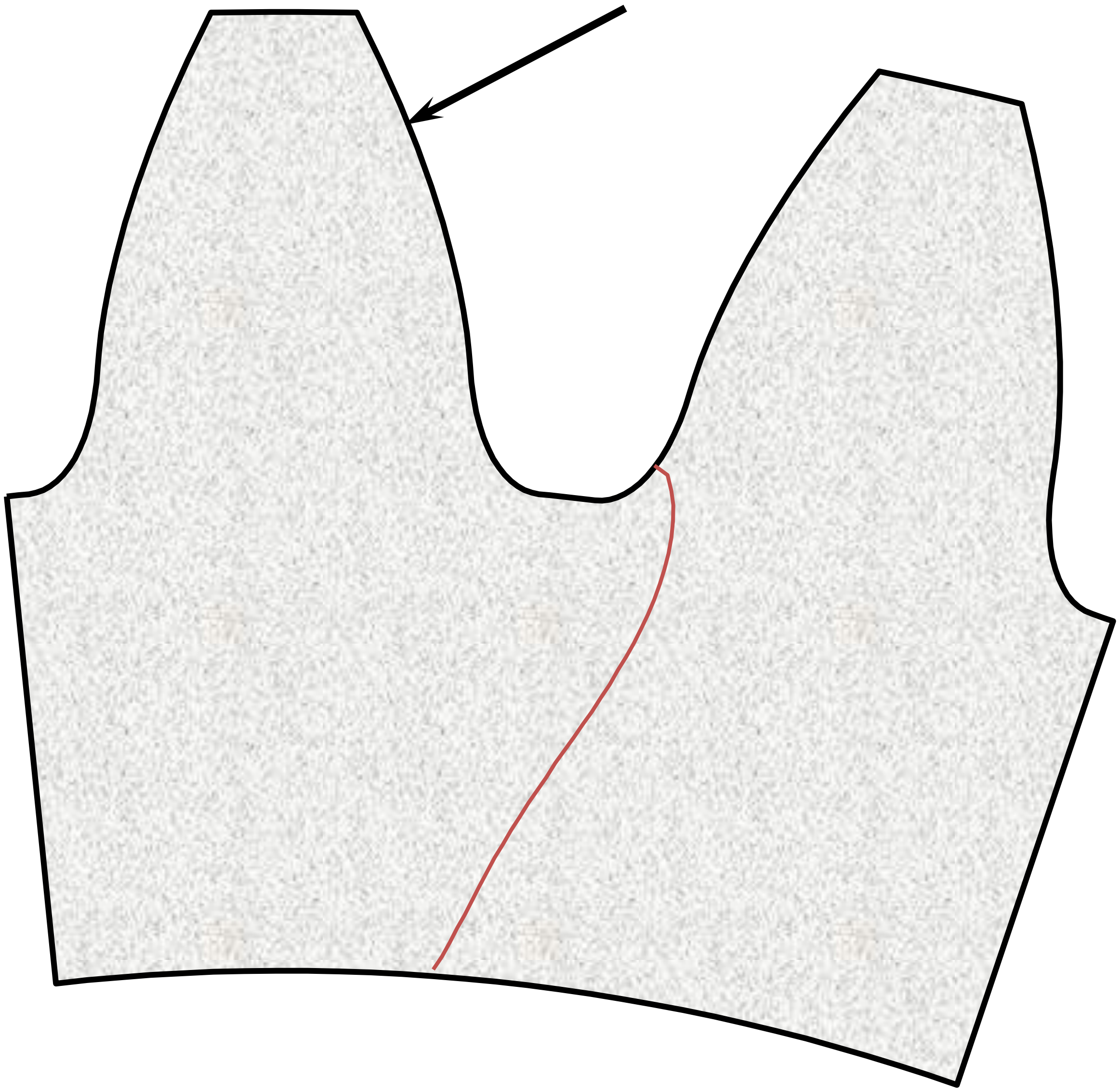

Initial crack location:
θ_0 = 68°

Failure mode:
Rim fracture

Effect of Initial Crack Location on Crack Path

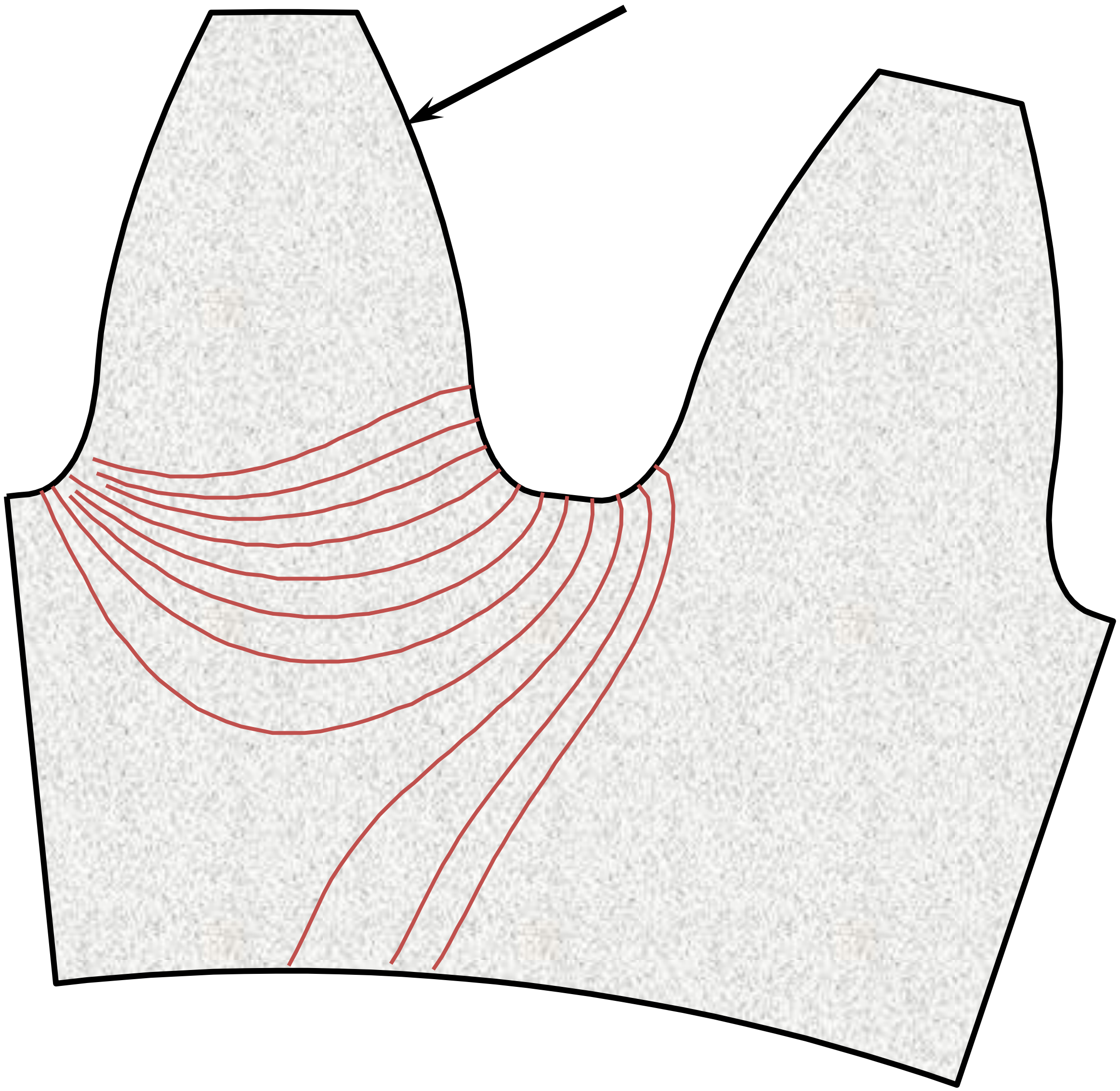

Stress Intensity Factors

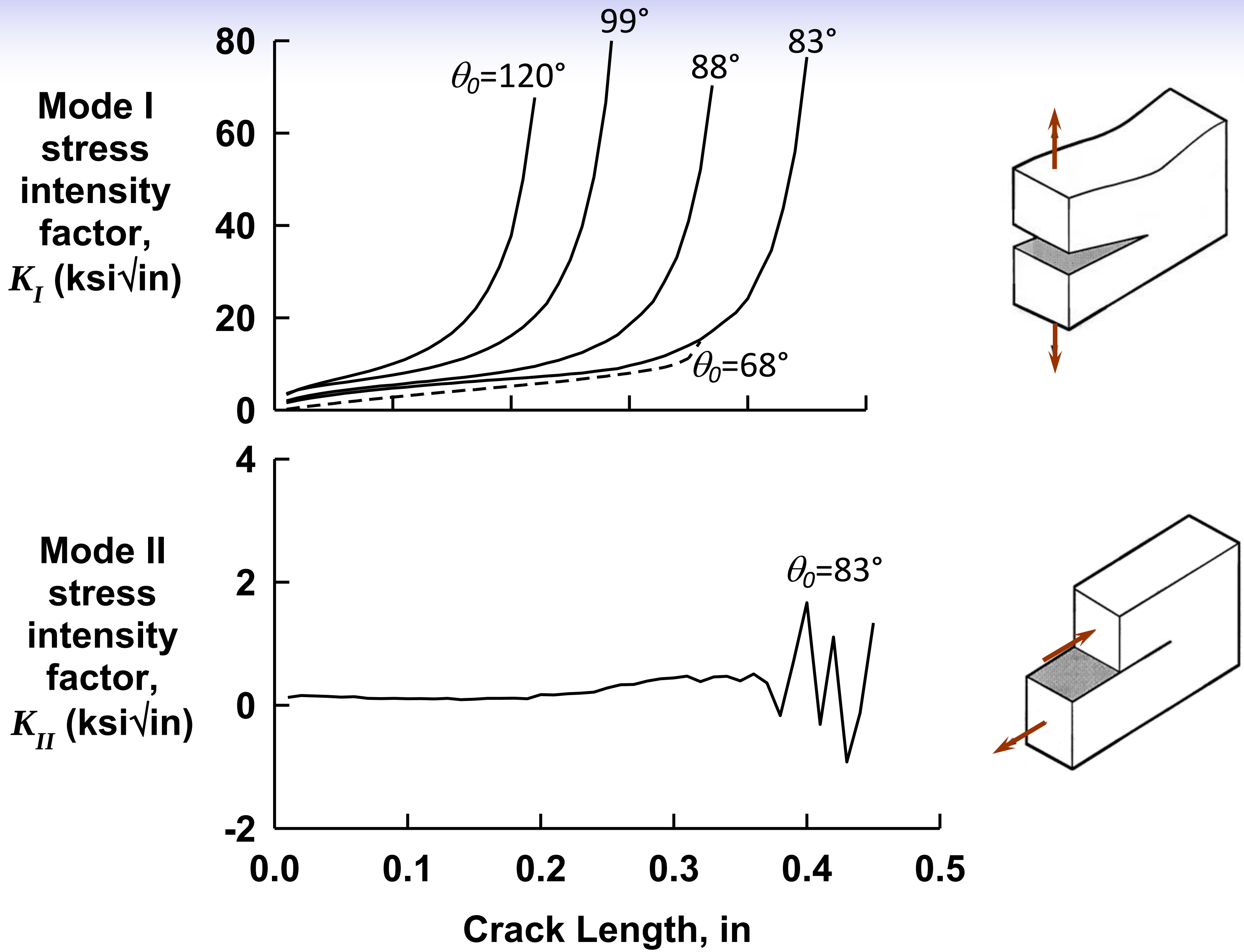

Effect of Backup Ratio on Crack Path

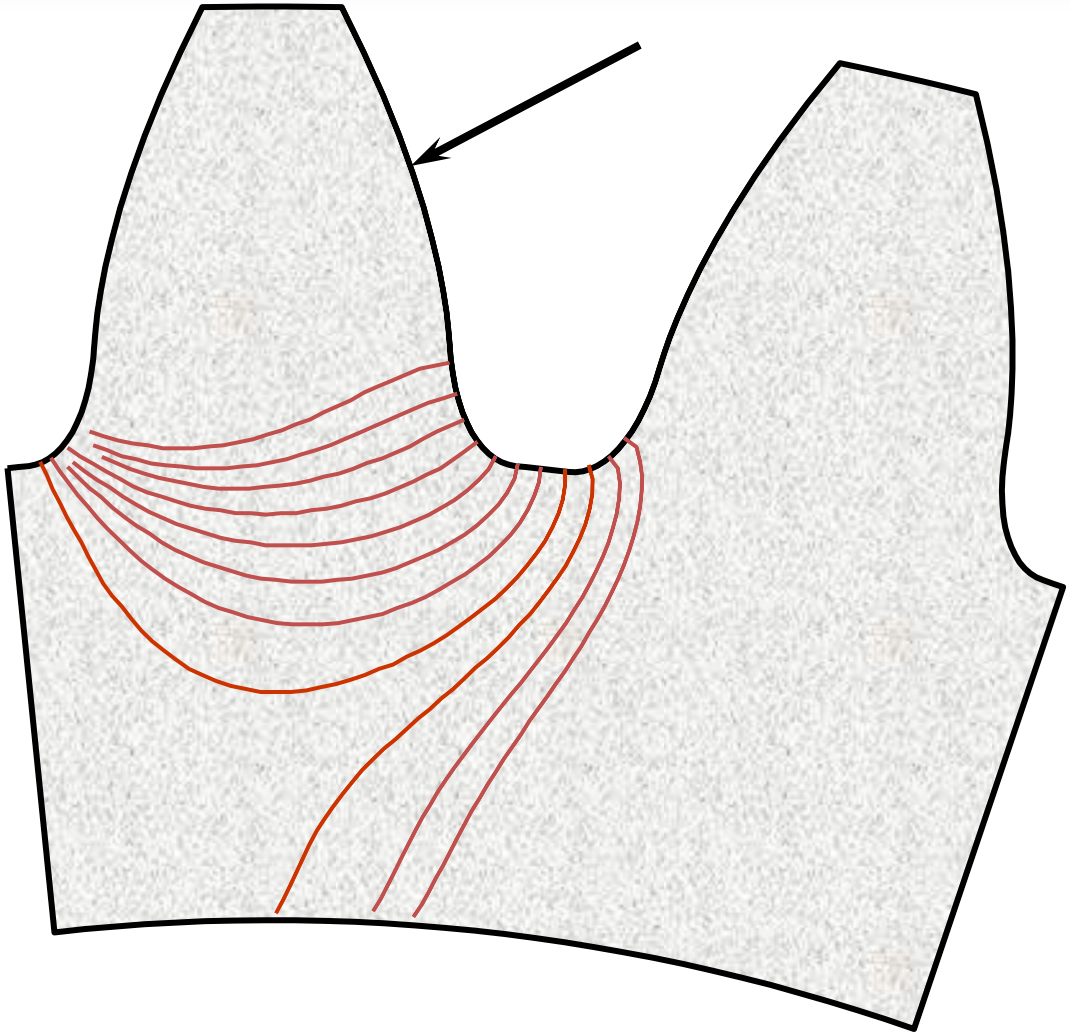

Backup ratio:
$m_B = 1.0$

Tooth/rim fracture transition:
$\theta_0 = 81^\circ$

Effect of Backup Ratio on Crack Path

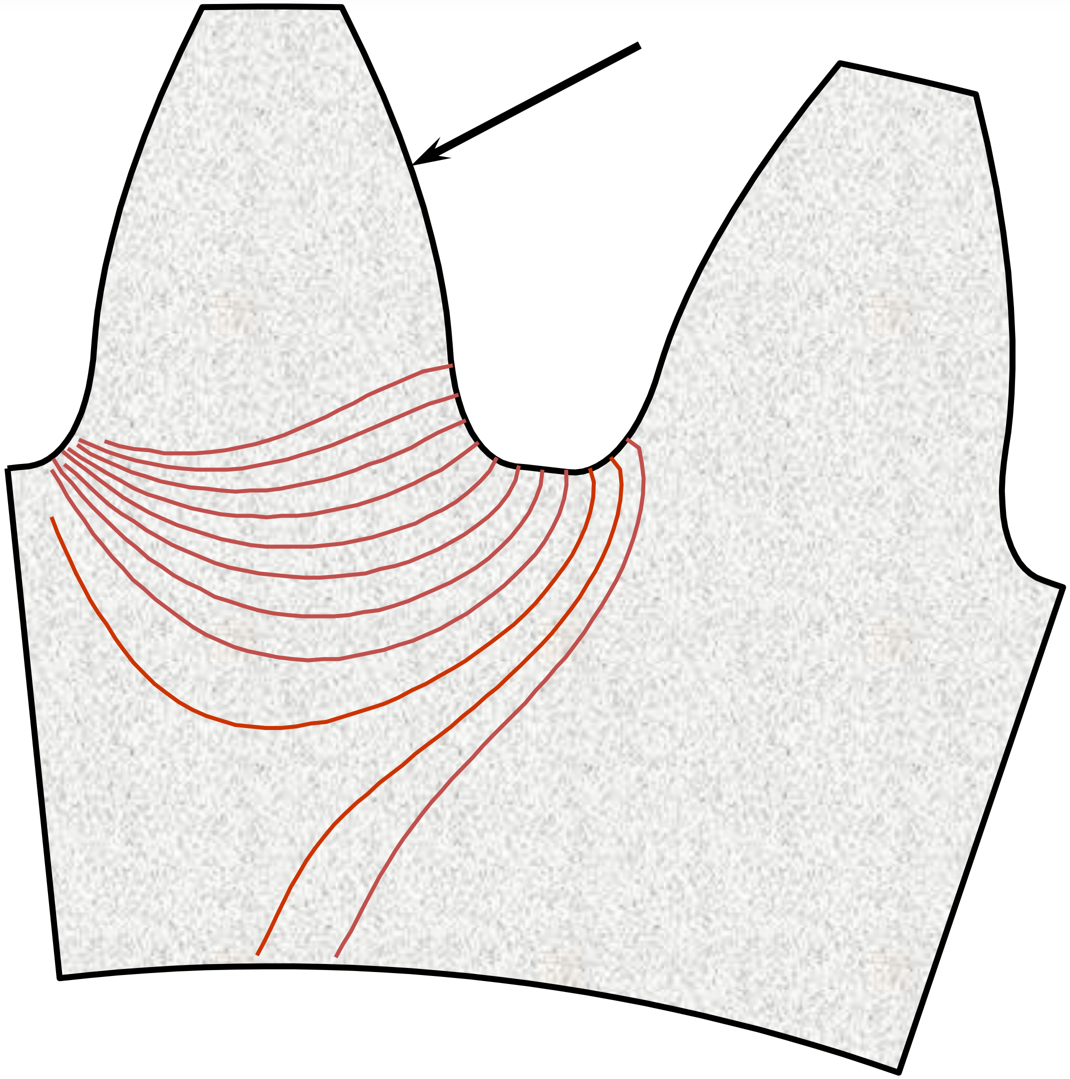

Backup ratio:
$m_B = 1.1$

Tooth/rim fracture transition:
$\theta_0 = 76^\circ$

Effect of Backup Ratio on Crack Path

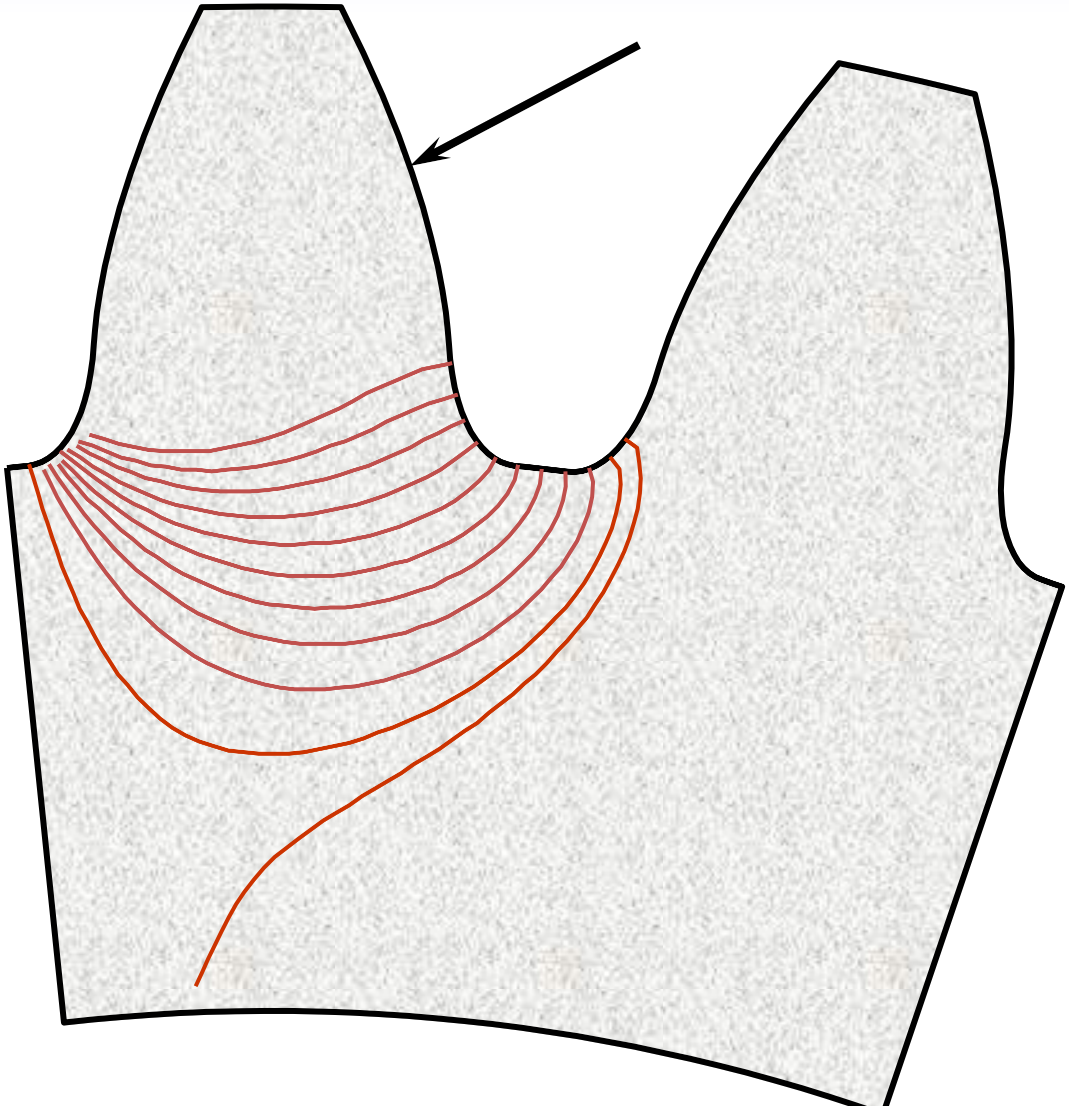

Backup ratio:
$m_B = 1.2$

Tooth/rim fracture transition:
$\theta_0 = 71°$

Effect of Backup Ratio on Crack Path

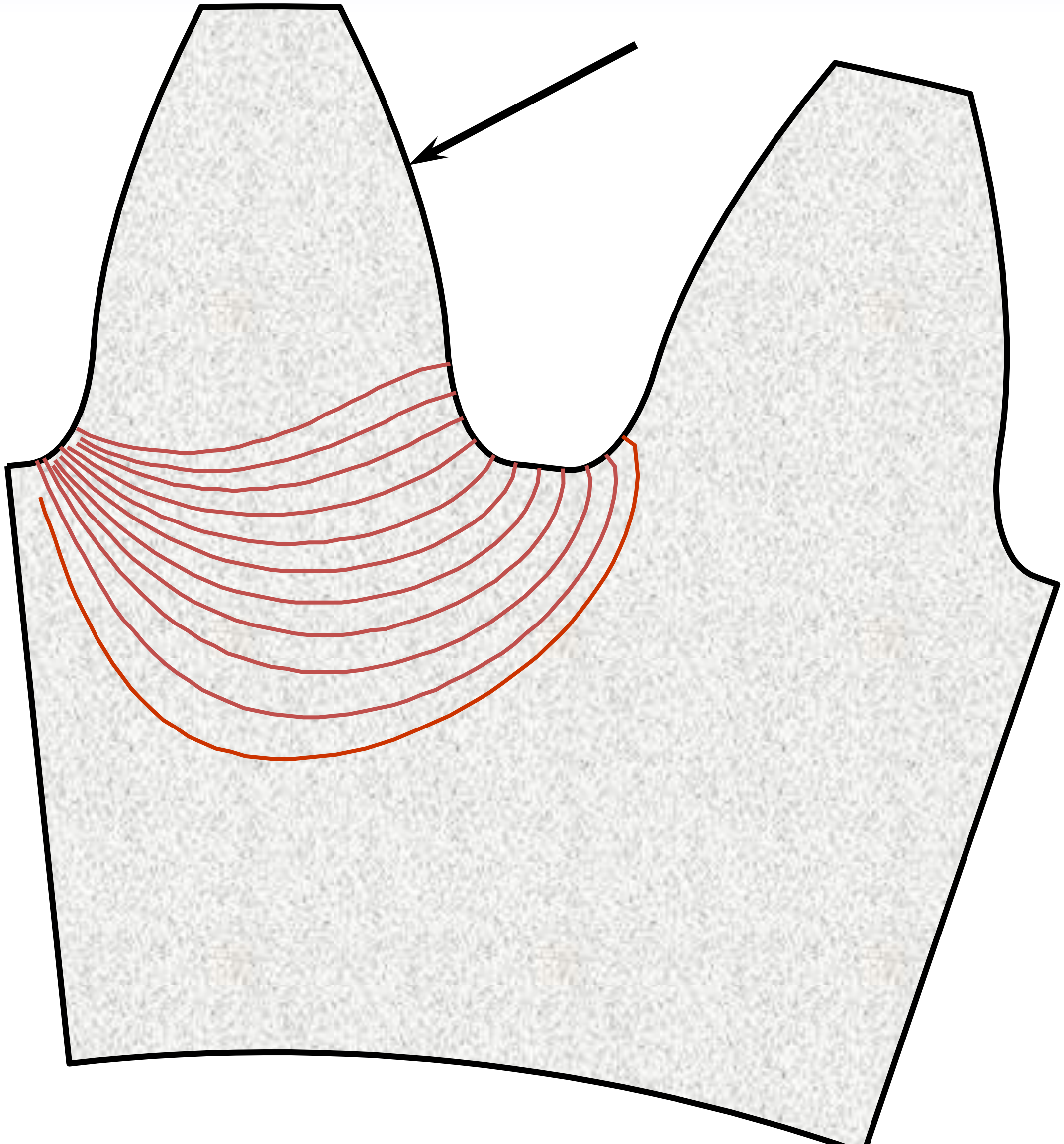

Backup ratio:
m_B = 1.3

Tooth/rim fracture transition:
All tooth fractures

Effect of Backup Ratio on Crack Path

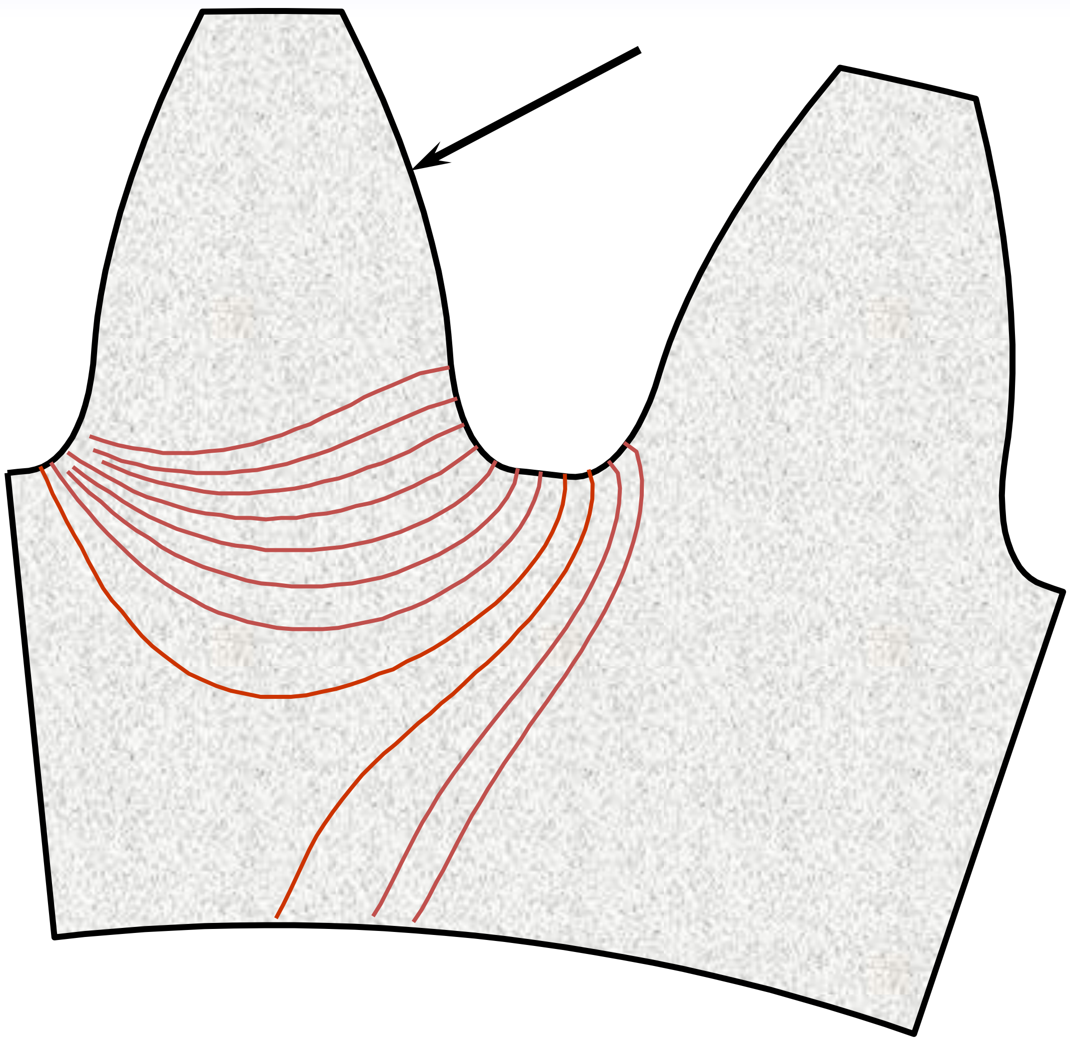

Backup ratio:
$m_B = 1.0$

Tooth/rim fracture transition:
$\theta_0 = 81^{\circ}$

Effect of Backup Ratio on Crack Path

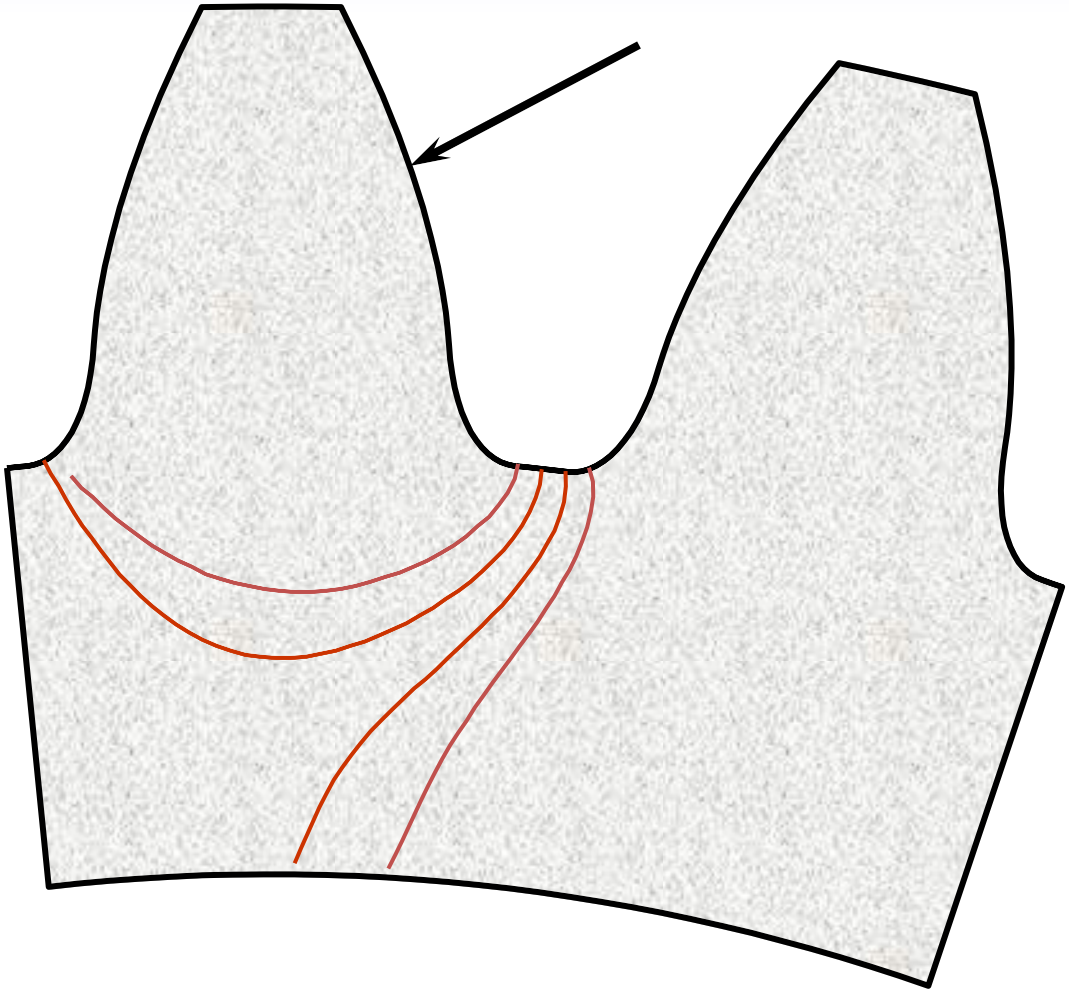

Backup ratio:
$m_B = 0.9$

Tooth/rim fracture transition:
$\theta_0 = 86^\circ$

Effect of Backup Ratio on Crack Path

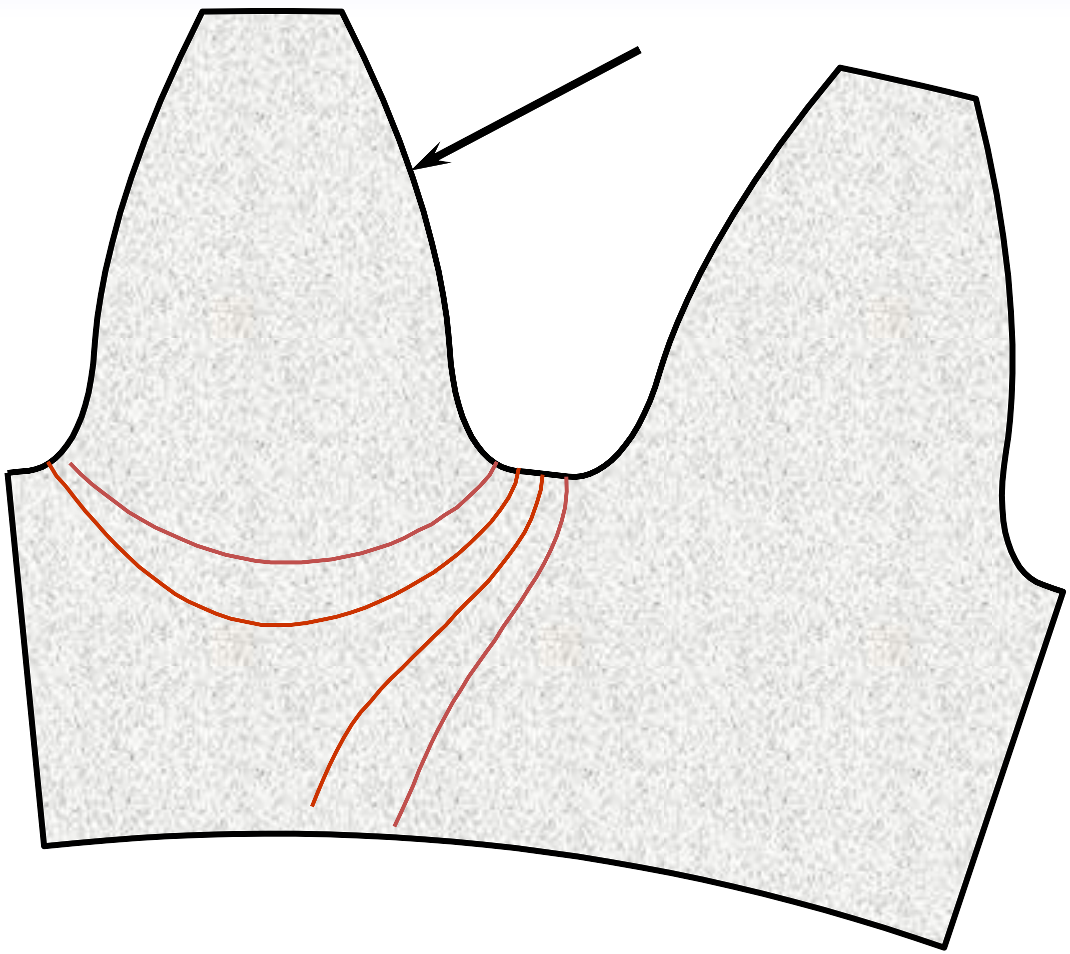

Backup ratio:
$m_B = 0.8$

Tooth/rim fracture transition:
$\theta_0 = 91^\circ$

Effect of Backup Ratio on Crack Path

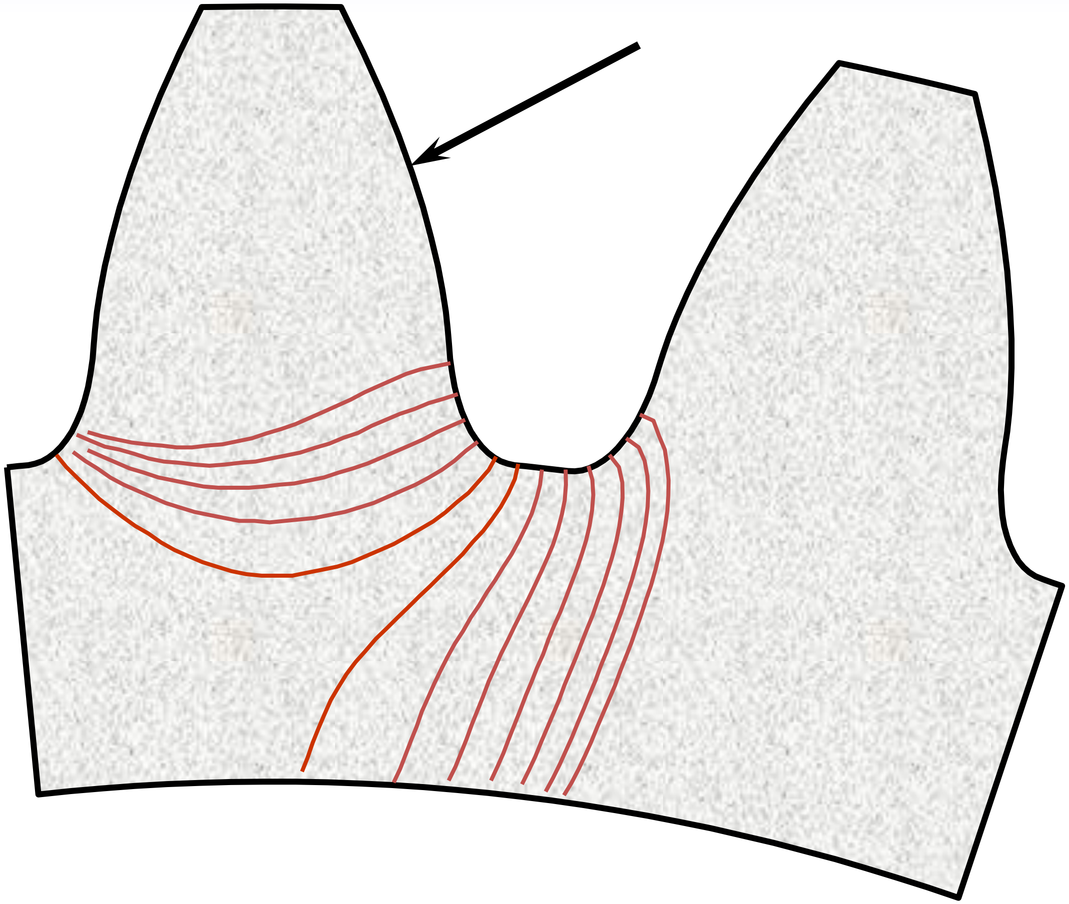

Backup ratio:
m_B = 0.7

Tooth/rim fracture transition:
θ_0 = 97°

Effect of Backup Ratio on Crack Path

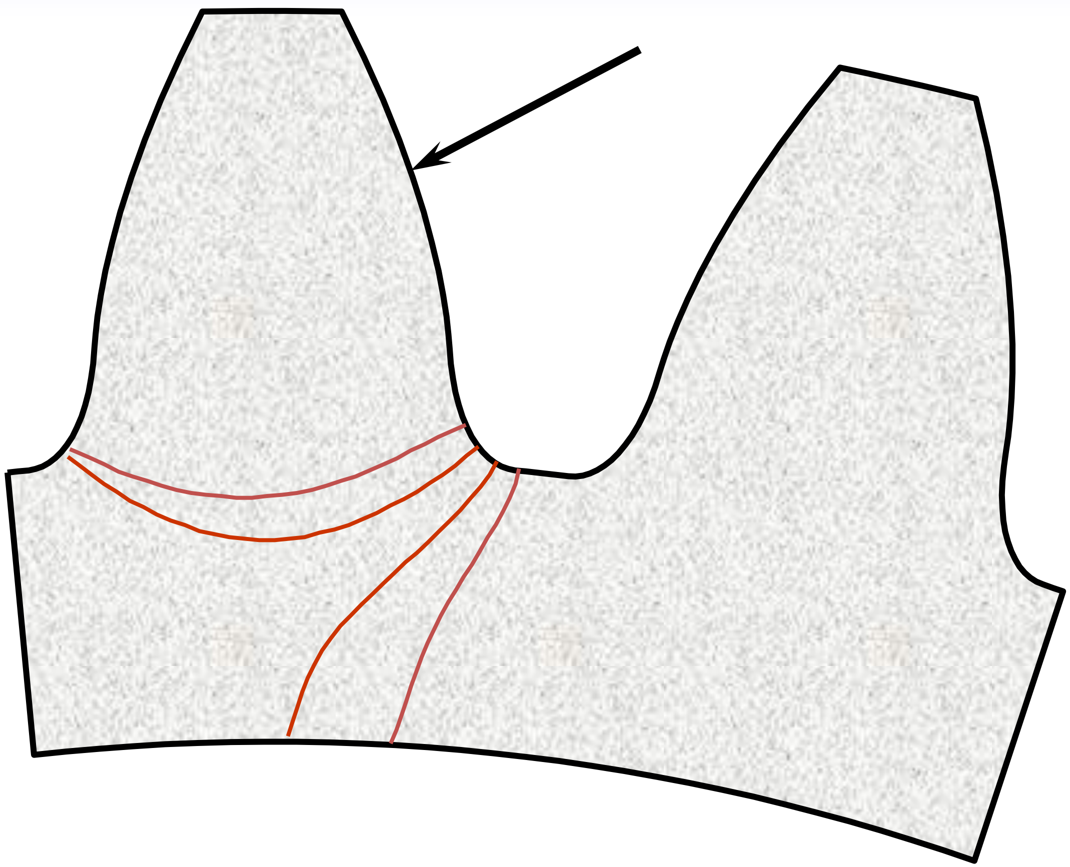

Backup ratio:
$m_B = 0.6$

Tooth/rim fracture transition:
$\theta_0 = 102^\circ$

Effect of Backup Ratio on Crack Path

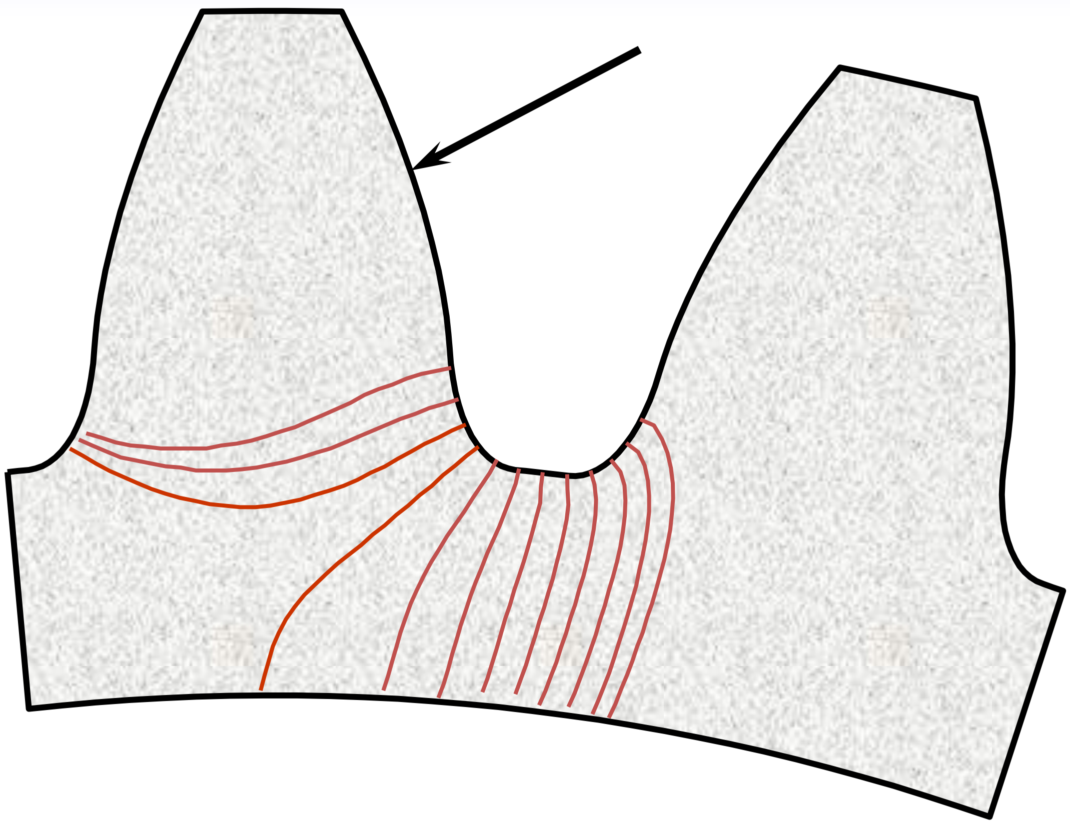

Backup ratio:
$m_B = 0.5$

Tooth/rim fracture transition:
$\theta_0 = 107°$

Validation of Finite Element Modeling

Backup ratio = 3.3

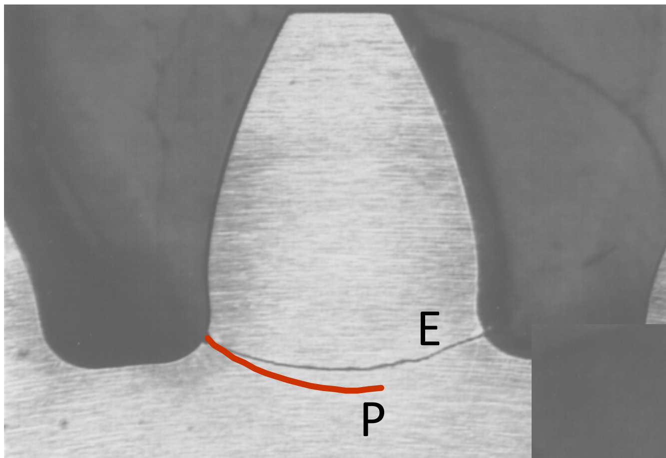

E = Experiment
P = Predicted

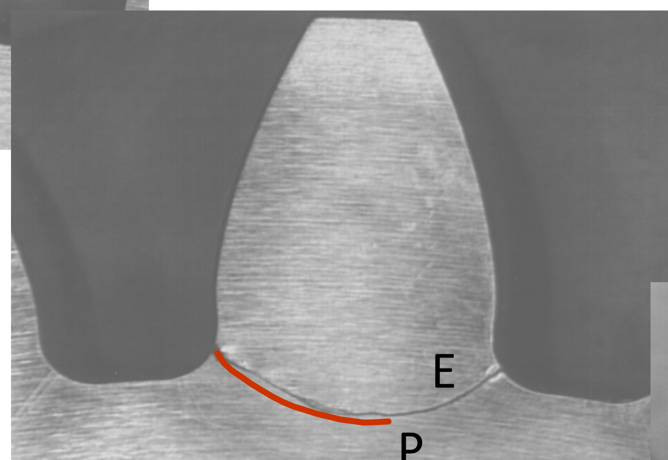

Backup ratio = 1.0

Backup ratio = 0.5

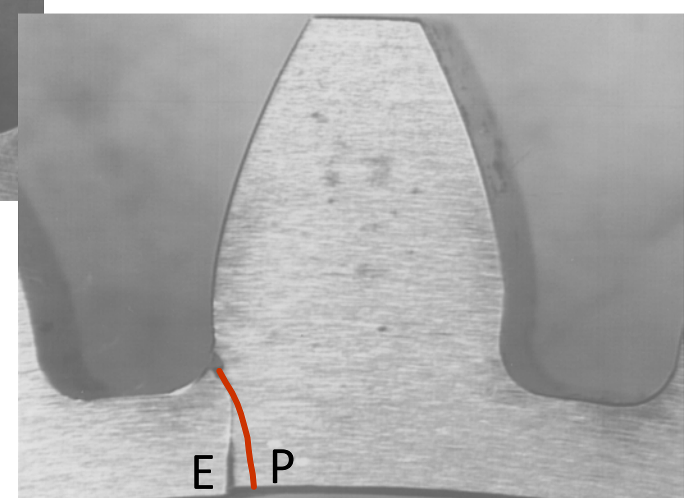

Design Map

T = tooth fractures
R = rim fractures
C = compression

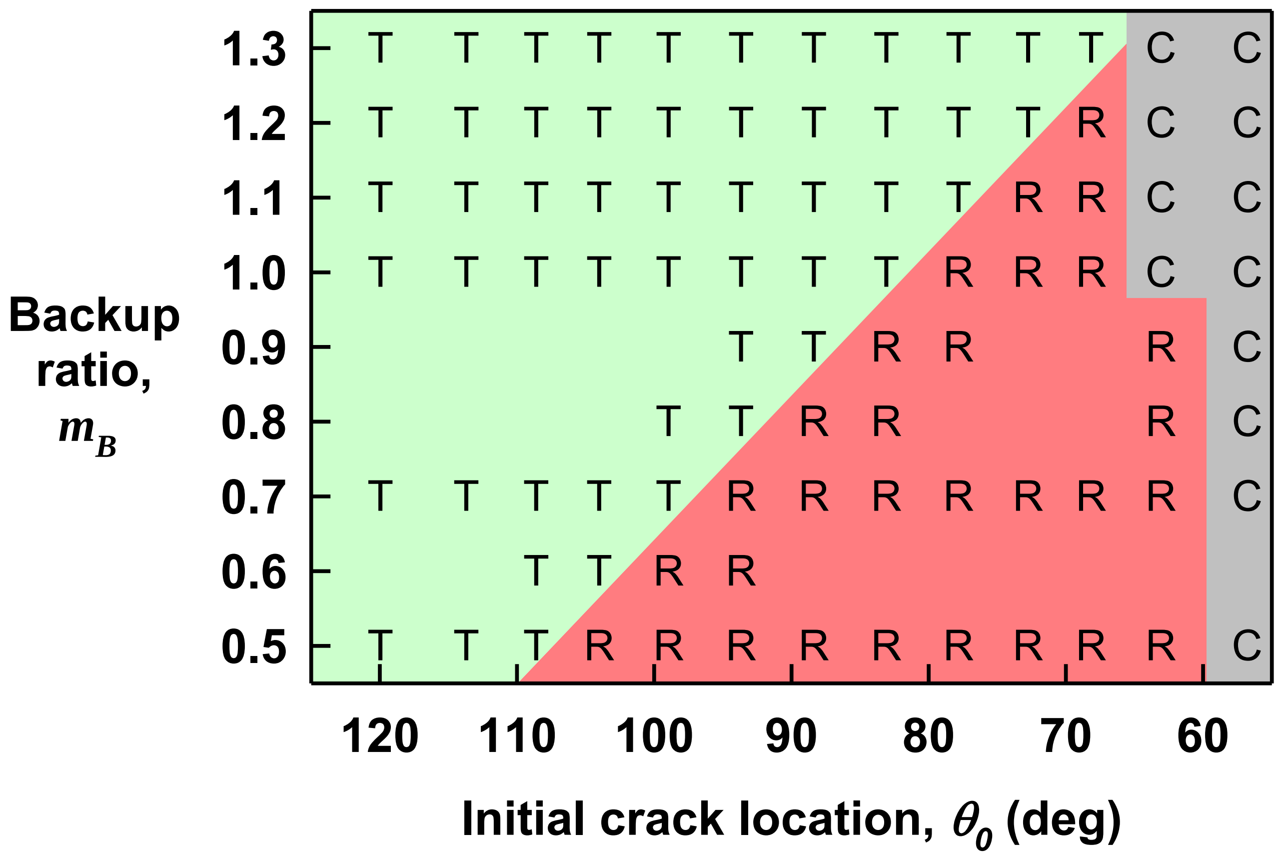

Mode I Stress Intensity Factors

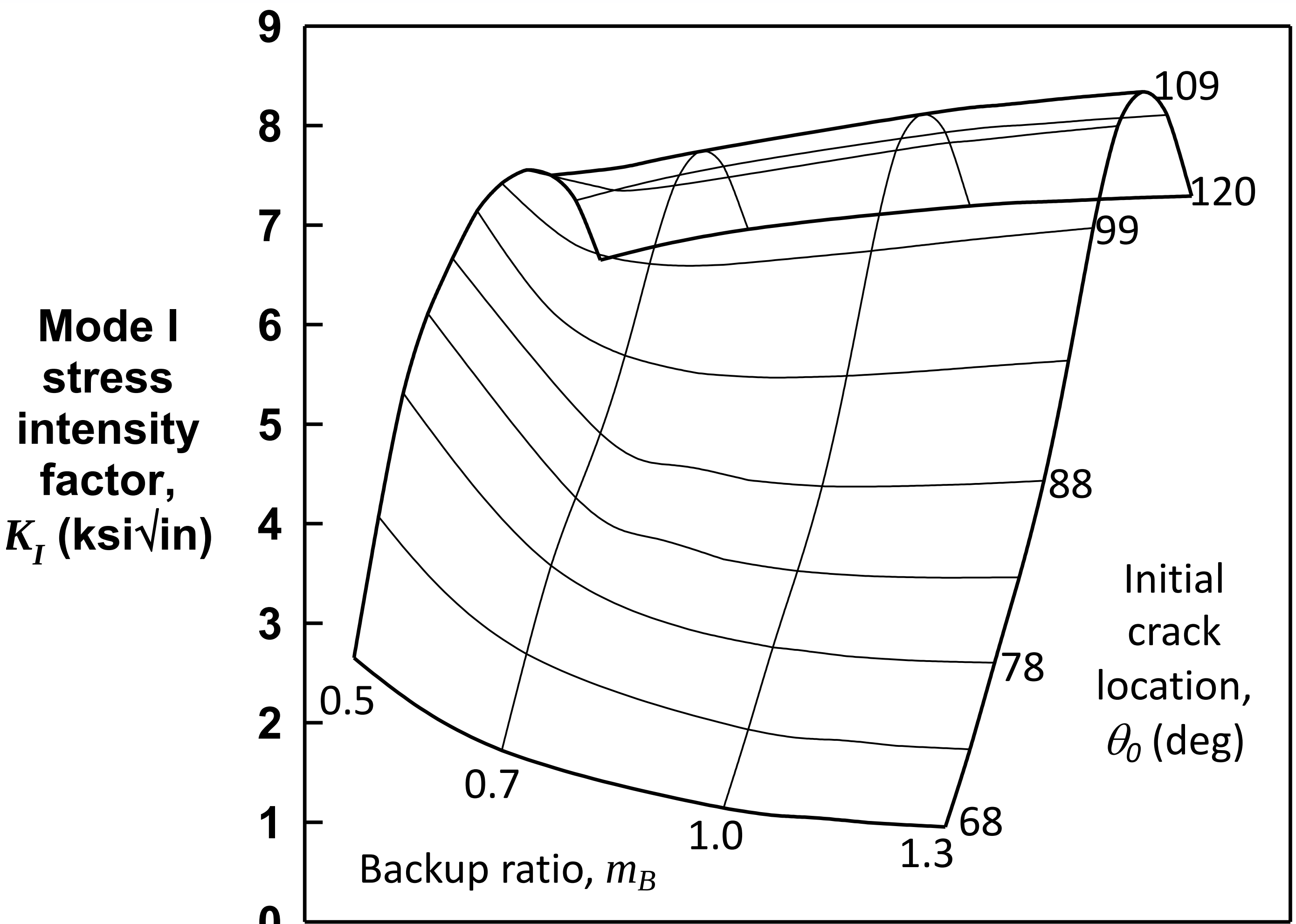

Gear Parameters:

- 28 teeth
- 8 pitch
- 1.75" pitch rad
- 20° press angle

- 500 lb tooth load
- 0.030" crack size

Mode I Stress Intensity Factors

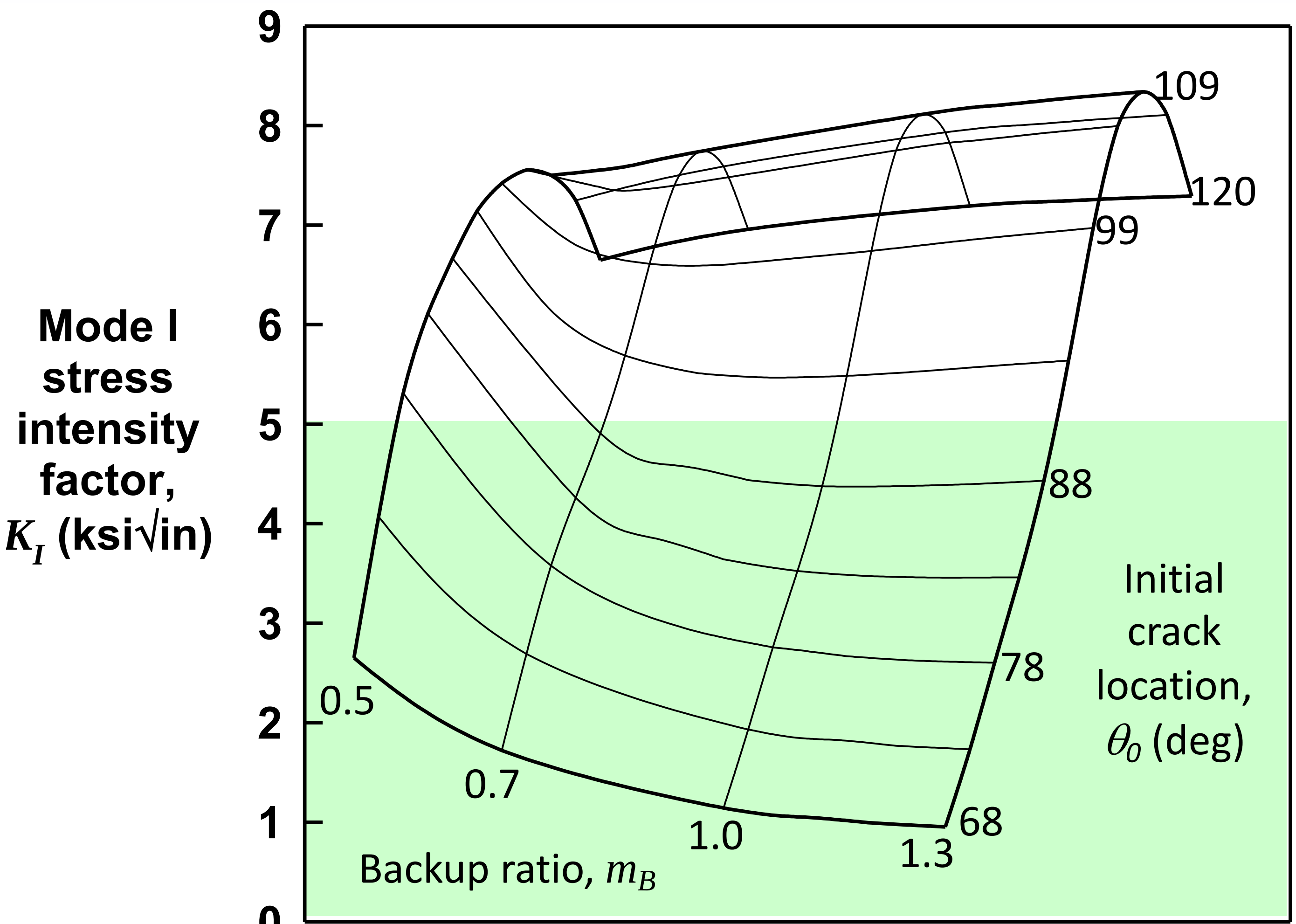

Gear Parameters:

- 28 teeth
- 8 pitch
- 1.75" pitch rad
- 20° press angle

- 500 lb tooth load
- 0.030" crack size

- AISI 9310 steel
- ΔK_{th} = 5 ksi√in

Crack Propagation Angle and Growth Rate

$$\theta_m = 2\tan^{-1}\left[\frac{\frac{K_I}{K_{II}} \pm \sqrt{\left(\frac{K_I}{K_{II}}\right)^2 + 8}}{4}\right]$$

3 Paris equation, n = 2.264, C = 1.149×10^{-15} in./cyc/(psi$\sqrt{\text{in.}}$)^n (Au and Ke, 1981)
4 Paris equation, n = 2.954, C = 6.027×10^{-19} in./cyc/(psi$\sqrt{\text{in.}}$)^n (Au and Ke, 1981)
5 Paris equation, n = 2.555, C = 2.721×10^{-17} in./cyc/(psi$\sqrt{\text{in.}}$)^n (Au and Ke, 1981)
6 Paris equation, n = 2.420, C = 1.084×10^{-16} in./cyc/(psi$\sqrt{\text{in.}}$)^n (Au and Ke, 1981)
10 Collipriest equation, n = 1.63, C = 8.36×10^{-9} in./cyc/(ksi$\sqrt{\text{in.}}$)^n, ΔK_{th} = 3.5 ksi$\sqrt{\text{in.}}$, K_{IC} = 200 ksi$\sqrt{\text{in.}}$, R = 0 (Forman and Hu, 1984)

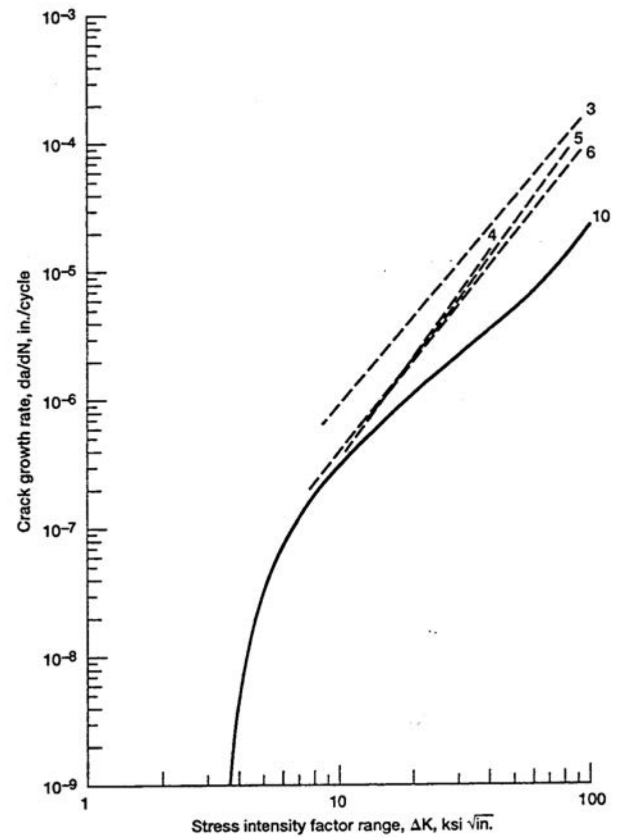

Figure 3.7.3.—Comparison of fatigue crack growth rates using Paris equation and Collipriest equation for AISI 9310 steel.

Design Map

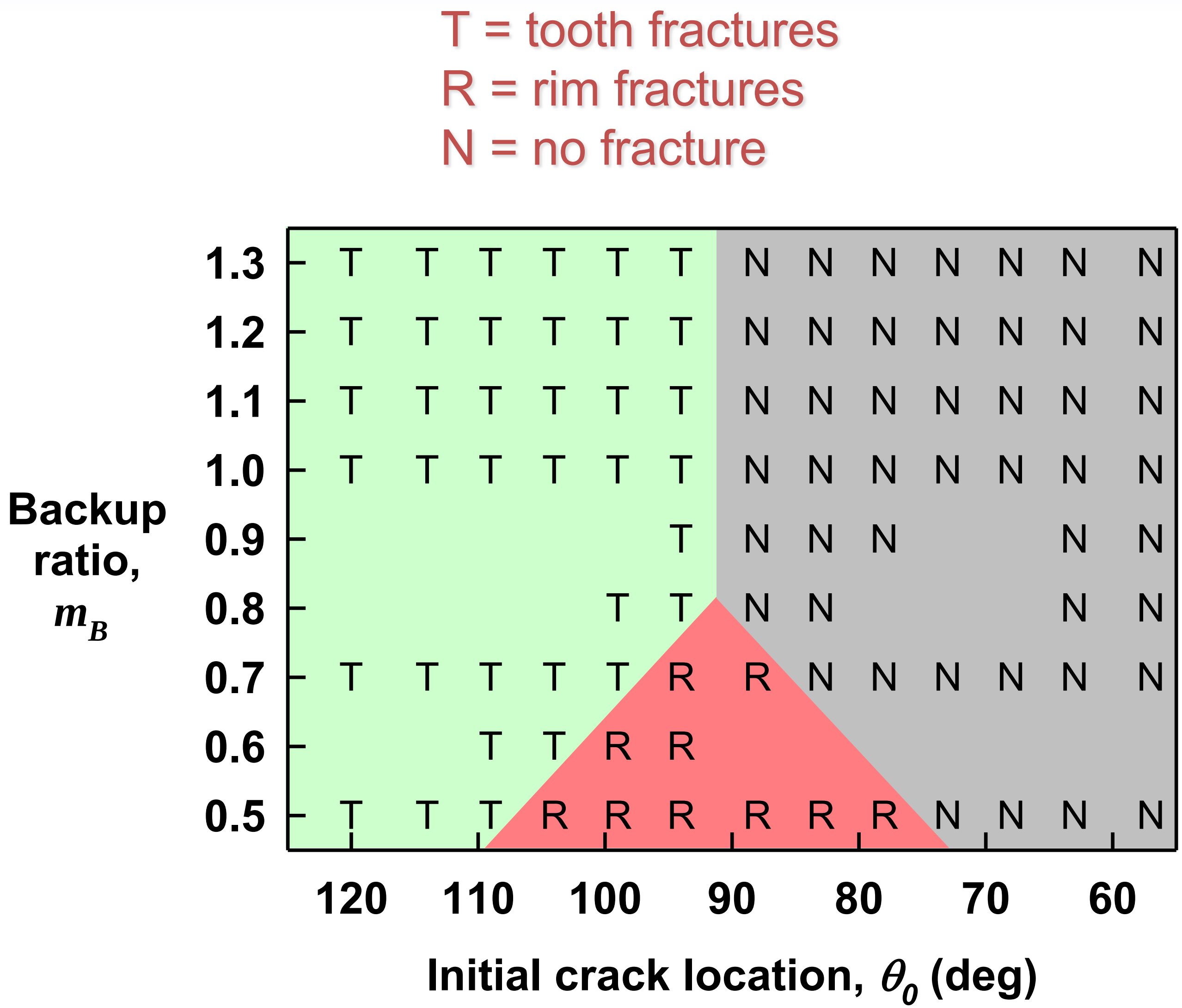
T = tooth fractures
R = rim fractures
N = no fracture
Backup ratio, m_B
1.3
1.2
1.1
1.0
0.9
0.8
0.7
0.6
0.5
T T T T T T N N N N N N N
T T T T T T N N N N N N N
T T T T T T N N N N N N N
T T T T T T N N N N N N N
T N N N N N
T T N N N N
T T T T T R R N N N N N N
T T R R
T T T R R R R R R N N N N
120
110
100
90
80
70
60
Initial crack location, θ_0 (deg)